PRODUCTION OF SCALARS AT ELECTRON COLLIDERS IN THE CONTEXT OF LITTLEST HIGGS MODEL

A THESIS SUBMITTED TO
THE GRADUATE SCHOOL OF NATURAL AND APPLIED SCIENCES
OF
MIDDLE EAST TECHNICAL UNIVERSITY

BY

AYŞE ÇAĞIL

IN PARTIAL FULFILLMENT OF THE REQUIREMENTS
FOR
THE DEGREE OF DOCTOR OF PHILOSOPHY
IN
PHYSICS

DECEMBER 2009

Approval of the thesis:

PRODUCTION OF SCALARS AT ELECTRON COLLIDERS IN THE CONTEXT OF LITTLEST HIGGS MODEL

submitted by **AYŞE ÇAĞIL** in partial fulfillment of the requirements for the degree of **Doctor of Philosophy in Physics Department, Middle East Technical University** by,

Prof. Dr. Canan Özgen
Dean, Graduate School of **Natural and Applied Sciences** _____

Prof. Dr. Sinan Bilikmen
Head of Department, **Physics** _____

Prof. Dr. Mehmet Zeyrek
Supervisor, **Physics Department, METU** _____

Examining Committee Members:

Prof. Dr. Ali Ulvi Yılmazer
Department of Physics Engineering, Ankara University _____

Prof. Dr. Mehmet T. Zeyrek
Department of Physics, METU _____

Prof. Dr. Takhmasib M. Aliev
Department of Physics, METU _____

Prof. Dr. Müge Boz Evinay
Department of Physics Engineering, Hacettepe University _____

Assoc. Prof. Dr. Altuğ Özpineci
Department of Physics, METU _____

Date: _____

I hereby declare that all information in this document has been obtained and presented in accordance with academic rules and ethical conduct. I also declare that, as required by these rules and conduct, I have fully cited and referenced all material and results that are not original to this work.

Name, Last Name: AYŞE ÇAĞIL

Signature :

ABSTRACT

PRODUCTION OF SCALARS AT ELECTRON COLLIDERS IN THE CONTEXT OF LITTLEST HIGGS MODEL

Çağıl, Ayşe
Ph. D., Department of Physics
Supervisor : Prof. Dr. Mehmet Zeyrek

December 2009, 91 pages

The littlest Higgs model is one of the most economical solution to the hierarchy problem of the standard model. It predicts existence of new gauge vectors and also new scalars, neutral and charged.

The littlest Higgs model predicts the existence of new scalars beside a scalar that can be assigned as Higgs scalar of the standard model. In this thesis, the production of scalars in e^+e^- colliders is studied. The scalar productions associated with standard model Higgs boson are also analyzed. The effects of the parameters of the littlest Higgs model to these processes are examined in detail.

The collider phenomenology of the littlest Higgs model is strongly dependant on the free parameters of the model, which are the mixing angles s, s' and the symmetry breaking scale f. The parameters of the model are strongly restricted when the fermions are charged under only one $U(1)$ subgroup. In this thesis, by charging fermions under two $U(1)$ subgroups, the constraints on the symmetry braking scale and the mixing angles are relaxed.

In the littlest Higgs model, the existence of charged heavy scalars also displays an interesting feature. By writing a Majorano like term in the Yukawa Lagrangian, these heavy charged scalars are allowed to decay in to lepton pairs, violating lepton number and flavor. In this thesis, the leptonic final states and also the lepton flavor and number violating final signals are also analyzed.

As a result of these thesis, it is predicted that the scalar production will be in the reach for a $\sqrt{S} = 2TeV$ e^+e^- collider, giving significant number of lepton flavor violating signals depending on the Yukawa couplings of the flavor violating term.

Keywords: heavy scalars, little Higgs, littlest Higgs

ÖZ

KÜÇÜCÜK HIGGS MODELİNDE AĞIR SKALARLARIN ELEKTRON ÇARPIŞTIRICILARINDA ÜRETİLMESİ

Çağıl, Ayşe
Doktora, Fizik Bölümü
Tez Yöneticisi : Prof. Dr. Mehmet Zeyrek

Aralık 2009, 91 sayfa

Küçücük Higgs modeli, standart model Higgs skalarına ilave olarak yeni ağır skalarların varlıklarını öngörmektedir. Bu tezde bu skalarların çizgisel e^+e^- çarpıştırıcılarındaki üretilme olasılıkları incelendi. Ayrıca yeni skalarların, standart model Higgs bozonu ile birlikte üretilme olasılıkları da inceledi. Küçücük Higgs model parametlerinin bu üretim süreçlerine etkileri de ayrıca araştırıldı.

Küçücük Higgs modeli, standart modeldeki hiyerarşi problemine getirilen en ekonomik çözümlerden biridir. Bu model, yeni, ağır, yüklü veya yüksüz skalar bozonların ve ayar vektoörlerinin varlıklarını öngörmektedir.

Küçücük Higgs modelinin parçacık hızlandırıcılarındaki fenomenolojisi modelin serbest parametrelerine doğrudan bağlıdır. Bu parametreler, karışım açıları s, s' ile simetri kırılma parametresi f olarak tanımlanmışlardır. Modelin parametre uzayı, fermionların sadece bir $U(1)$ alt grubu altında yüklü oldukları durumda güçlü kısıtlamalara tabiidirler. Biz bu çalışmada fermionları her iki $U(1)$ grupları altında ayarlı kabul ederek simetri kırılma parametresi üzerindeki kısıtlamaları azalttık.

Küçücük Higgs modelinde yüklü yeni parcacıkların varlıkları ilgi çekici bir ilaveye izin vermektedir. Bu modele fermionlar için lepton çeşnisinin korunumunu kıran Majorano tarzı kutle terimleri eklenebilmektedir. Bunun sonucu olarakta, bu tezde araştılan üretim süreçleri, son sistemlerinde lepton çeşnisini ve sayısını kıran parçacıklar bulundurabilmektedirler. Bu tezde üretim süreçlerine ilave olarak, bu son sistemler de ayrıca işlenmiştir.

Bu tezin sonucunda, ağır skalarların enerji ölçeği $2TeV$ ve üzeri olan çizgisel e^+e^- çarpıştırıcılarında üretilebileceği, ve lepton sayısını ve çeşnisini korumayan son sistemlerin gözlemlenebileceği bulunmuştur.

Anahtar Kelimeler: küçücük Higgs modeli, küçük Higgs modelleri, ağır skalarlar, yüklü Higgs bozonu, lepton çeşnisi bozunumu

to my family

ACKNOWLEDGMENTS

I would like to thank to my supervisor Prof. Dr. Mehmet Zeyrek, for his encouragement, and guidance during this work. I would also thank to Prof. Dr. T. M. Aliev, for suggesting a wonderful and a timely topic, and his guidance. I am deeply thankful to Assoc. Prof. Dr. A. Özpineci, for the scientific discussions that we had, for proof reading this thesis, and especially for his support and his friendly attitude.

Last but not least, I thank to my family, my dear father and mother, for every support and help, up to this stage.

TABLE OF CONTENTS

LIST OF TABLES

TABLES

LIST OF FIGURES

FIGURES

CHAPTER 1

INTRODUCTION

Standard model (SM) is an effective theory with a cutoff scale around electroweak symmetry breaking (EWSB) scale. In SM, symmetry is broken by Higgs mechanism giving mass to fermions and gauge bosons Z and W. From experimental data of Z and W masses vacuum expectation value of the Higgs field (VEV) is calculated as $v \sim 246GeV$ indicating that $M_H \sim 240GeV$. However the Higgs mass suffers from loop corrections, which is known as the hierarchy problem. In order to get a light Higgs mass many theories are proposed, such as supersymmetry (SUSY), models with dynamical symmetry breaking, extra dimensional models and little Higgs models.

The little Higgs (LH) models are proposed as an alternative solution to hierarchy problem as an ultraviolet completion of SM [1, 2, 3, 4]. In LH models collective symmetry breaking mechanism is used. First a global symmetry at scale $\Lambda \sim 10TeV$ is broken and Higgs boson appears as a pseudo goldstone boson, and than ordinary EWSB occurs. As a consequence of collective symmetry breaking, LH models contain extra scalar and vector gauge bosons that cancel out the divergences in Higgs scalar mass. The phenomenology of the little Higgs models are reviewed in [5, 6, 7], and constraints on little Higgs models are studied in [9, 10, 12, 13, 14, 15]. The little Higgs models are also expected to give significant signatures in future high energy colliders[16, 17, 18, 22]. The phenomenology of the little Higgs models are also well studied at the literature [20, 21, 22, 23, 24, 25, 26, 27, 28, 29, 30, 31, 32, 33]. The Little Higgs models also have significant effects on the observables of flavor physics, due to the existence of heavy charged bosons and a new T quark [34, 35, 36, 37, 38, 39]

The littlest Higgs model [1] is one of the LH models, in which the global symmetry $SU(5)$ containing a gauged subgroup $(SU(2) \otimes U(1))^2$ is broken to $SO(5)$ by nonlinear sigma model

(NLSM), resulting in the appearance of a set of Nambu-Goldstone bosons. At the same time diagonal subgroup $(SU(2) \otimes U(1))^2$ is broken to $(SU(2) \otimes U(1))$ at a scale $f \sim 2\pi v$ around $1TeV$. These collective symmetry breaking in the littlest Higgs model results in new neutral scalars ϕ^0 and ϕ^P, and a charged scalar $\phi^{\pm}$, and a double charged scalar $\phi^{\pm\pm}$ besides the SM Higgs scalar. Also the littlest Higgs model contains new heavy (H) vector bosons A_H (heavy photon), Z_H and $W_H^{\pm}$, besides the light (L) gauge bosons, A_L, Z_L and $W_L^{\pm}$ which are the SM gauge bosons. Since there is a large quadratic contribution to Higgs mass from loops of fermions, especially from t quark loop, a new fermion with charge $\frac{2}{3}$ called the T quark is introduced. As a result extra fermion T quark cancels the quadratic divergences coming from fermion loops, new gauge bosons cancel the quadratic divergences coming from the loop corrections of Z_L and W_L of SM, and new scalars cancel the divergences of Higgs self loops.

The appearance of new scalars in littlest Higgs model also allows Majorano type mass terms in Yukawa Lagrangian without need of right handed neutrinos to give mass to neutrinos [40, 41, 42, 43]. These type of interactions result in lepton flavor and number violating processes which can be distinct signatures in high energy colliders.

In this thesis the productions of new scalars and their decays at future linear e^+e^- colliders, namely, International Linear Collider (ILC) [45] and Compact Linear Collider (CLIC) [46] in the context of littlest Higgs model[1] are studied.

This thesis is organized as follows. In chapter 2, the hierarchy problem in the Standard Model is discussed. In chapter 3, the littlest Higgs model is reviewed in detail. Also the parameter space of the littlest Higgs model is discussed. In the last section of this chapter, the littlest Higgs model with T parity is reviewed briefly. The theoretical explanations of the calculations done in this thesis are explained in chapter 4. In chapter 5, the Z_L associated production channels are examined. The Z_L associated production of charged scalars and their lepton flavor violating decay modes are discussed in section 5.2. In chapter 6 the direct production processes of scalars are discussed. Finally, the results are discussed and the thesis is concluded in chapter 7. The Feynman rules for the littlest Higgs model are presented in appendix A.

CHAPTER 2

STANDARD MODEL AND THE HIERARCHY PROBLEM

Standard model (SM) has been a successful model explaining the physics up to a cut off scale $\Lambda \simeq 1TeV$. For higher cut off scales Higgs boson mass suffers from quadratically divergent loop corrections, and needs to be fine tuned.

Standard model is a gauge theory based model. Its group structure consists of $SU(3)_c \otimes SU(2)_L \otimes U(1)_Y$. In order to give mass to gauge bosons and fundamental fermions, $SU(2)_L \otimes U(1)_Y$ symmetry is spontaneously broken to $U(1)_Y$ symmetry by Higgs mechanism.

The Lagrangian for the Higgs scalar in SM is written as:

$$\mathcal{L}(H) = (D_\mu H)(D^\mu H)^\dagger - V(H^\dagger H), \tag{2.1}$$

where the covariant derivative is defined as;

$$D_\mu \equiv \partial_\mu - ig_1 A^a_\mu T^a - ig_2 B_\mu. \tag{2.2}$$

The A^a_μ and B_μ are the gauge fields and g_1 and g_2 are the coupling constants of corresponding $SU(2)$ and $U(1)$ groups. The $SU(2)$ invariant Higgs potential is written in the form:

$$V(HH) = -\mu^2 H^\dagger H + \lambda (H^\dagger H)^2, \tag{2.3}$$

where H is the Higgs doublet, λ is the coupling constant and μ^2 is the mass term. The coupling constant λ in Higgs potential (Eq. 2.3) is restricted to have a positive sign to have a stable vacua. The mass term μ^2 naturally has no restrictions on its sign but it is chosen to be negative to have the spontaneous symmetry breaking.

The interactions of the Higgs scalar with fermions are written in Yukawa Lagrangian, as:

$$\begin{aligned} \mathcal{L}_{\mathcal{Y}} &= g_d \bar{L} H R_d + g_u \bar{L} H^C R_u \\ &\quad + h.c., \end{aligned} \tag{2.4}$$

where L is the left handed doublet, R_d and R_u are right handed singlets of leptons and quarks and $H^C = i\sigma_2 H^*$.

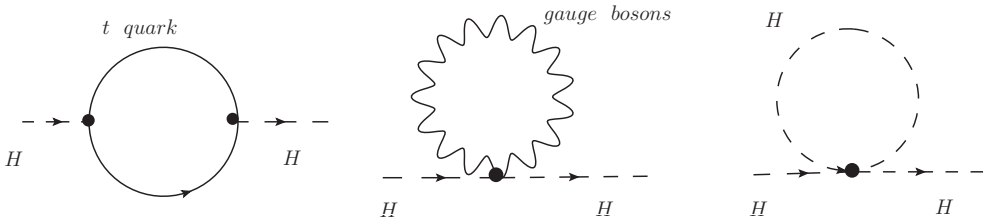

Figure 2.1: The diagrams for contributions to Higgs mass in SM.

The hierarchy problem of the Higgs mechanism in SM arises when loop contributions at first level to bare mass term are calculated. The main contributions are from Higgs self coupling loop, gauge boson loops and the top quark loop due to the large value of the Yukawa coupling g_t (see Fig.2.1).

The corrections to Higgs mass due to loops are calculated as:

$$\begin{aligned} \delta_{m^2}(t-quark) &\sim -\frac{3}{8\pi^2} g_t^2 \Lambda^2 \,, \\ \delta_{m^2}(gaugeloops) &\sim \frac{9}{64\pi^2} g^2 \Lambda^2 \\ \delta_{m^2}(selfloops) &\sim \frac{1}{16\pi^2} \lambda^2 \Lambda^2 \,, \end{aligned} \tag{2.5}$$

thus;

$$m_H^2 = m_{tree}^2 + \delta m_{total}^2, \tag{2.6}$$

where Λ is a cutoff scale introduced to regularize the divergent loop integrals. These divergent contributions given in Eq. 2.5 do not cancel each other at a single scale for Λ.

The theoretical bounds on Higgs mass depends on vacuum stability; meaning that the Higgs potential should have the Mexican hat shape in order the get symmetry breaking and triviality; to avoid infinities, the bare Higgs mass should not be too large. The recent experimental data also constraints the Higgs mass[47, 55]. The current bounds on the Higgs mass are given in Fig. 2.2. The yellow region in Fig. 2.2 indicates considering both theoretical and experimental limits m_H is valid up to Planck scale with severe fine tuning.

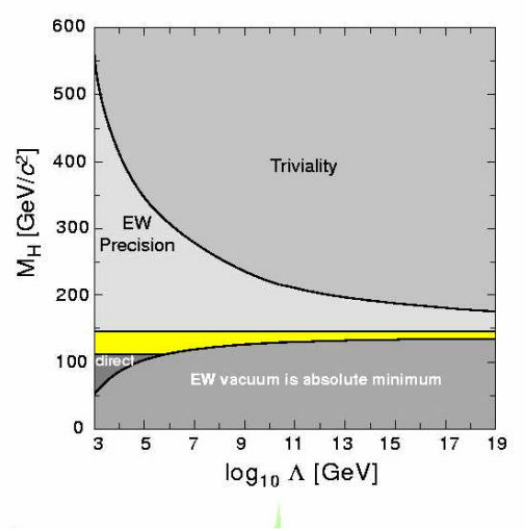

Figure 2.2: The current theoretical and experimental bounds on Higgs mass[48].

CHAPTER 3

LITTLE HIGGS MODELS

A possible solution to the hierarchy problem is the little Higgs models. In the little Higgs models collective symmetry breaking mechanism is used to stabilize Higgs mass. In symmetry breaking mechanism, an enlarged global symmetry with extra gauged subgroups is broken at a scale higher than EWSB scale.

In this chapter, the littlest Higgs model, one of the little Higgs models, is reviewed.

3.1 The Littlest Higgs Model

The littlest Higgs model has a global symmetry $SU(5)$ and a locally gauged symmetry $(SU(2)\otimes U(1))^2$[1]. At an energy scale $f \sim 1TeV$ by nonlinear sigma model[8], $SU(5)$ is broken to subgroup $SO(5)$ spontaneously. This leaves $14(= 24 - 10)$ broken generators thus 14 Goldstone bosons, denoted by $\Pi^a(x)$ $(a = 1, 2, ..., 14)$. The pion matrix (alteratively Goldstone boson matrix)is defined as

$$\Pi(x) = \sum_{a=1}^{14} \Pi^a(x) X^a \tag{3.1}$$

where X^a are broken generators of $SU(5)$. Vacuum bases can be chosen such that

$$\Sigma_0 = \begin{pmatrix} 0 & 0 & \mathbb{1} \\ 0 & 1 & 0 \\ \mathbb{1} & 0 & 0 \end{pmatrix}, \tag{3.2}$$

and the Σ field is defined as

$$\Sigma(x) \;=\; e^{i\Pi/f}\Sigma_0 e^{i\Pi/f} \;=\; e^{2i\Pi/f}\Sigma_0. \tag{3.3}$$

Effective theory can be written by expanding the Σ field around its vacuum expectation value Σ_0, such as,

$$\Sigma = \Sigma_0 + \frac{2i}{f}\Sigma_0\Pi - \frac{1}{f^2}\Pi^\dagger\Sigma_0\Pi + O(\frac{1}{f^2}). \tag{3.4}$$

Then the leading term of the effective Lagrangian is the so called kinetic term:

$$\mathcal{L}_\Sigma = \frac{f^2}{8}\mathrm{Tr}|\mathcal{D}_\mu\Sigma|^2. \tag{3.5}$$

The covariant derivative here is defined by the gauged subgroup $[SU(2)_1 \otimes U(1)_1]\otimes[SU(2)_2 \otimes U(1)_2]$ of $SU(5)$, such as:

$$\mathcal{D}_\mu\Sigma = \partial_\mu\Sigma - i\sum_{j=1}^{2}\left(g_j(W_j\Sigma + \Sigma W_j^T) + g'_j(B_j\Sigma + \Sigma B_j^T)\right), \tag{3.6}$$

where B_i and W_i are the gauge fields and g'_i and g_i are the corresponding couplings of $U(1)_i$ and $SU(2)_i$ respectively. The gauge fields of $U(1)_i$ are given as

$$B_{1(2)} = B_{\mu,1(2)}Y_{1(2)}, \tag{3.7}$$

where Y_i is the generator of B_i, and given as

$$\begin{aligned} Y_1 &= \frac{1}{10}diag(-3,-3,2,2,2) \\ Y_2 &= \frac{1}{10}diag(-2,-2,-2,3,3). \end{aligned} \tag{3.8}$$

The gauge fields of $SU(2)_i$ are given as

$$W_{1(2)} = \sum_{a=1}^{3} W^a_{\mu,1(2)}Q^a_{1(2)}, \tag{3.9}$$

where the generators Q^a_i are given as

$$Q^a_1 = \begin{pmatrix} \frac{\sigma^a}{2} & 0 \\ 0 & 0 \end{pmatrix}, \qquad Q^a_2 = \begin{pmatrix} 0 & 0 \\ 0 & -\frac{\sigma^{*a}}{2} \end{pmatrix}, \tag{3.10}$$

with σ^a being the usual Pauli matrices. The VEV of Σ field in the Lagrangian breaks $(SU(2)\otimes U(1))^2$ symmetry to diagonal subgroup $(SU(2)\otimes U(1))$ of SM, and the unbroken generators are

$$Q^{a\prime} = \frac{1}{\sqrt{2}}(Q_1^a + Q_2^a), \qquad Y = Y_1 + Y_2. \tag{3.11}$$

In this process four of the Goldstone bosons are eaten by gauge bosons, and new vectors gain mass with mass eigenstates

$$\begin{aligned} W &= sW_1 + cW_2, \\ W' &= -cW_1 + sW_2, \\ B &= s'B_1 + c'B_2, \\ B' &= -c'B_1 + s'B_2, \end{aligned} \tag{3.12}$$

and the masses

$$M_{W'} = \frac{g}{2sc} f \ , \qquad M_{B'} = \frac{g'}{2\sqrt{5}s'c'} f \ , \tag{3.13}$$

where s, s'[1] are the mixing angles such as

$$s = \frac{g_2}{\sqrt{g_1^2 + g_2^2}} \ , \qquad s' = \frac{g_2'}{\sqrt{g_1'^2 + g_2'^2}} \ . \tag{3.14}$$

The remaining Goldstone bosons forming the scalar field content consist of a doublet h and a triplet ϕ

$$h = \begin{pmatrix} h^0 \\ h^\dagger \end{pmatrix} \ , \qquad \phi = \begin{pmatrix} \phi^{++} & \frac{\phi^+}{\sqrt{2}} \\ \frac{\phi^+}{\sqrt{2}} & \phi^0 \end{pmatrix} \ . \tag{3.15}$$

In littlest Higgs model, SM fermions have $SU(2)_1$ group charges but are considered to be singlets under $SU(2)_2$. Also they are charged under $U(1)_1$ and $U(1)_2$, and their charges are assigned such as diagonal $U(1)$ group matches SM hypercharge, thus

[1] In this work $s(s')$ will denote the $\sin\theta(\theta')$ of the mixing angle $\theta(\theta')$, and c will be the *cosine*.

$$Y_1 = xY \ , \ \ Y_2 = (1-x)Y \ , \tag{3.16}$$

where Y is the SM hypercharge. In this work, x is chosen to be $\frac{3}{5}$.

In general fermion scalar interactions are written such that Yukawa Lagrangian is invariant under $[SU(2)_1 \otimes U(1)_1] \otimes [SU(2)_2 \otimes U(1)_2]$ with fermions carrying both $U(1)$ and $U(2)$ hypercharge, such as:

$$\begin{aligned} \mathcal{L}_Y &= \frac{\lambda_u f}{2} \epsilon_{ijk} \epsilon_{mn} \chi_i \Sigma_{jm} \Sigma_{kn} u^c \\ &+ \frac{\lambda_d f}{2} \epsilon_{ijk} \epsilon_{mn} \chi_i \Sigma^*_{jm} \Sigma^*_{kn} d^c, \end{aligned} \tag{3.17}$$

where u is the upper and d is the lower components of lepton doublet, with $i, j, k = 1, 2, 3$ and $m, n = 4, 5$.

From this Yukawa Lagrangian top quark coupling to Higgs boson results in a quadratic divergence in M_H. To cancel out this divergence a new set of fermion singlets u_R and u_L are introduced to model. u_R and u_L have quantum numbers assigned as $(3, 1)_{Y_i}$, $(3, 1)_{-Y_i}$, allowing them to have bare mass term.

The extra terms of Yukawa Lagrangian preserving $[SU(2)_1 \otimes U(1)_1] \otimes [SU(2)_2 \otimes U(1)_2]$ symmetry can be written as [1];

$$-\frac{\lambda_1 f}{2} \epsilon_{ijk} \epsilon_{mn} \chi_i \Sigma_{jm} \Sigma_{kn} u_{3R} - \lambda_2 f u^\dagger_L u_R, \tag{3.18}$$

where $i, j, k = 1, 2, 3$ and $m, n = 4, 5$, u_{3R} is the third generation singlet and λ_1 and λ_2 are arbitrary couplings at this stage.

In the littlest Higgs model, one can also add lepton number violating terms to Yukawa Lagrangian. At low energies $\mathcal{L}_Y$ does not have to preserve full gauge symmetry so the terms that are invariant under SM $SU(2) \otimes U(1)$ symmetry can be added to Lagrangian such as a Majorano type mass term [41, 40];

$$\mathcal{L}_{LFV} = i Y_{ij} L_i^T \ \phi \, C^{-1} L_j + \text{h.c.}, \tag{3.19}$$

where L_i are the lepton doublets $\begin{pmatrix} \nu_l \\ l \end{pmatrix}$.

For top quark $[SU(2)_1 \otimes U(1)_1] \otimes [SU(2)_2 \otimes U(1)_2]$ symmetry should be preserved for this kind of term since the interactions between scalars and the top quark result in divergent contributions to Higgs mass. For the third generation of quarks, the lepton number violating term can be written as;

$$\mathcal{L}_{LFV} = Y_{ij} f \epsilon^{\alpha\beta} \epsilon^{\gamma\sigma} \left(L_i^T\right)_\alpha \Sigma^*_{\beta\gamma} C^{-1} \left(L_j\right)_\sigma + \text{h.c.}, \tag{3.20}$$

where $\alpha, \beta = 1, 2$. This term in the Lagrangian violates the lepton number for the third generation of quarks by 2.

Higgs potential to trigger EWSB can be written by Weinberg-Coleman method[49]. The Weinberg-Coleman potential includes terms generated by gauge bosons and fermions at one loop level, and is parameterized as,

$$\begin{aligned} V_{CW} &= \lambda_{\phi^2} f^2 \text{Tr}(\phi^\dagger \phi) + i\lambda_{h\phi h} f (H\phi^\dagger H^T - H^* \phi H^\dagger) \\ &\quad -\mu^2 H H^\dagger + \lambda_{h^4} (H H^\dagger)^2 \\ &\quad +\lambda_{h\phi\phi h} H\phi^\dagger \phi H^\dagger + \lambda_{h^2\phi^2} H H^\dagger \text{Tr}(\phi^\dagger \phi) + \lambda_{\phi^2\phi^2} [\text{Tr}(\phi^\dagger \phi)]^2 \\ &\quad +\lambda_{\phi^4} \text{Tr}(\phi^\dagger \phi \phi^\dagger \phi), \end{aligned} \tag{3.21}$$

where the coefficients λ_{ϕ^2}, λ_{ϕ^4}, $\lambda_{\phi^2\phi^2}$, $\lambda_{h\phi\phi h}$, $\lambda_{h\phi h}$ and λ_{h^4} in equation 3.21 are given by

$$\begin{aligned} \lambda_{\phi^2} &= \frac{a}{2}\left[\frac{g^2}{s^2c^2} + \frac{g'^2}{s'^2c'^2}\right] + 8a'\lambda_1^2, \\ \lambda_{h\phi h} &= -\frac{a}{4}\left[g^2\frac{(c^2 - s^2)}{s^2c^2} + g'^2\frac{(c'^2 - s'^2)}{s'^2c'^2}\right] + 4a'\lambda_1^2, \\ \lambda_{h^4} &= \frac{a}{8}\left[\frac{g^2}{s^2c^2} + \frac{g'^2}{s'^2c'^2}\right] + 2a'\lambda_1^2 = \frac{1}{4}\lambda_{\phi^2}, \\ \lambda_{h\phi\phi h} &= \frac{-3}{4}\lambda_{\phi^2}, \\ \lambda_{\phi^2\phi^2} &= -16a'\lambda_1^2, \\ \lambda_{\phi^4} &= \frac{2a}{3}\left(\frac{g^2}{s^2c^2} + \frac{g'^2}{s'^2c'^2}\right) + \frac{16a'}{3}\lambda_1^2. \end{aligned} \tag{3.22}$$

If the loop contributions to lepton number violating term $\mathcal{L}_{LFV}$ are considered in Coleman Weinberg potential, λ_{ϕ^2} receives a correction term such that, it becomes:

$$\lambda_{\phi^2} = \frac{a}{2}\left[\frac{g^2}{s^2c^2} + \frac{g'^2}{s'^2c'^2}\right] + 8a'\lambda_1^2 + a''Tr(Y^\dagger), \tag{3.23}$$

where a and a' are parameters of Coleman Weinberg potential depending on ultraviolet completion of the model. For $\mu^2 > 0$, EWSB is triggered and h and ϕ fields acquire vacuum expectation values: $\langle h^0\rangle = v/\sqrt{2}$ and $\langle i\phi^0\rangle = v'$, with

$$v^2 = \frac{\mu^2}{\lambda_{h^4} - \lambda_{h\phi h}^2/\lambda_{\phi^2}}, \qquad v' = \frac{\lambda_{h\phi h}}{2\lambda_{\phi^2}}\frac{v^2}{f}. \tag{3.24}$$

Diagonalizing the mass matrices for scalar fields mass eigenstates; i.e. physical states, of scalar bosons are found:

$$\begin{aligned}
h^0 &= \left(c_0 H_m - s_0\phi_m^0 + v\right)/\sqrt{2} + i\left(c_P G^0 - s_P\phi_m^P\right)/\sqrt{2},\\
\phi^0 &= \left(s_P G^0 + c_P\phi_m^P\right)/\sqrt{2} - i\left(s_0 H_m + c_0\phi_m^0 + \sqrt{2}v'\right)/\sqrt{2},\\
h^+ &= c_+ G^+ - s_+\phi_m^+, \qquad \phi^+ = \left(s_+ G^+ + c_+\phi_m^+\right)/i\\
\phi^{++} &= \phi_m^{++}/i.
\end{aligned} \tag{3.25}$$

Physical states are these mass eigenstates consisting of the SM Higgs scalar H_m, and new neutral scalar ϕ_m^0 and neutral pseudo scalar ϕ_m^P, a single charged scalar ϕ_m^+ and a double charged scalar ϕ_m^{++}[2]. The G^+ and G^0 are the Goldstone bosons, and will be eaten by SM vector bosons Z_L and W_L (it is reviewed in detail in [5, 6, 9]).

The scalar mixing angles appearing in Eq.3.25 are:

$$\begin{aligned}
s_P &= \frac{2\sqrt{2}v'}{\sqrt{v^2 + 8v'^2}} \simeq 2\sqrt{2}\frac{v'}{v}\ , \qquad s_+ = \frac{2v'}{\sqrt{v^2 + 4v'^2}} \simeq 2\frac{v'}{v}\\
s_0 &\simeq 2\sqrt{2}\frac{v'}{v}.
\end{aligned} \tag{3.26}$$

The masses of scalars H and ϕ are:

[2] The subscript m in Eq.(3.25) is to denote that they are mass eigenstates and will not be used in the rest of this work. From now on only the physical states will be mentioned.

$$M_\phi^2 \simeq \lambda_{\phi^2} f^2, \qquad M_H^2 \simeq 2\left(\lambda_{h^4} - \lambda_{h\phi h}^2/\lambda_{\phi^2}\right)v^2 = 2\mu^2, \tag{3.27}$$

where M_ϕ is the common mass of ϕ^0, ϕ^P, $\phi^+$and ϕ^{++}.

After EWSB, vector bosons get extra mixing due to vacuum expectation values of h doublet and ϕ triplet. Again by diagonalizing the mass matrices, final states of vector bosons are expressed as:

$$\begin{aligned}
W_L &= W + \frac{v^2}{2f^2} sc(c^2 - s^2)W', \\
W_H &= W' - \frac{v^2}{2f^2} sc(c^2 - s^2)W, \\
A_L &= s_{\rm w} W^3 + c_{\rm w} B, \\
Z_L &= c_{\rm w} W^3 - s_{\rm w} B + x_Z^{W'} \frac{v^2}{f^2} W'^3 + x_Z^{B'} \frac{v^2}{f^2} B', \\
A_H &= B' + x_H \frac{v^2}{f^2} W'^3 - x_Z^{B'} \frac{v^2}{f^2}(c_{\rm w} W^3 - s_{\rm w} B), \\
Z_H &= W'^3 - x_H \frac{v^2}{f^2} B' - x_Z^{W'} \frac{v^2}{f^2}(c_{\rm w} W^3 - s_{\rm w} B),
\end{aligned} \tag{3.28}$$

where

$$\begin{aligned}
x_H &= \frac{5}{2} g' \frac{sc s' c'(c^2 s'^2 + s^2 c'^2)}{(5g^2 s'^2 c'^2 - g'^2 s^2 c^2)}, \\
x_Z^{W'} &= -\frac{1}{2c_{\rm w}} sc(c^2 - s^2), \qquad x_Z^{B'} = -\frac{5}{2s_{\rm w}} s' c'(c'^2 - s'^2).
\end{aligned} \tag{3.29}$$

And their masses are given to the order of $\frac{v^2}{f^2}$:

$$\begin{aligned}
M_{W_L^\pm}^2 &= m_w^2 \left[1 - \frac{v^2}{f^2}\left(\frac{1}{6} + \frac{1}{4}(c^2 - s^2)^2\right) + 4\frac{v'^2}{v^2}\right], \\
M_{W_H^\pm}^2 &= \frac{f^2 g^2}{4s^2 c^2} - \frac{1}{4} g^2 v^2 + O(v^4/f^2) = m_w^2 \left(\frac{f^2}{s^2 c^2 v^2} - 1\right), \\
M_{A_L}^2 &= 0, \\
M_{Z_L}^2 &= m_z^2 \left[1 - \frac{v^2}{f^2}\left(\frac{1}{6} + \frac{1}{4}(c^2 - s^2)^2 + \frac{5}{4}(c'^2 - s'^2)^2\right) + 8\frac{v'^2}{v^2}\right], \\
M_{A_H}^2 &= \frac{f^2 g'^2}{20 s'^2 c'^2} - \frac{1}{4} g'^2 v^2 + g^2 v^2 \frac{x_H}{4s^2 c^2} = m_z^2 s_{\rm w}^2 \left(\frac{f^2}{5 s'^2 c'^2 v^2} - 1 + \frac{x_H c_{\rm w}^2}{4 s^2 c^2 s_{\rm w}^2}\right), \\
M_{Z_H}^2 &= \frac{f^2 g^2}{4s^2 c^2} - \frac{1}{4} g^2 v^2 - g'^2 v^2 \frac{x_H}{4 s'^2 c'^2} = m_w^2 \left(\frac{f^2}{s^2 c^2 v^2} - 1 - \frac{x_H s_{\rm w}^2}{s'^2 c'^2 c_{\rm w}^2}\right),
\end{aligned} \tag{3.30}$$

where $m_w \equiv gv/2$ and $m_z \equiv gv/(2c_{\rm w})$. In these equations $s_{\rm w}$ and $c_{\rm w}$ are the usual weak mixing angles:

$$s_{\rm w} = \frac{g'}{\sqrt{g^2+g'^2}}, \qquad c_{\rm w} = \frac{g}{\sqrt{g^2+g'^2}}, \tag{3.31}$$

and s and s' are given in Eq. 3.14.

As a result of EWSB, fermions gain their masses. For top quark and new singlets of littlest Higgs model, by expanding the Σ matrix and diagonalizing the mass matrix, physical states and corresponding masses for top quark and the new fermion called T quark can be found as:

$$\begin{aligned} t_L &= c_L t_3 - s_L \tilde{t}, \qquad & t_R^c &= c_R u_3'^c - s_R \tilde{t}'^c, \\ T_L &= s_L t_3 + c_L \tilde{t}, \qquad & T_R^c &= s_R u_3^{\tilde{c}} + c_R \tilde{t}'^c, \end{aligned} \tag{3.32}$$

where the quark mixing angles are

$$\begin{aligned} s_R &= \frac{\lambda_1}{\sqrt{\lambda_1^2+\lambda_2^2}}\left[1-\frac{v^2}{f^2}\frac{\lambda_2^2}{\lambda_1^2+\lambda_2^2}\left(\frac{1}{2}+\frac{\lambda_1^2}{\lambda_1^2+\lambda_2^2}\right)\right], \\ c_R &= \frac{\lambda_2}{\sqrt{\lambda_1^2+\lambda_2^2}}\left[1+\frac{v^2}{f^2}\frac{\lambda_1^2}{\lambda_1^2+\lambda_2^2}\left(\frac{1}{2}+\frac{\lambda_1^2}{\lambda_1^2+\lambda_2^2}\right)\right], \\ s_L &= -i\frac{\lambda_1^2}{\lambda_1^2+\lambda_2^2}\frac{v}{f}\left[1-\frac{v^2}{f^2}\left(\frac{5}{6}-\frac{fv'}{v^2}-\frac{1}{2}\frac{\lambda_1^4}{(\lambda_1^2+\lambda_2^2)^2}\right)\right], \\ c_L &= 1-\frac{v^2}{2f^2}\frac{\lambda_1^4}{(\lambda_1^2+\lambda_2^2)^2}. \end{aligned} \tag{3.33}$$

The corresponding masses are:

$$\begin{aligned} m_t &= \frac{i\lambda_1\lambda_2}{\sqrt{\lambda_1^2+\lambda_2^2}}v\left\{1+\frac{v^2}{f^2}\left[-\frac{1}{3}+\frac{fv'}{v^2}+\frac{1}{2}\frac{\lambda_1^2}{\lambda_1^2+\lambda_2^2}\left(1-\frac{\lambda_1^2}{\lambda_1^2+\lambda_2^2}\right)\right]\right\}, \\ M_T &= -f\sqrt{\lambda_1^2+\lambda_2^2}\left[1+O(v^2/f^2)\right]. \end{aligned} \tag{3.34}$$

Since top quark mass is known in SM, the bound on the free parameters λ_1 and λ_2 can be expressed as:

$$\frac{(\lambda_1\lambda_2)^2}{(\lambda_1^2+\lambda_2^2)} \approx (\frac{v}{M_t})^2. \tag{3.35}$$

The Feynman rules for the littlest Higgs model are presented in Appendix A.

3.2 The Constraints on the Littlest Higgs Model Parameters

In the littlest Higgs model the symmetry breaking scale f, and the mixing angles s and s' are not restricted by the model. These parameters are constrained by the electroweak observables, and experimental limits from Tevatron data[11, 12, 13, 14]. Especially direct searches for a light gauge boson, takes the minimum limits on the mass of A_H up to 900GeV[11]. This results increases the limits of the symmetry breaking scale up to few TeVs, i.e. $f \geq 4$TeV, for the models in which the fermions are gauged under only one $U(1)$ subgroups. When the fermions are charged in both $U(1)$ groups, the couplings of fermions to A_H become very small and the constraints on the parameter space are relaxed[15]. In this thesis, leptons are charged under both $U(1)$ groups, with corresponding hypercharge of Y_1 and Y_2. The restriction for Y_1 and Y_2 is that $Y_1 + Y_2$ should reproduce $U(1)_Y$ hypercharge Y of SM, thus $Y_1 = xY$ and $Y_2 = (1 - x)Y$ can be written. Due to gauge invariance, x can be taken as $3/5$[6, 15].

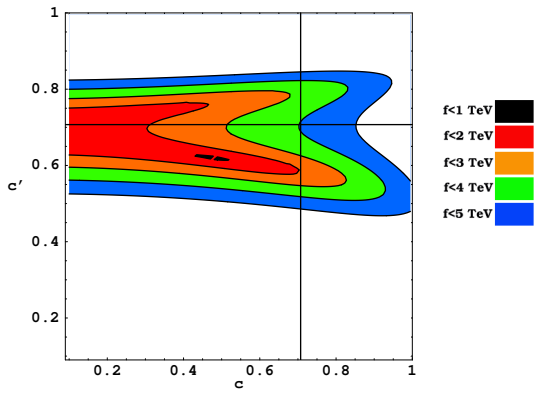

Figure 3.1: The allowed values of s/s' for various values of f[15].

The constraints on symmetry breaking scale f, and the mixing angles s and s' are plotted in Fig. 3.1. Also for the values of symmetry breaking scale f, the limits on mixing angles s and s' are given in table 3.1.

It is seen from Fig 3.1 that, when the value of symmetry breaking scale reaches is large, $f \sim 4$ TeV, the mixing angles are less constrained. But for this values of symmetry breaking scale,

Table 3.1: The limits on littlest Higgs model parameters $f/s/s'$[15].

$1TeV \leq f \leq 2TeV$	$0.75 \leq s \leq 0.99$	$0.6 \leq s' \leq 0.75$
$2TeV \leq f \leq 3TeV$	$0.6 \leq s \leq 0.99$	$0.6 \leq s' \leq 0.8$
$3TeV \leq f \leq 4TeV$	$0.4 \leq s \leq 0.99$	$0.6 \leq s' \leq 0.85$
$f \geq 4TeV$	$0.15 \leq s \leq 0.99$	$0.4 \leq s' \leq 0.9$

the Higgs boson mass within the littlest Higgs model needs to be fine tuned, thus the model goes out of its purpose.

3.3 Littlest Higgs Model with T Parity

The littlest Higgs model with T parity(LHT) is introduced to solve the requirement of high symmetry breaking scale of the original littlest Higgs model[50, 51, 52]. As mentioned in section 3.2, the littlest Higgs model is out favored by electroweak constraints and the recent experimental data when fermions are gauged under only one $U(1)$ subgroup. The phenomenology of the LHT model is reviewed in [53, 54]. In this section the littlest Higgs model with T parity is summarized following reference [5].

The T parity act on the pion matrix given in Eq. 3.1, such as;

$$T : \Pi \rightarrow -\Omega\Pi\Omega \tag{3.36}$$

where $\Omega = \text{diag}(1, 1, -1, 1, 1)$. This transformation law ensures that $SU(2)_L$ triplet ϕ is odd under T parity, where the Higgs doublet H is T even .

In the gauge sector of the model, T parity acts as an automorphism that exchanges $[SU(2) \otimes U(1)]_1$ and $[SU(2) \otimes U(1)]_2$, thus the kinetic Lagrangian in Eq. 3.5 is only invariant if $g_1 = g_2$ and $g'_1 = g'_2$. In this case, following the same manner of the littlest Higgs model without T parity, the mass eigenstates are found to be;

$$W_{\pm} = \frac{W_1 \pm W_2}{\sqrt{2}}, \quad B_{\pm} = \frac{B_1 \pm B_2}{\sqrt{2}}, \tag{3.37}$$

where W_+ and B_+ are the standard model gauge bosons and are T-even, whereas W_- and B_-

are the additional, heavy, T-odd states. After EWSB, the T-even states W_+ and B_+ mix to produce the SM Z an W and the photon.

In the fermion sector all SM model fermions other than top quark are T even. Thus introducing T parity automatically eliminates the tree level electroweak precision constraints.

CHAPTER 4

THEORETICAL FRAMEWORK

The littlest Higgs model with global symmetry $SU(5)$ and extra gauged subgroups $[SU(2)_1 \otimes U(1)_1] \otimes [SU(2)_2 \otimes U(1)_2]$, as a consequence of collective symmetry breaking, has extra charged and neutral scalar gauge bosons, charged and neutral vector gauge bosons and a neutral pseudo scalar, compared to standard model. In the littlest Higgs model, an extra quark like fermion is also introduced. These new particles have interactions between themselves and also interact with SM particles. Due to existence of vacuum expectation value of new scalars (v'), existing interaction vertices of SM also receive corrections. In this chapter the masses of the necessary particles , their decay widths and the necessary Feynman rules for calculating differential cross sections and cross sections of Z_L associated production of scalars in littlest Higgs model at e^+e^- interactions are presented.

In this thesis, the couplings between e^+e^- and neutral vector bosons are necessary for all processes. The couplings of fermions with gauge bosons are written as $i\gamma_\mu(g_{V_i} + g_{A_i}\gamma_5)$ where $i = 1, 2, 3$ corresponds to Z_L, Z_H and A_H respectively. These couplings are given in table 4.1, where $x_Z^{W'}$ and $x_Z^{B'}$ are given in Eq. 3.29, and $y_e = \frac{3}{5}$.

It is seen from table 4.1 that vector and axial vector couplings of SM $Z_L e^+e^-$ vertex gets contributions from littlest Higgs model. As a result total decay widths of SM vector bosons, receive corrections of the order $\frac{v^2}{f^2}$, which are written as; $\Gamma(V_i \rightarrow f\bar{f}) = \frac{N}{24\pi}(g_V^2 + g_A^2)M_{V_i}$ where $N = 3$ for quarks, and $N = 1$ for leptons.

In this thesis, decay widths of new vectors and scalars are also needed, because they contribute

Table 4.1: The vector and axial vector couplings of e^+e^- with vector bosons. Feynman rules for $e^+e^-V_i$ vertices are given as $i\gamma_\mu(g_{V_i} + g_{A_i}\gamma_5)$.

i	vertices	g_{V_i}	g_{A_i}
1	$e^+e^-Z_L$	$-\frac{g}{2c_\mathrm{w}}\left\{(-\frac{1}{2}+2s_\mathrm{w}^2)\right.$ $-\frac{v^2}{f^2}\left[-c_\mathrm{w}x_Z^{W'}c/2s\right.$ $\left.\left.+\frac{s_\mathrm{w}x_Z^{B'}}{s'c'}\left(2y_e-\frac{9}{5}+\frac{3}{2}c'^2\right)\right]\right\}$	$-\frac{g}{2c_\mathrm{w}}\left\{\frac{1}{2}-\frac{v^2}{f^2}\left[c_\mathrm{w}x_Z^{W'}c/2s\right.\right.$ $\left.\left.+\frac{s_\mathrm{w}x_Z^{B'}}{s'c'}\left(-\frac{1}{5}+\frac{1}{2}c'^2\right)\right]\right\}$
2	$e^+e^-Z_H$	$-gc/4s$	$gc/4s$
3	$e^+e^-A_H$	$\frac{g'}{2s'c'}\left(2y_e-\frac{9}{5}+\frac{3}{2}c'^2\right)$	$\frac{g'}{2s'c'}\left(-\frac{1}{5}+\frac{1}{2}c'^2\right)$

to the production processes. The lightest new vector boson in littlest Higgs model is the so called heavy photon A_H. The heavy photon decays to leptons and to hadrons and also to Z_LH. Total decay width of heavy photon is given as [22]:

$$\begin{aligned}
\Gamma_{A_H} &= 3\Gamma(A_H\to\bar{l}l)+3\Gamma(A_H\to\overline{\nu}\nu)+3\Gamma(A_H\to\overline{d}d)\\
&\quad +2\Gamma(A_H\to\overline{u}u)+\Gamma(A_H\to\overline{t}t)+\Gamma(A_H\to Z_LH)\\
&\approx \frac{\alpha_e M_{A_H}}{4c_W^2}\{\frac{85(c'^2-\frac{2}{5})^2}{18s'^2c'^2}+\frac{\sqrt{1-4\frac{M_t^2}{M_{A_H}^2}}}{s'^2c'^2}\{[\frac{5}{6}(\frac{2}{5}-c'^2)-\frac{1}{5}x_L]^2(1+2\frac{M_t^2}{M_{A_H}^2})\\
&\quad +[\frac{1}{2}(\frac{2}{5}-c'^2)-\frac{1}{5}x_L]^2(1-4\frac{M_t^2}{M_{A_H}^2})\}\\
&\quad +\frac{(c'^2-s'^2)^2}{24c'^2s'^2}\lambda^{\frac{1}{2}}[(1+\frac{M_{Z_L}^2}{M_{A_H}^2}-\frac{M_H^2}{M_{A_H}^2})^2+8\frac{M_{Z_L}^2}{M_{A_H}^2}]\},
\end{aligned} \tag{4.1}$$

where $\lambda = 1+(\frac{M_{Z_L}^2}{M_{A_H}^2})^2+(\frac{M_H^2}{M_{A_H}^2})^2+2(\frac{M_{Z_L}^2}{M_{A_H}^2})+2(\frac{M_H^2}{M_{A_H}^2})+2(\frac{M_{Z_L}^2}{M_{A_H}^2})(\frac{M_H^2}{M_{A_H}^2})$, and $x_L=\lambda_1^2/(\lambda_1^2+\lambda_2^2)$ is the t - T mixing parameter, in which λ_1 and λ_2 are the couplings of the Yukawa Lagrangian 3.18.

The second neutral vector boson named as Z_H in the littlest Higgs model decays to leptons and hadrons and also to Z_LH and $W_L^+W_L^-$. Total decay width of Z_H is given by [22]:

$$\begin{aligned}\Gamma_{Z_H} &= 6\Gamma(Z_H \to \overline{q}q) + 6\Gamma(Z_H \to \bar{l}l) + \Gamma(Z_H \to Z_L H) + \Gamma(Z_H \to W^+W^-) \\ &\approx \frac{g^2(193 - 388s^2 + 196s^4)}{768\pi s^2(s^2-1)} M_{Z_L}. \end{aligned} \tag{4.2}$$

Finally the charged heavy vector $W_H^{\pm}$ decays to leptons and hadrons and also to $W_L^{\pm}H$ and $W_L^{\pm}Z_L$. The total width of the W_H is calculated as:

$$\begin{aligned}\Gamma_{W_H} &= 3\Gamma(W_H^{\pm} \to l^{\pm}\nu) + 3\Gamma(W_H^{\pm} \to \bar{q'}q) + \Gamma(W_H^{\pm} \to W_L^{\pm}H) + \Gamma(W_H^{\pm} \to W_L^{\pm}Z_L) \\ &\approx \frac{g^2(97 - 196s^2 + 100s^4)}{384\pi s^2(s^2-1)} M_{W_H}. \end{aligned} \tag{4.3}$$

The decay widths of heavy vectors for the relevant values of littlest Higgs model parameter set are presented in table 4.3.

The new scalars and pseudo scalars also contribute to the analysis done in this study. Their decay modes and decay widths are studied in [40] in detail. Since these new scalars have lepton number and flavor violating decay modes, their total widths will depend on the Yukawa couplings Y_{ij}. The decay width of ϕ^{++} is given as:

$$\begin{aligned}\Gamma_{\phi^{++}} &= \Gamma(\phi^{++} \to W_L^+W_L^+) + 3\Gamma(\phi^{++} \to \ell_i^+\ell_j^+(i=j) + 3\Gamma(\phi^{++} \to \ell_i^+\ell_j^+(i \neq j)) \\ &\approx \frac{v'^2 M_\phi^3}{2\pi v^4} + \frac{3}{8\pi}|Y|^2 M_\phi + \frac{3}{4\pi}|Y'|^2 M_\phi \end{aligned} \tag{4.4}$$

For the single charged scalar, the decay width is given by:

$$\begin{aligned}\Gamma_{\phi^+} &= 3\Gamma(\phi^+ \to \ell_i^+\bar{\nu}_j(i=j)) + 6\Gamma(\phi^+ \to \ell_i^+\bar{\nu}_j(i \neq j)) \\ &+ \Gamma(\phi^+ \to W_L^+H) + \Gamma(\phi^+ \to W_L^+Z_L) + \Gamma(\phi^+ \to t\bar{b}) + \Gamma(\phi^+ \to T\bar{b}) \\ &\approx \frac{N_c M_t^2 M_\phi}{32\pi f^2} \\ &\quad + \frac{v'^2 M_\phi^3}{2\pi v^4} + \frac{3}{8\pi}|Y|^2 M_\phi + \frac{3}{4\pi}|Y'|^2 M_\phi. \end{aligned} \tag{4.5}$$

For the neutral scalar ϕ^0, the total decay width is given by:

$$
\begin{aligned}
\Gamma_{\phi^0} &= 3\Gamma(\phi^0 \to \nu_i\nu_j + \bar{\nu}_i\bar{\nu}_j(i=j)) + 3\Gamma(\phi^0 \to \nu_i\nu_j + \bar{\nu}_i\bar{\nu}_j(i\neq j)) \\
&+ \Gamma(\phi^0 \to HH) + \Gamma(\phi^0 \to Z_L Z_L) + \Gamma(\phi^0 \to t\bar{t}) \\
&+ \Gamma(\phi^0 \to b\bar{b}) + \Gamma(\phi^0 \to T\bar{t} + t\bar{T}) \\
&\approx \frac{N_c M_\phi}{32\pi f^2}(M_b^2 + M_t^2) \\
&\quad + \frac{v'^2 M_\phi^3}{2\pi v^4} + \frac{3}{8\pi}|Y|^2 M_\phi + \frac{3}{4\pi}|Y'|^2 M_\phi. \qquad (4.6)
\end{aligned}
$$

For the pseudoscalar ϕ^P, the total decay width is given by:

$$
\begin{aligned}
\Gamma_{\phi^P} &= 3\Gamma(\phi^P \to \nu_i\nu_j + \bar{\nu}_i\bar{\nu}_j(i=j)) + 3\Gamma(\phi^P \to \nu_i\nu_j + \bar{\nu}_i\bar{\nu}_j(i\neq j)) \\
&+ \Gamma(\phi^P \to Z_L H) + \Gamma(\phi^P \to t\bar{t}) \\
&+ \Gamma(\phi^P \to b\bar{b}) + \Gamma(\phi^P \to T\bar{t} + t\bar{T}) \\
&\approx \frac{N_c M_\phi}{32\pi f^2}(M_b^2 + M_t^2) \\
&\quad + \frac{v'^2 M_\phi^3}{2\pi v^4} + \frac{3}{8\pi}|Y|^2 M_\phi + \frac{3}{4\pi}|Y'|^2 M_\phi. \qquad (4.7)
\end{aligned}
$$

It is seen from the decay widths of the scalars that lepton number violation is proportional to $|Y|^2$ if the final state leptons are from the same family and to $|Y'|^2$ for final state leptons are from different generations . The branching ratios of scalars decaying to same family of leptons is denoted as $BR[Y]$ and to leptons of different flavor as $BR[Y']$.

The values of Yukawa couplings Y and Y' are restricted by the current constraints on the neutrino masses[44], given as; $M_{ij} = Y_{ij}v' \simeq 10^{-10}GeV$. Since the vacuum expectation value v' has only an upper bound in order to get symmetry breaking (Eq. 3.24); $v' < 1GeV$, Y_{ij} can be taken up to order of unity without making v' unnaturally small. In this work the values of the Yukawa mixings are taken to be $10^{-4} \leq Y, Y' \leq 1$, and the vacuum expectation value $1GeV > v' > 1eV$.

The branching ratios of scalars to final state lepton number violating modes are plotted in figure 4.1 with respect to Yukawa couplings Y, Y'.

In this thesis the differential and total cross sections are calculated for the production processes. The masses of new heavy bosons for the various values of littlest Higgs parameters are presented in table 4.2. The double differential cross section is given by:

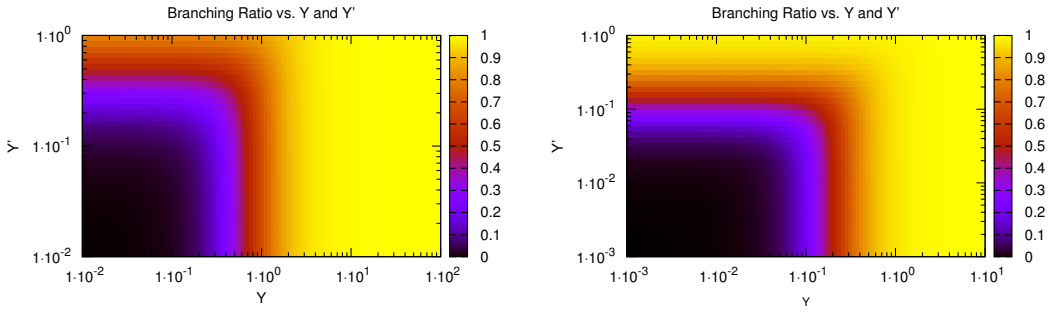

Figure 4.1: The Branching Ratio of scalars into leptons plotted with respect to Yukawa couplings in the range $10^{-2} < Y < 10^2$ and $10^{-2} < Y' < 1$ for $f = 1TeV$ (left) and $f = 2460GeV$ (right).

$$\frac{d\sigma}{dE_Z d\cos\theta_Z} = \frac{|M|^2 E_Z}{128\pi^3 S}, \tag{4.8}$$

where M is the sum of the all amplitudes of the corresponding sub processes for the considered process and S is the center of mass energy[1]. The numerical calculation of total and differential cross sections are performed using `CalcHep` [56] after implementing all necessary vertices. In performing the numerical calculations, we take the electromagnetic coupling constant $e = \sqrt{4\pi\alpha} = 0.092$, the Higgs mass $M_H = 120GeV$ and the mass of the SM bosons $M_{Z_L} = 91GeV$, $M_{W_L} = 80GeV$ and the SM mixing angle $s_W = 0.47$ using the recent data[55]. In the calculations, we ignored v^2/f^2 terms in the couplings, since we are not dealing with the corrections to a SM process.

[1] In literature, usually the abbreviation s is used instead of S for center of mass energy. Since the abbreviation s is used for expressing the *sine* of the mixing angle (Eq. 3.14), in this thesis, S is preferred for center of mass energy.

Table 4.2: Masses of new particles with respect to littlest Higgs parameters in GeV.

$s/s'/f(GeV)$	M_{Z_H}	M_{A_H}	M_{W_H}	M_ϕ
0.8/0.6/2460	1678	396	1678	1626
0.8/0.7/2460	1678	380	1678	1626
0.95/0.6/2460	2717	397	2717	1626
0.95/0.4/2460	2717	521	2717	1626
0.5/0.1/2460	2098	1902	1860	1626
0.8/0.6/1000	677	159	678	661
0.8/0.7/1000	678	192	679	661
0.95/0.6/1000	1101	161	1102	661
0.5/0.1/1000	1228	748	752	661

Table 4.3: Decay widths of new heavy vectors with respect to littlest Higgs parameters in GeV.

$s/s'/f(GeV)$	Γ_{Z_H}	Γ_{A_H}	Γ_{W_H}
0.8/0.6/2460	32.4	6.73	32.9
0.8/0.7/2460	32.4	3.80	32.9
0.95/0.6/2460	13.61	6.75	13.18
0.95/0.4/2460	13.67	3.78	17.2
0.5/0.1/2460	215	1817	191
0.8/0.6/1000	13.08	2.7	13.10
0.8/0.7/1000	13.06	1.8	13.18
0.95/0.6/1000	5.6	2.8	6.96
0.5/0.1/1000	126	714	77

CHAPTER 5

Z_L ASSOCIATED PRODUCTION OF SCALARS

5.1 Production of Neutral Scalars in Littlest Higgs model

The littlest Higgs model implies existence of a heavy neutral scalar, ϕ^0 and a heavy neutral pseudo scalar, ϕ^P, within SM Higgs scalar. In this section Z_L associated production of new neutral scalar and pseudo scalar are examined through processes, $e^+e^- \to Z_L\phi^0$, $e^+e^- \to Z_L\phi^0\phi^0$, $e^+e^- \to Z_L\phi^0\phi^P$ and $e^+e^- \to Z_L\phi^P\phi^P$.

5.1.1 $e^+e^- \to Z_L\phi^0$

The single production of ϕ^0 associated with Z_L is the one of the most dominant channels in electron colliders. Since ϕ^0 couples to Z_L and new neutral bosons, A_H and Z_H, this channel provides a quite deep information about the littlest Higgs model. In the final state, lepton number and flavor violating signals can be observed in colliders since ϕ^0 have decays into $\nu_i\nu_j + \bar{\nu}_j\bar{\nu}_i$ including all three generations of leptons as mentioned(equations 3.19,3.20 and 4.6). The decays of ϕ^0 into SM particles will provide final states such as $Z_LZ_LZ_L$, in which ϕ^0 can be reconstructed and observed [16, 17].

The couplings of ϕ^0 to Z_L and vectors are in the form $ig_{\mu\nu}B_i$, where $i = 1, 2, 3$ corresponds to Z_L, Z_H, A_H respectively and given in table 5.1. The Feynman diagrams contributing this process are given in figure 5.1.

The corresponding amplitude for the Feynman diagrams in figure 5.1 can be written as;

Table 5.1: The Feynman rules for $\phi^0 Z_L V_i$ vertices where μ and ν are Lorentz indices for vectors and V_i denotes Z_L, Z_H and A_H respectively for $i = 1, 2, 3$.

	vertices	$ig_{\mu\nu}B_i$
1	$\phi^0 Z_L Z_L$	$-\frac{i}{2}\frac{g^2}{c_w^2}(vs_0 - 4\sqrt{2}v')g_{\mu\nu}$
2	$\phi^0 Z_L Z_H$	$\frac{i}{2}\frac{g^2}{c_w}\frac{(c^2-s^2)}{2sc}(vs_0 - 4\sqrt{2}v')g_{\mu\nu}$
3	$\phi^0 Z_L A_H$	$\frac{i}{2}\frac{gg'}{c_w}\frac{(c'^2-s'^2)}{2s'c'}(vs_0 - 4\sqrt{2}v')g_{\mu\nu}$

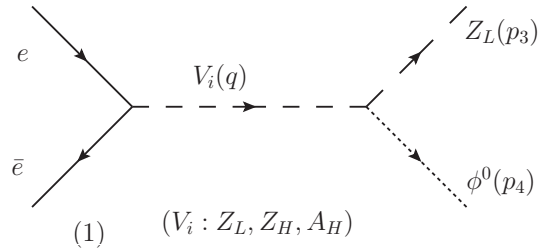

Figure 5.1: Feynman diagrams contributing to $e^+e^- \to Z_L\phi^0$ in littlest Higgs model.

$$M = \sum_{i=1}^{3} \bar{u}[-p_2]i\gamma_\mu(g_{V_i} + g_{A_i}\gamma_5)u[p_1](-i)\frac{g^{\mu\nu} - \frac{q^\mu q^\nu}{M_i^2}}{q^2 - M_i^2 + iM_i\Gamma_i}iB_i g^{\nu\alpha}\epsilon^\alpha[p_3], \tag{5.1}$$

where B_i are the vertex factors for $V_i Z_L \phi^0$ given in table 5.1.

For this process, the total cross section of the event is examined and the results are presented in figure 5.2. Value of cross section depends strongly on center of mass energy $\sqrt{S}$, as well as the free parameters of the littlest Higgs model parameters f, s, s' and mass of the Higgs boson. In this work, the mass of the Higgs boson is assumed to be $M_H = 120GeV$[55], in the range of Higgs mass constraints. Dependence of total cross section to littlest Higgs model mixing angles s, s' are presented in the bottom plot of figure 5.2. It is seen that for $s' = 0.6$, the cross section peaks at $s = 0.4$, and at $s = 0.8$ it starts to increase for lower values of s' for

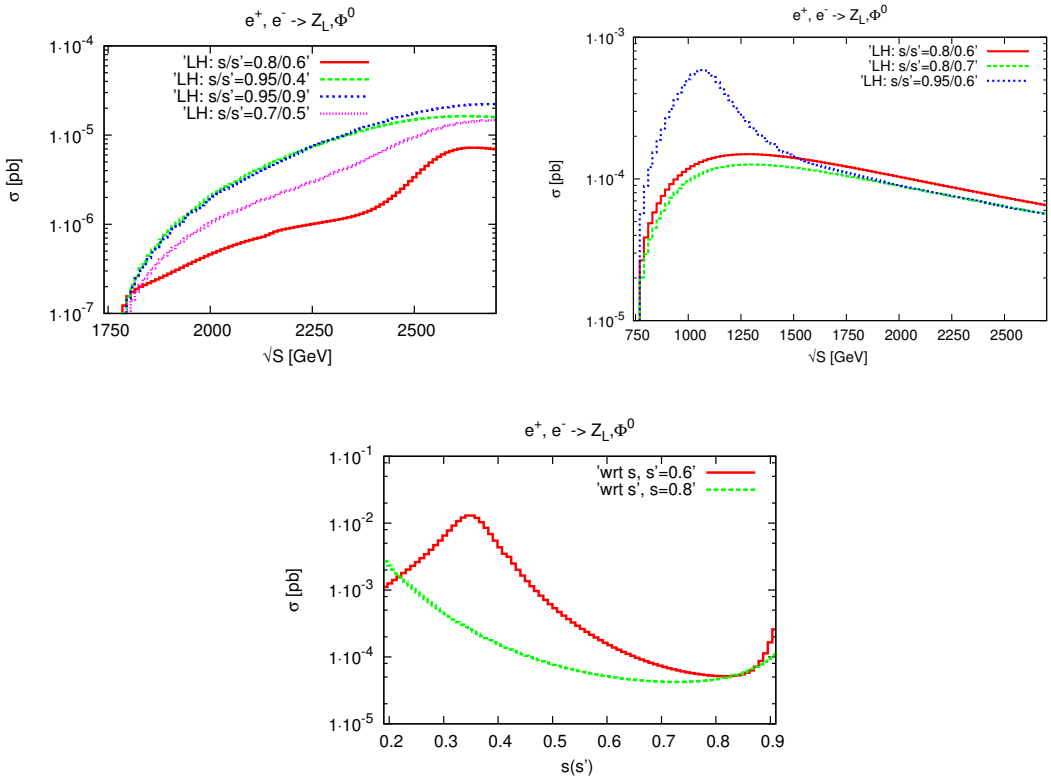

Figure 5.2: Total cross section vs. $\sqrt{S}$ graphs for $e^+e^- \rightarrow Z_L\phi^0$, for parameters $f = 2460GeV$(left-up),$f = 1000GeV$(right-up). The dependance of cross section on mixing angles $s(s')$(bottom).

$f = 2460GeV$.

The first two graphs in figure 5.2 present the total cross section vs. center of mass energy plots for different parameters $s/s' = 0.8/0.6, 0.95/0.4, 0.95/0.9, 0.7/0.5$ at $f = 2460GeV$, and for parameters $s/s' = 0.8/0.6, 0.8/0.7, 0.95/0.6$ at $f = 1000GeV$ allowed by the electroweak data. It is seen that for $f = 2460GeV$, the total cross section reaches to $10^{-5}pb$ at $\sqrt{S} = 3TeV$, which would yield one event per year at a luminosity of $100fb^{-1}$. The situation is more promising for low symmetry breaking scale $f = 1000GeV$, such that the total cross section reaches to $8.0 \times 10^{-4}pb$ for $s/s' = 0.95/0.6$ and to $10^{-4}pb$ for parameters $s/s' = 0.8/0.6, 0.8/0.7$ at $\sqrt{S} = 1TeV$. This would result in $10 \sim 100$ events per year at this channel for an integrated luminosity of $100fb^{-1}$. The peak of the cross section for parameters

$s/s' = 0.95/0.6$ appears around $\sqrt{S} = 1100GeV$ corresponding to heavy vector resonances. The resonances for the rest of the parameters are not seen since the masses of heavy vectors are the same order as the scalar mass.

The production of neutral scalar ϕ^0 via $e^+e^- \to Z_L\phi^0$ channel is possible for low values of symmetry breaking scale parameter $f \sim 1TeV$ for both ILC($\sqrt{S} = 1TeV$) and CLIC($\sqrt{S} = 3TeV$), but for higher f values this channel is not promising. The lepton number violating final states in this channel can be observed at this production process, since the branching ratio of ϕ^0 to leptons can get values up to 0.5. But the final leptonic states will be in the form $\nu_i\nu_j + \bar{\nu}_j\bar{\nu}_i$, so the final state signatures of these signals will be missing energy and experimentally not promising.

5.1.2 $e^+e^- \to Z_L\phi^0\phi^0$

The direct double production of ϕ^0 via $e^+e^- \to \phi^0\phi^0$ process is not possible in littlest Higgs model at tree level and the loop level production processes are suppressed by terms $\frac{v^3}{f^3}$. The double production of neutral heavy scalar associated with Z_L via ϕ^0 via $e^+e^- \to Z_L\phi^0\phi^0$ is examined in this section. This production channel can give contributions of four point vector scalar couplings besides three point couplings of a vectors and scalars. The Feynman rules for ϕ^0 couplings to scalars and vectors are given in tables 5.2, 5.5 and 5.3, and the Feynman diagrams contributing to this process are given in figure 5.3.

Table 5.2: The Feynman rules for four point interaction vertices between scalars and vectors. Their couplings are given in the form $iC_{ij}g_{\mu\nu}$ and $iC^P_{ij}g_{\mu\nu}$ respectively for $\phi^0\phi^0V_iV_j$ and $\phi^P\phi^PV_iV_j$, where $g_{\mu\nu}$ carries the Lorentz indices of vectors.

i/j	vertices	$iC_{ij}g_{\mu\nu}$	vertices	$iC^P_{ij}g_{\mu\nu}$
1/1	$\phi^0\phi^0Z_LZ_L$	$2i\frac{g^2}{c_w^2}g_{\mu\nu}$	$\phi^P\phi^PZ_LZ_L$	$2i\frac{g^2}{c_w^2}g_{\mu\nu}$
1/2	$\phi^0\phi^0Z_LZ_H$	$-2i\frac{g^2}{c_w}\frac{(c^2-s^2)}{2sc}g_{\mu\nu}$	$\phi^P\phi^PZ_LZ_H$	$-2i\frac{g^2}{c_w}\frac{(c^2-s^2)}{2sc}g_{\mu\nu}$
1/3	$\phi^0\phi^0Z_LA_H$	$-2i\frac{gg'}{c_w}\frac{(c'^2-s'^2)}{2s'c'}g_{\mu\nu}$	$\phi^P\phi^PZ_LA_H$	$-2i\frac{gg'}{c_w}\frac{(c'^2-s'^2)}{2s'c'}g_{\mu\nu}$

The amplitude corresponding to first diagram in figure 5.3;

Table 5.3: The Feynman rules for $\phi^0 V_i V_j$ vertices. Their couplings are given in the form $ig_{\mu\nu}B_{ij}$.

i/j	vertices	$ig_{\mu\nu}B_{ij}$
1/1	$\phi^0 Z_L Z_L$	$-\frac{i}{2}\frac{g^2}{c_w^2}(vs_0 - 4\sqrt{2}v')g_{\mu\nu}$
2/2	$\phi^0 Z_H Z_H$	$\frac{i}{2}g^2\left(vs_0 + \frac{(c^2-s^2)^2}{s^2c^2}\sqrt{2}v'\right)g_{\mu\nu}$
1/2	$\phi^0 Z_L Z_H$	$\frac{i}{2}\frac{g^2}{c_w}\frac{(c^2-s^2)}{2sc}(vs_0 - 4\sqrt{2}v')g_{\mu\nu}$
2/3	$\phi^0 Z_H A_H$	$\frac{i}{4}gg'\frac{1}{scs'c'}\left((c^2s'^2 + s^2c'^2)vs_0\right.$
1/3	$\phi^0 Z_L A_H$	$\frac{i}{2}\frac{gg'}{c_w}\frac{(c'^2-s'^2)}{2s'c'}(vs_0 - 4\sqrt{2}v')g_{\mu\nu}$
3/3	$\phi^0 A_H A_H$	$\frac{i}{2}g'^2\left(vs_0 + \frac{(c'^2-s'^2)^2}{s'^2c'^2}\sqrt{2}v'\right)g_{\mu\nu}$

$$M_1 = \sum_{i=1}^{3} \bar{u}[-p_2]i\gamma_\mu(g_{V_i} + g_{A_i}\gamma_5)u[p_1](-i)\frac{g^{\mu\nu} - \frac{q^\mu q^\nu}{M_i^2}}{q^2 - M_i^2 + iM_i\Gamma_i}iC_{1i}g^{\nu\alpha}\epsilon^\alpha[p_3], \tag{5.2}$$

where $iC_{1i}g_{\mu\nu}$ is the vertex factors of $V_i Z_L \phi^0 \phi^0$ given in table 5.2.

The amplitude corresponding to second diagram in figure 5.3;

$$\begin{aligned} M_2 &= \sum_{i,j=1,1}^{3,3} \bar{u}[-p_2]i\gamma_\mu(g_{V_i} + g_{A_i}\gamma_5)u[p_1](-i)\frac{g^{\mu\nu} - \frac{q^\mu q^\nu}{M_i^2}}{q^2 - M_i^2 + iM_i\Gamma_i}iB_{ij}g^{\nu\alpha} \\ &\quad (-i)\frac{g^{\alpha\nu} - \frac{q'^\alpha q^\nu}{M_j^2}}{q'^2 - M_j^2 + iM_j\Gamma_j}iB_{1j}g_{\beta\sigma}\epsilon^\sigma[p_3], \end{aligned} \tag{5.3}$$

where $iB_{ij}g_{\mu\nu}$ and $iB_{1j}g_{\mu\nu}$ are the vertex factors of $V_i V_j \phi^0$ and $V_j Z_L \phi^0$ respectively, and $q' = q - p_5$ given in table 5.3.

The amplitude corresponding to third diagram in figure 5.3;

$$\begin{aligned} M_3 &= \sum_{i=1}^{3} \bar{u}[-p_2]i\gamma_\mu(g_{V_i} + g_{A_i}\gamma_5)u[p_1](-i)\frac{g^{\mu\nu} - \frac{q^\mu q^\nu}{M_i^2}}{q^2 - M_i^2 + iM_i\Gamma_i}iE_{i2}^P P_\nu \\ &\quad \frac{-i}{q'^2 - M_\phi^2}iE_{12}^P P'_\alpha \epsilon^\alpha[p_3], \end{aligned} \tag{5.4}$$

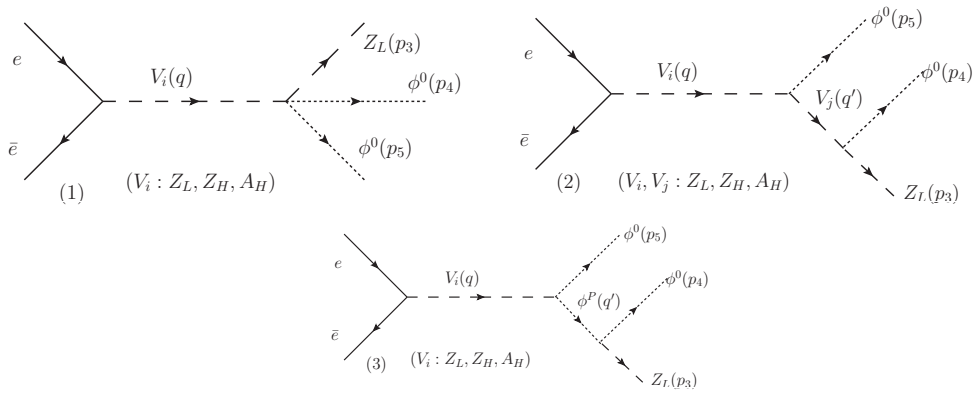

Figure 5.3: Feynman diagrams contributing to $e^+e^- \rightarrow Z_L\phi^0\phi^0$ in littlest Higgs model.

where $iE^P_{i2}P_\nu$ and $iE^P_{12}P'_\alpha$ are the vertex factors of $V_i\phi^P\phi^0$ and $Z_L\phi^P\phi^0$ given in table 5.5, and $P = q$ and $P' = q' - p_4$.

In this production process the change of differential cross section with respect to energy of the Z_L boson is analyzed with exploring the effects of variations of littlest Higgs model parameters s/s' for $f = 1TeV$ and mass of the SM Higgs boson is taken to be $M_H = 120GeV$ at $\sqrt{S} = 3TeV$. The resulting differential cross section vs. E_{Z_L} graphs are presented in figure 5.4. The plot of total cross section vs $\sqrt{S}$ of the process is presented in figure 5.13 in comparison with other associated production processes, and the total cross sections for necessary values of s/s' are presented in table 5.4. The peak values for differential cross section are at the order of $2 \times 10^{-4} \sim 10^{-6}\frac{pb}{GeV}$ in figure 5.4. Highest value of differential cross section is observed for parameters $s/s' = 0.5/0.1$ at low E_{Z_L} values and corresponding cross section for these parameters are $\sigma \sim 10^{-2}pb$ resulting in 1000 events per year for a luminosity of $100fb^{-1}$ expected for CLIC. But these values of s/s' do not quite satisfy the electroweak precision data for $f = 1TeV$.

For the values of parameters within the range of constraints from electroweak precision observables such as $\frac{M_{W_L}}{M_{Z_L}}$ and couplings of light fermions to gauge bosons at $f = 1TeV$, differential cross sections for this production process reduces to lower values. At $\sqrt{S} = 3TeV$, for the parameters $s/s' = 0.8/0.6, 0.8/0.7$ and $s/s' = 0.95/0.6$ the peak values of differential

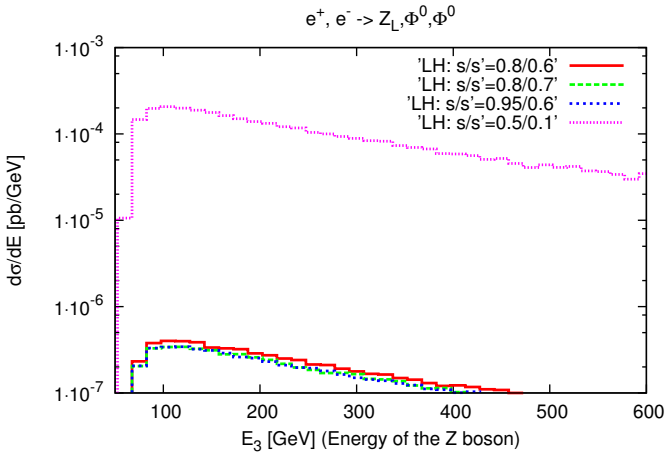

Figure 5.4: Differential cross section vs. E_Z graphs for $e^+e^- \to Z_L\phi^0\phi^0$, the behavior of differential cross section for parameters $f = 1000GeV$, s/s' : 0.8/0.6, 0.8/0.7, 0.95/0.6, 0.5/0.1 of littlest Higgs model .

cross sections of process $e^+e^- \to Z_L\phi^0\phi^0$ is about $5 \times 10^{-7}\frac{pb}{GeV}$ and the corresponding cross sections are $\sigma \sim 10^{-4}pb$. At CLIC($\sqrt{S} = 3TeV$), the expected luminosity is $100fb^{-1}$ per year resulting in $10 \sim 100$ production events for these low values free from SM backgrounds. The lepton number violating signals at the final state of this process depends on the value of the Yukawa couplings Y and Y'. For high values of $Y \simeq 1$, this channel would yield $1 \sim 10$ leptonic final states per year. Since the leptonic final states can only be neutrinos, the signature will be huge missing energy in the order of two scalar masses.

For ILC ($\sqrt{S} = 0.5 \sim 1TeV$), this production channel is out of reach because of kinematical limits coming from large M_ϕ.

5.1.3 $e^+e^- \to Z_L\phi^P\phi^P$

The littlest Higgs model implies the existence of new pseudoscalar ϕ^P degenerate in mass with other heavy scalars. The single production of ϕ^P within Z_L boson in littlest Higgs model is absent in tree level, and ϕ^P has no decay modes to two vectors, and also the direct double production without Z_L is not allowed in littlest Higgs model. The most dominant vector

Table 5.4: The total cross sections in *pb* for double production of neutral scalars for $f = 1TeV$ and at $\sqrt{S} = 3TeV$.

s/s'	$\sigma_{Z_L\phi^0\phi^0}$	$\sigma_{Z_L\phi^0\phi^P}$	$\sigma_{Z_L\phi^P\phi^P}$
0.8/0.6	$1.2\ 10^{-4}$	$5.4\ 10^{-5}$	$1.2\ 10^{-4}$
0.8/0.7	$1.0\ 10^{-4}$	$4.8\ 10^{-5}$	$1.0\ 10^{-4}$
0.95/0.6	$1.0\ 10^{-4}$	$4.7\ 10^{-5}$	$1.1\ 10^{-4}$
0.5/0.1	$5.8\ 10^{-2}$	$2.4\ 10^{-2}$	$5.9\ 10^{-2}$

associated production of ϕ^P is at the channel $e^+e^- \to Z_L\phi^P\phi^P$. This channel is sensitive to four point interaction vertices of ϕ^P with itself and two vectors and their couplings are given in table 5.2. ϕ^P also couples to a scalar and a vector, and these three point couplings are given in table 5.5. It also has lepton flavor violating decays so this channel can provide interesting signals. The Feynman diagrams contributing to this process are given in figure 5.5.

Table 5.5: The Feynman rules for $\phi^P V_i S_j$ vertices. Their couplings are given in the form $iE^P_{ij}P_\mu$, with P_μ is the difference of two scalars momentum, $(p_j - p_{\phi^P})$.

i/j	vertices	$-iE^P_{ij}(p_j - p_{\phi^P})$
1/1	$\phi^P H Z_L$	$\frac{1}{2}\frac{g}{c_w}(s_P - 2s_0)(p_{\phi^P} - p_H)_\mu$
1/2	$\phi^P\phi^0 Z_L$	$-\frac{g}{c_w}(p_{\phi^P} - p_{\phi^0})_\mu$
2/1	$\phi^P H Z_H$	$-\frac{1}{2}g\frac{(c^2-s^2)}{2sc}(s_P - 2s_0)(p_{\phi^P} - p_H)_\mu$
2/2	$\phi^P\phi^0 Z_H$	$g\frac{(c^2-s^2)}{2sc}(p_{\phi^P} - p_{\phi^0})_\mu$
3/1	$\phi^P H A_H$	$-\frac{1}{2}g'\frac{(c'^2-s'^2)}{2s'c'}(s_P - 2s_0)(p_{\phi^P} - p_H)_\mu$
3/2	$\phi^P\phi^0 A_H$	$g'\frac{(c'^2-s'^2)}{2s'c'}(p_{\phi^P} - p_{\phi^0})_\mu$

The amplitude corresponding to first Feynman diagram giving four point interactions can be written as:

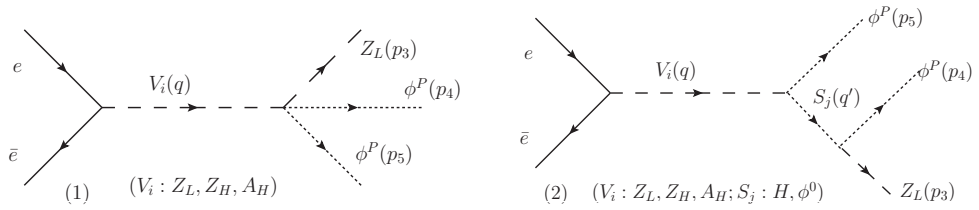

Figure 5.5: Feynman diagrams contributing to $e^+e^- \to Z_L\phi^P\phi^P$ in littlest Higgs model.

$$M_1 = \sum_{i=1}^{3} \bar{u}[-p_2]i\gamma_\mu(g_{V_i} + g_{A_i}\gamma_5)u[p_1](-i)\frac{g^{\mu\nu} - \frac{q^\mu q^\nu}{M_i^2}}{q^2 - M_i^2 + iM_i\Gamma_i} iC_{1i}^P g^{\nu\alpha}\epsilon^\alpha[p_3], \tag{5.5}$$

where $iC_{1i}^P g_{\mu\nu}$ is the vertex factor of $V_i Z_L \phi^P \phi^P$ given in table 5.2.

The amplitude corresponding to diagram 2 in figure 5.5 is:

$$\begin{aligned} M_2 \quad = \quad & \sum_{i,j=1,1}^{3,2} \bar{u}[-p_2]i\gamma_\mu(g_{V_i} + g_{A_i}\gamma_5)u[p_1](-i)\frac{g^{\mu\nu} - \frac{q^\mu q^\nu}{M_i^2}}{q^2 - M_i^2 + iM_i\Gamma_i} iE_{ij}^P P_\nu \\ & \frac{-i}{q'^2 - M_j^2 + iM_j\Gamma_j} iE_{1j}^P P'_\sigma \epsilon^\sigma[p_3], \end{aligned} \tag{5.6}$$

where $iE_{ij}^P P_\mu$ and $iE_{1j}^P P'_\nu$ are the vertex factors of $V_i S_{\,j}\phi^P$ and $Z_L S_{\,j}\phi^P$ respectively given in table 5.5, and $q' = q - p_5$, $P = q$ and $P' = p_3$.

For this process the differential cross section, and its dependence on the model parameters are analyzed. The resulting differential cross section vs. energy of the Z_L boson for various values of parameters of littlest Higgs model s/s' are given in figure 5.6. The total cross section vs center off mass energy graph is plotted in comparison with other double production channels in figure 5.13, and the total cross sections of this production channel for various values of parameters s/s' are given in table 5.4. Since the pseudo scalar ϕ^P have similar features with heavy scalar ϕ^0, the results for this process is close to results of double production of neutral heavy scalar associated with Z_L presented in previous section.

For parameters $s/s' = 0.5/0.1$ at symmetry breaking scale $f = 1TeV$, differential cross

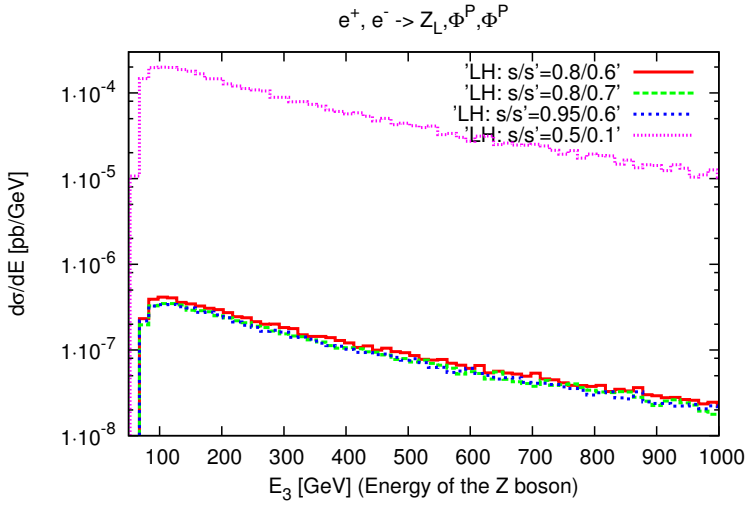

Figure 5.6: Differential cross section vs. E_{Z_L} graphs for $e^+e^- \to Z_L\phi^P\phi^P$, the behavior of differential cross section with respect to parameters s/s' : $0.8/0.6,\ 0.8/0.7, 0.95/0.6,\ 0.5/0.1$ at $f = 1000GeV$.

section of the process reads $10^{-4}\frac{pb}{GeV}$, and by integrating out E_{Z_L} total cross section is found $\sigma \sim 10^{-2}pb$ for $\sqrt{S} = 3TeV$. For $s/s' = 0.8/0.6, 0.8/0.7, 0.95/0.6$ the differential cross section takes lower values. For these set of parameters total cross section of the process takes $\sigma \sim 10^{-4}pb$ at $\sqrt{S} = 3TeV$. And for CLIC ($\sqrt{S} = 3TeV$) these values are in the reach of ϕ^P production resulting in $10 \sim 100$ events per year which can be observed for a yearly luminosity of $100fb^{-1}$. The final state lepton number violation signal for this process is four neutrinos, which can be detected as huge missing energy accompanied with Z_L.

In the littlest Higgs model, the single Z_L associated production of ϕ^P is not allowed. Since the double production is out of the energy limits of ILC $\sqrt{S} = 0.5 \sim 1TeV$, the pseudo scalar ϕ^P can not be observed associated with Z_L at ILC.

5.1.4 $e^+e^- \to Z_L\phi^0\phi^P$

In this section the associated production ϕ^0 and ϕ^P within Z_L boson is investigated. Since littlest Higgs model allows $V_i\phi^0\phi^P$ interactions, the neutral scalar and the pseudo scalar can

be produced through $e^+e^- \rightarrow Z_L\phi^0\phi^P$ process in electron colliders. Feynman diagrams are given in figure 5.7.

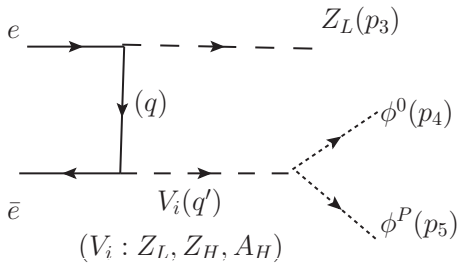

Figure 5.7: Feynman diagrams contributing to $e^+e^- \rightarrow Z_L\phi^0\phi^P$ in littlest Higgs

The amplitude of the Feynman diagram contributing this process can be written as:

$$\begin{aligned} M &= \sum_{i=1}^{3} \bar{u}[-p_2] i\gamma_\mu (g_{V_1} + g_{A_1}\gamma_5)\epsilon^\mu[p_3] \frac{\not{q}}{q^2} i\gamma_\nu (g_{V_i} + g_{A_i}\gamma_5) u[p_1] \\ &\quad \frac{g^{\nu\alpha} - \frac{q'^\alpha q^\nu}{M_i^2}}{q'^2 - M_i^2 + iM_i\Gamma_i} iE_i' P_\alpha, \end{aligned} \tag{5.7}$$

where $iE_i'P_\mu$ is the vertex factor of $V_i\phi^0\phi^P$, $P = q - q'$, $E_i' = E_{i2}^P$ given in table 5.5, and all of the momentums are defined in Fig.5.7.

For this process the differential cross section versus energy of the Z_L boson graphs are presented in figure 5.8. It is seen that similar to $Z_L\phi^0\phi^0$ and $Z_L\phi^P\phi^P$ final states, for $s/s' = 0.5/0.1$, the differential cross section reaches the highest values $\sim 10^{-4}\frac{pb}{GeV}$, and for parameter set $s/s' = 0.8/0.6, 0.95/0.6, 0.8/0.7$ allowed by electroweak precision constraints differential cross section gets values $\sim 10^{-6}\frac{pb}{GeV}$ at $\sqrt{S} = 3TeV$ for $f = 1TeV$. Since CLIC is expected to work at energies up to $\sqrt{S} = 3TeV$ and reach luminosities as much as $100fb^{-1}$, $Z_L\phi^0\phi^P$ production can be observed. Since the parameters $s/s' = 0.5/0.1$ are not acceptable due to electroweak precision data, the number of productions for this channel will be limited to $1 \sim 10$ events per year with events production cross section $\sigma \sim 5 \times 10^{-5} pb$ for acceptable parameter set $s/s' = 0.7/0.9$ at $f = 1TeV$. Since the number of production events is slightly

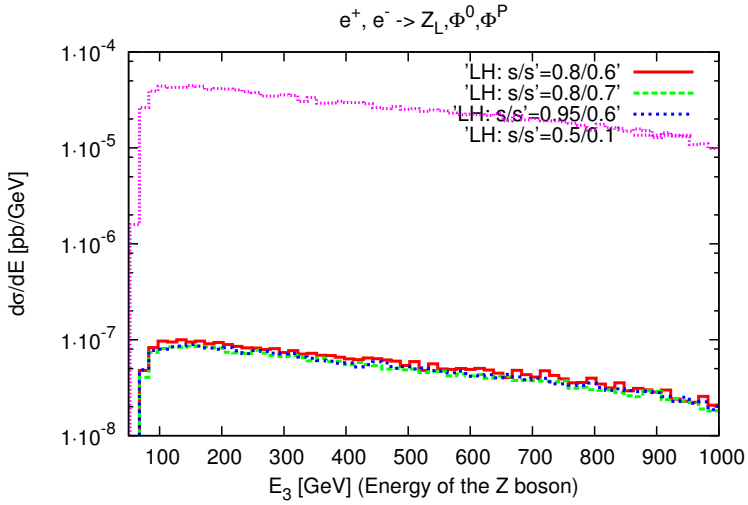

Figure 5.8: Differential cross section vs. E_Z graphs for $e^+e^- \rightarrow Z_L\phi^0\phi^P$, the behavior of differential cross section with respect to parameters s/s' : $0.8/0.6,\ 0.8/0.7, 0.95/0.6,\ 0.5/0.1$ at $f = 1000GeV$.

lower than $Z_L\phi^P\phi^P$ and $Z_L\phi^0\phi^0$ channels, the final number of lepton violating signals will not be remarkable at this channel.

In the littlest Higgs model, ϕ^0 and ϕ^P can also be produced directly in the $e^+e^- \rightarrow \phi^0\phi^P$ channel. This process will be discussed in chapter 6.

5.2 Production of Charged Scalars in the Littlest Higgs Model

In the littlest Higgs model, one of the decay modes of the single charged scalar in littlest Higgs model is a lepton and a neutrino which violates lepton flavor, resulting in signature of lepton and missing transverse energy of the neutrino. And also for the double charged scalar in the final state two charged leptons violating the lepton flavor can be observed.

In this section, the Z_L associated double production of single and double charged heavy scalars at electron colliders in littlest Higgs model is discussed. The results of this section is published in [57].

5.2.1 $e^+e^- \to Z_L\phi^+\phi^-$

In the littlest Higgs model, the masses of all heavy scalars are degenerate and proportional to symmetry breaking scale f, so for lower values of f double production $\phi^+\phi^-$ can be produced at e^+e^- colliders via $e^+e^- \to Z_L\phi^+\phi^-$ process. At the final state this channel is promising for lepton flavor and number violating signals such as missing energy of the neutrino and two leptons of different or same families. In this model $\phi^-\phi^+$ couples to neutral vectors through four point interactions, so this production channel is sensitive to these couplings given in table 5.6. The couplings of ϕ^- with a neutral vector and a charged vector are given in table 5.8. The single charged heavy scalars can also be produced via the decay of heavy vectors, because littlest Higgs model allows these interactions given in table 5.7. The Feynman diagrams contributing to this associated production process are given in figure 5.9.

Table 5.6: The four point Feynman rules for $\phi^+\phi^- V_i V_j$ vertices. Their couplings are given in the form $iC_{ij}^{\phi\phi} g_{\mu\nu}$ where $g_{\mu\nu}$ carries the Lorentz indices for vectors.

i/j	vertices	$iC_{ij}^{\phi\phi} g_{\mu\nu}$
1/1	$\phi^+\phi^- Z_L Z_L$	$2i\frac{g^2}{c_w^2} s_w^4 g_{\mu\nu}$
2/1	$\phi^+\phi^- Z_H Z_L$	$O(v^2/f^2) \sim 0$
3/1	$\phi^+\phi^- A_H Z_L$	$2i\frac{gg'}{c_w}\frac{(c'^2-s'^2)}{2s'c'} s_w^2 g_{\mu\nu}$
4/1	$\phi^+\phi^- A_L Z_L$	$-2ie\frac{g}{c_w} s_w^2 g_{\mu\nu}$

Table 5.7: The three point interaction vertices for $\phi^+(p_1)\phi^-(p_2)V_i$ vertices. Their couplings are given in the form $iE_i^{\phi\phi} P_\mu$, where $P_\mu = (p_1 - p_2)_\mu$ is the difference of outgoing momentum of two charged scalars.

i/j	vertices	i $E_i^{\phi\phi} P_\mu$
1	$\phi^+\phi^- Z_L$	$i\frac{g}{c_w} s_w^2 (p_1 - p_2)_\mu$
2	$\phi^+\phi^- Z_H$	$O(v^2/f^2) \sim 0$
3	$\phi^+\phi^- A_H$	$ig'\frac{(c'^2-s'^2)}{2s'c'}(p_1 - p_2)_\mu$
4	$\phi^+\phi^- A_L$	$-ie(p_1 - p_2)_\mu$

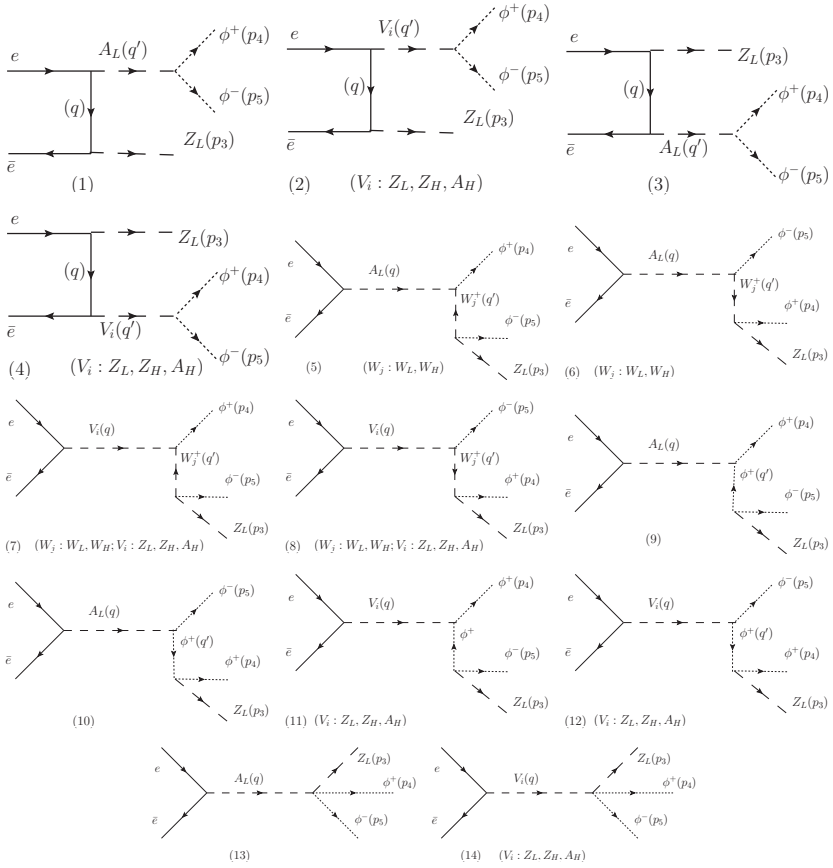

Figure 5.9: Feynman diagrams contributing to $e^+e^- \to Z_L\phi^+\phi^-$ in littlest Higgs model

Table 5.8: The Feynman rules for $\phi^+ V_i W_j^-$ vertices. Their couplings are given in the form $iB_{ij}^{\phi W} g_{\mu\nu}$ where $g_{\mu\nu}$ carries the Lorentz indices of vectors and $j = 1, 2$ denotes W_L, W_H respectively.

i/j	vertices	$iB_{ij}^{\phi W} g_{\mu\nu}$
1/1	$\phi^+ W_L^- Z_L$	$-i\frac{g^2}{c_w} v' g_{\mu\nu}$
1/2	$\phi^+ W_H^- Z_L$	$i\frac{g^2}{c_w}\frac{(c^2-s^2)}{2sc} v' g_{\mu\nu}$
2/1	$\phi^+ W_L^- Z_H$	$ig^2\frac{(c^2-s^2)}{2sc} v' g_{\mu\nu}$
2/2	$\phi^+ W_H^- Z_H$	$-ig^2\frac{(c^4+s^4)}{2s^2c^2} v' g_{\mu\nu}$
3/1	$\phi^+ W_L^- A_H$	$-\frac{i}{2}gg'\frac{(c'^2-s'^2)}{2s'c'}(vs_+ - 4v')g_{\mu\nu}$
3/2	$\phi^+ W_H^- A_H$	$-\frac{i}{2}gg'\frac{(c^2c'^2+s^2s'^2)}{scs'c'} v' g_{\mu\nu}$

The first four Feynman diagrams contributing to the process $e^+e^- \to \phi^+\phi^- Z_L$ are sensitive to $e^+e^- V_i$ couplings because in them two vectors are created from e^+e^- annihilation processes, and one of them decays to scalars. The amplitudes for the first two diagrams in figure 5.9, are given as:

$$\begin{aligned} M_1 &= \bar{u}[-p_2] i\gamma_\mu (g_{V_1} + g_{A_1}\gamma_5)\epsilon^\mu[p_3]\frac{i\not{q}}{q^2} i\gamma_\nu g_{V_4} u[p_1](i)\frac{g^{\alpha\nu}}{q'^2} \\ &\quad iE_4^{\phi\phi}(p_4 - p_5)_\alpha, \end{aligned} \tag{5.8}$$

$$\begin{aligned} M_2 &= \sum_{i=1}^{3} \bar{u}[-p_2] i\gamma_\mu (g_{V_1} + g_{A_1}\gamma_5)\epsilon^\mu[p_3]\frac{i\not{q}}{q^2} i\gamma_\nu (g_{V_i} + g_{A_i}\gamma_5) u[p_1] \\ &\quad (i)\frac{g^{\alpha\nu} - \frac{q'^\nu q'^\alpha}{M_i^2}}{q'^2 - M_i^2 + iM_i\Gamma_i} iE_i^{\phi\phi}(p_4 - p_5)_\alpha, \end{aligned} \tag{5.9}$$

where $q = p_2 - p_3$, $q' = p_4 + p_5$ and coefficients $E_i^{\phi\phi}$ are given in table 5.7.

The amplitudes for diagrams 3 and 4 in figure 5.9, are given as:

$$M_3 = \bar{u}[-p_2] i\gamma_\mu (g_{V_4})\frac{ig^{\mu\nu}}{q^2} iE_4^{\phi\phi}(p_4 - p_5)_\nu \gamma_\alpha (g_{V_1} + g_{A_1}\gamma_5)\epsilon^\alpha[p_3] u[p_1], \tag{5.10}$$

$$M_4 = \sum_{i=1}^{3} \bar{u}[-p_2] i\gamma_\mu (g_{V_i} + g_{A_i}\gamma_5) i \frac{g^{\mu\nu} - \frac{q'^\mu q'^\nu}{M_i^2}}{q'^2 - M_i^2 + iM_i\Gamma_i} iE_i^{\phi\phi} (p_4 - p_5)_\nu$$
$$i\frac{\not{q}}{q^2} i\gamma_\alpha (g_{V_1} + g_{A_1}\gamma_5)\epsilon^\alpha[p_3]u[p_1], \tag{5.11}$$

where $q = p_1 - p_3$, $q' = p_4 + p_5$ and coefficients $E_i^{\phi\phi}$ are given in table 5.7.

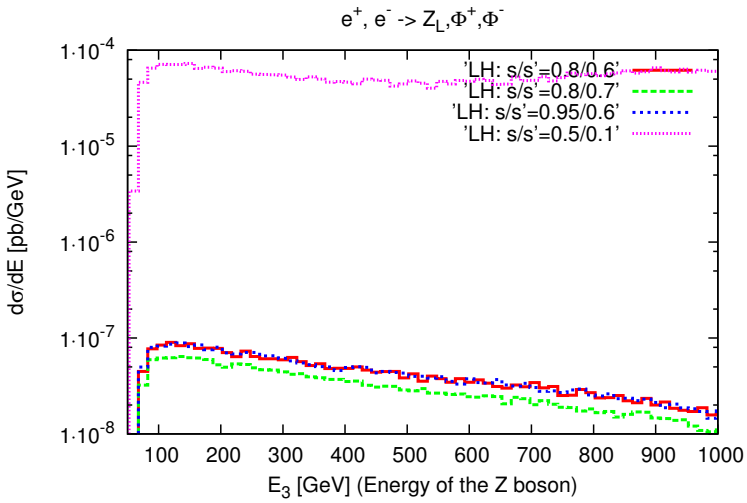

Figure 5.10: Differential cross section vs. E_Z graphs for $e^+e^- \to Z_L\phi^+\phi^-$, the variation of differential cross section with respect to parameters s/s' : 0.8/0.6, 0.8/0.7, 0.95/0.6, 0.5/0.1 for $f = 1000GeV$.

The rest of the amplitudes from 5 to 14 in figure 5.9 are s channel processes with $q = p_1 + p_2$. The amplitudes 5 to 8 correspond to diagrams 5 to 8 in figure 5.9, where an electric charge is carried by a W propagator. These sub processes are proportional to the couplings of a vector with a charged scalar and a charged vector W_j, where $j = 1, 2$ corresponds to W_L and W_H respectively. Their amplitudes are given as:

$$M_5 = \sum_{j=1}^{2} \bar{u}[-p_2] i\gamma_\mu (g_{V_4}) u[p_1] \frac{ig^{\mu\nu}}{q^2} (iB_{4j}^{\phi W}) g_{\nu\alpha} i \frac{g^{\alpha\beta} - \frac{q'^\alpha q'^\beta}{M_{W_j}^2}}{q^2 - M_{W_j}^2 + iM_{W_j}\Gamma_{W_j}}$$
$$(iB_{1j}^{\phi W}) g_{\beta\sigma}\epsilon^\sigma[p_3], \tag{5.12}$$

$$M_6 = \sum_{j=1}^{2} \bar{u}[-p_2] i\gamma_\mu (g_{V_4}) u[p_1] \frac{ig^{\mu\nu}}{q^2} (iB_{4j}^{\phi W}) g_{\nu\alpha} i \frac{g^{\alpha\beta} - \frac{q'^\alpha q'^\beta}{M_{W_j}^2}}{q^2 - M_{W_j}^2 + iM_{W_j}\Gamma_{W_j}} (iB_{1j}^{\phi W}) g_{\beta\sigma} \epsilon^\sigma[p_3], \tag{5.13}$$

$$M_7 = \sum_{i,j=1,1}^{3,2} \bar{u}[-p_2] i\gamma_\mu (g_{V_i} + g_{A_i}\gamma_5) u[p_1] i \frac{g^{\mu\nu} - \frac{q^\mu q^\nu}{M_i^2}}{q^2 - M_i^2 + iM_i\Gamma_i} (iB_{ij}^{\phi W}) g_{\nu\alpha} \frac{g^{\alpha\beta} - \frac{q'^\alpha q'^\beta}{M_{W_j}^2}}{q^2 - M_{W_j}^2 + iM_{W_j}\Gamma_{W_j}} (iB_{1j}^{\phi W}) g_{\beta\sigma} \epsilon^\sigma[p_3], \tag{5.14}$$

$$M_8 = \sum_{i,j=1,1}^{3,2} \bar{u}[-p_2] i\gamma_\mu (g_{V_i} + g_{A_i}\gamma_5) u[p_1] i \frac{g^{\mu\nu} - \frac{q^\mu q^\nu}{M_i^2}}{q^2 - M_i^2 + iM_i\Gamma_i} (iB_{ij}^{\phi W}) g_{\nu\alpha} \frac{g^{\alpha\beta} - \frac{q'^\alpha q'^\beta}{M_{W_j}^2}}{q^2 - M_{W_j}^2 + iM_{W_j}\Gamma_{W_j}} (iB_{1j}^{\phi W}) g_{\beta\sigma} \epsilon^\sigma[p_3], \tag{5.15}$$

where $B_{ij}^{\phi W}$ are given in table 5.8, and $q' = q - p_5$ for amplitudes 6 and 8 and $q' = q - p_4$ for 5 and 7.

The diagrams 9 to 12 in figure 5.9, corresponding to amplitudes 9 to 12, have a heavy scalar as a propagator, and are proportional to the square of the couplings of two vectors with a charged scalar. These amplitudes are given as:

$$M_9 = \bar{u}[-p_2] i\gamma_\mu g_{V_4} u[p_1] i \frac{g^{\mu\nu}}{q^2} iE_4^{\phi\phi} (p_4 - q')_\nu \frac{i}{q'^2 - M_{\phi^2}} iE_1^{\phi\phi} (-q' - p_3)_\sigma \epsilon^\sigma[p_3], \tag{5.16}$$

$$M_{10} = \bar{u}[-p_2] i\gamma_\mu g_{V_4} u[p_1] i \frac{g^{\mu\nu}}{q^2} iE_4^{\phi\phi} (p_5 + q')_\nu \frac{i}{q'^2 - M_{\phi^2}} iE_1^{\phi\phi} (-q' - p_3)_\sigma \epsilon^\sigma[p_3], \tag{5.17}$$

$$M_{11} = \sum_{i=1}^{3} \bar{u}[-p_2] i\gamma_\mu (g_{V_i} + g_{A_i}\gamma_5) u[p_1] i \frac{g^{\mu\nu} - \frac{q^\mu q^\nu}{M_i^2}}{q^2 - M_i^2 + iM_i\Gamma_i}$$
$$(iE_i^{\phi\phi})(p_4 - q')_\nu \frac{i}{q'^2 - M_\phi^2} (iE_1^{\phi\phi})(-q' - p_3)_\sigma \epsilon^\sigma[p_3], \quad (5.18)$$

$$M_{12} = \sum_{i=1}^{3} \bar{u}[-p_2] i\gamma_\mu (g_{V_i} + g_{A_i}\gamma_5) u[p_1] i \frac{g^{\mu\nu} - \frac{q^\mu q^\nu}{M_i^2}}{q^2 - M_i^2 + iM_i\Gamma_i}$$
$$(iE_i^{\phi\phi})(p_5 + q')_\nu \frac{i}{q'^2 - M_\phi^2} (iE_1^{\phi\phi})(-q' - p_3)_\sigma \epsilon^\sigma[p_3], \quad (5.19)$$

where $E_i^{\phi\phi}$ are given in table 5.7, and $q' = q - p_5$ for amplitudes 10 and 12 and $q' = q - p_4$ for 9 and 11.

The rest of the diagrams in figure 5.9 are sub processes in which the four point couplings of vectors and scalars contribute. Their amplitudes are given as:

$$M_{13} = \bar{u}[-p_2] i\gamma_\mu g_{V_4} u[p_1] i \frac{ig^{\mu\nu}}{q^2} iC_{41}^{\phi\phi} g_{\nu\sigma} \epsilon^\sigma[p_3], \quad (5.20)$$

$$M_{14} = \sum_{i=1}^{3} \bar{u}[-p_2] i\gamma_\mu (g_{V_i} + g_{A_i}\gamma_5) u[p_1] i \frac{g^{\mu\nu} - \frac{q^\mu q^\nu}{M_i^2}}{q^2 - M_i^2 + iM_i\Gamma_i}$$
$$(iC_{i1}^{\phi\phi}) g_{\nu\alpha} \epsilon^\alpha[p_3], \quad (5.21)$$

where $C_{ij}^{\phi\phi}$ are four point couplings given in table 5.6.

For the double production of single charged heavy scalars associated with Z_L , the differential cross sections versus energy of the Z_L boson graphs for different values of mixing angle parameters s/s' for symmetry breaking scale $f = 1TeV$ at total center of mass energy $\sqrt{S} = 3TeV$ appropriate for CLIC are presented in figure 5.10. The total cross sections for these process for parameters $s/s' = 0.8/0.6, 0.8/0.7, 0.95/0.6, 0.5/0.1$ are given in table 5.9, and also total cross section versus $\sqrt{S}$ graph for this process is presented in figure 5.13, in comparison with other scalar production channels. The differential cross section gets its maximum value of about $10^{-4}\frac{pb}{GeV}$ for $s/s' = 0.5/0.1$, corresponding to a remarkable cross section of $5.9 \times 10^{-2} pb$, resulting in thousands of productions per year at high integrated luminosity

Table 5.9: The total cross sections in pb for double production of single charged scalars associated with Z_L for $f = 1TeV$ and at $\sqrt{S} = 3TeV$.

s/s'	$\sigma_{Z_L\phi^+\phi^-}$
0.8/0.6	$4.2\ 10^{-5}$
0.8/0.7	$3.1\ 10^{-5}$
0.95/0.6	$4.3\ 10^{-5}$
0.5/0.1	$5.9\ 10^{-2}$

of $100fb^{-1}$, but this parameter set is not allowed for low symmetry breaking scales $f = 1TeV$ by electroweak precision data. So to search this parameter space the center of mass energy should be increased for parameter space $f > 3TeV$, where the parameters are less restricted.

For parameters $s/s' = 0.8/0.6, 0.8/0.7, 0.95/0.6$, the peak values of differential cross sections are obtained at the order of $10^{-7}\frac{pb}{GeV}$ for low E_Z values, $E_Z \sim 100GeV$. The total cross section is calculated as $4\times10^{-5}pb$. This result implies $1 \sim 10$ events per year accessible for a collider luminosity of $100fb^{-1}$.

The lepton number violating signals in the final state will be at the order of one event per year, for high values of lepton mixing Yukawa couplings Y, Y'. The final signals are two leptons of same or different families and missing energy of neutrinos.

5.2.2 $e^+e^- \to Z_L\phi^{++}\phi^{--}$

The littlest Higgs model has global symmetry breaking by nonlinear sigma model resulting in 14 Goldstone bosons among which a doublet and a triplet remain physical and gain mass through Coleman Weinberg potential. The doublet is assigned as SM Higgs doublet and the triplet contains the new scalars and the pseudo scalar of the model. Since the triplet carries hypercharge 1 under electroweak group, it has charged components.

This feature results in one of the most interesting aspect of the littlest Higgs model; the existence of double charged heavy scalars $\phi^{\pm\pm}$ and their lepton number violating decay modes. These double charged scalars have three point interaction vertices with vector bosons given in

table 5.11, and four point interaction vertices with vectors given in table 5.10. The couplings of these vertices strongly depend on the littlest Higgs parameter set f, s, s'.

In this section the associated production of double charged scalars in $e^+e^- \rightarrow Z_L\phi^{++}\phi^{--}$ channel is analyzed. In this model, ϕ^{++} has decay modes to charged vectors $W_L^+W_L^+$ and also to leptons $l_i^+l_j^+$ proportional to squares of the values of the Yukawa couplings (Y_{ij}); $|Y^2|$ for same families and $|Y'^2|$ for different lepton families when lepton violating modes are considered. Hence this channel provides very interesting final signals for $\phi^{\pm\pm}$ discovery, and four leptons at the final step violating lepton flavor, such as $l_il_il_j^+l_j^+$, $l_il_jl_j^+l_j^+$ and $l_il_il_i^+l_j^+$. The final state $l_il_jl_i^+l_j^+$ in this channel also proceeds through a lepton flavor violating process but does not give violation signals.

The Feynman diagrams contributing to this process are given in figure 5.12.

Table 5.10: The four point Feynman rules for $\phi^{++}\phi^{--}V_iV_j$ vertices. Their couplings are given in the form $iC'^{\phi\phi}_{ij}g_{\mu\nu}$ where $g_{\mu\nu}$ carries the Lorentz indices of vectors.

i/j	vertices	$iC'^{\phi\phi}_{ij}g_{\mu\nu}$
1/1	$\phi^{++}\phi^{--}Z_LZ_L$	$2i\frac{g^2}{c_w^2}(1-2s_w^2)^2g_{\mu\nu}$
2/1	$\phi^{++}\phi^{--}Z_HZ_L$	$2i\frac{g^2}{c_w}\frac{(c^2-s^2)}{2sc}(1-2s_w^2)g_{\mu\nu}$
3/1	$\phi^{++}\phi^{--}A_HZ_L$	$-2i\frac{gg'}{c_w}\frac{(c'^2-s'^2)}{2s'c'}(1-2s_w^2)g_{\mu\nu}$
4/1	$\phi^{++}\phi^{--}A_LZ_L$	$4ie\frac{g}{c_w}(1-2s_w^2)g_{\mu\nu}$

Table 5.11: The three point interaction vertices for $\phi^{++}(p_1)\phi^{--}(p_2)V_i$ vertices. Their couplings are given in the form $iE_i'^{\phi\phi}P_\mu$, where $P_\mu = (p_1 - p_2)_\mu$ is the difference of outgoing momentum of the scalars.

i/j	vertices	$iE_i'^{\phi\phi}P_\mu$
1	$\phi^{++}\phi^{--}Z_L$	$-i\frac{g}{c_w}\left(1-2s_w^2\right)(p_1-p_2)_\mu$
2	$\phi^{++}\phi^{--}Z_H$	$ig\frac{(c^2-s^2)}{2sc}(p_1-p_2)_\mu$
3	$\phi^{++}\phi^{--}A_H$	$ig'\frac{(c'^2-s'^2)}{2s'c'}(p_1-p_2)_\mu$
4	$\phi^{++}\phi^{--}A_L$	$-2ie(p_1-p_2)_\mu$

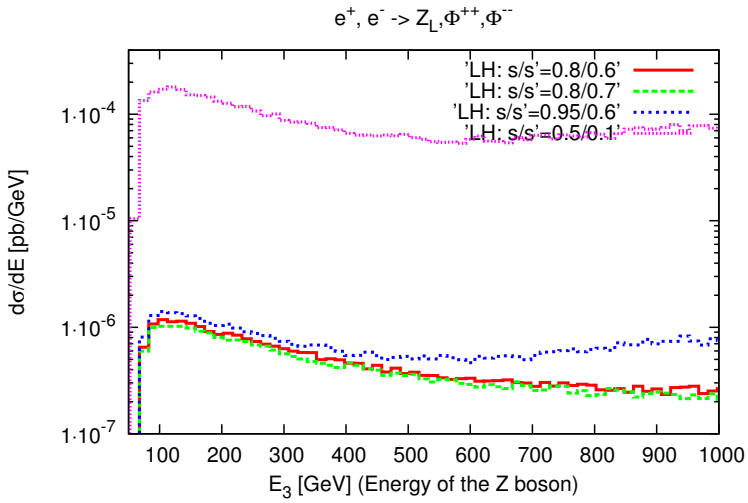

Figure 5.11: Differential cross section vs. E_Z graphs for $e^+e^- \to Z_L\phi^{++}\phi^{--}$, the variation of differential cross section with respect to parameters s/s' : $0.8/0.6,\ 0.8/0.7, 0.95/0.6,\ 0.5/0.1$ for $f = 1000GeV$.

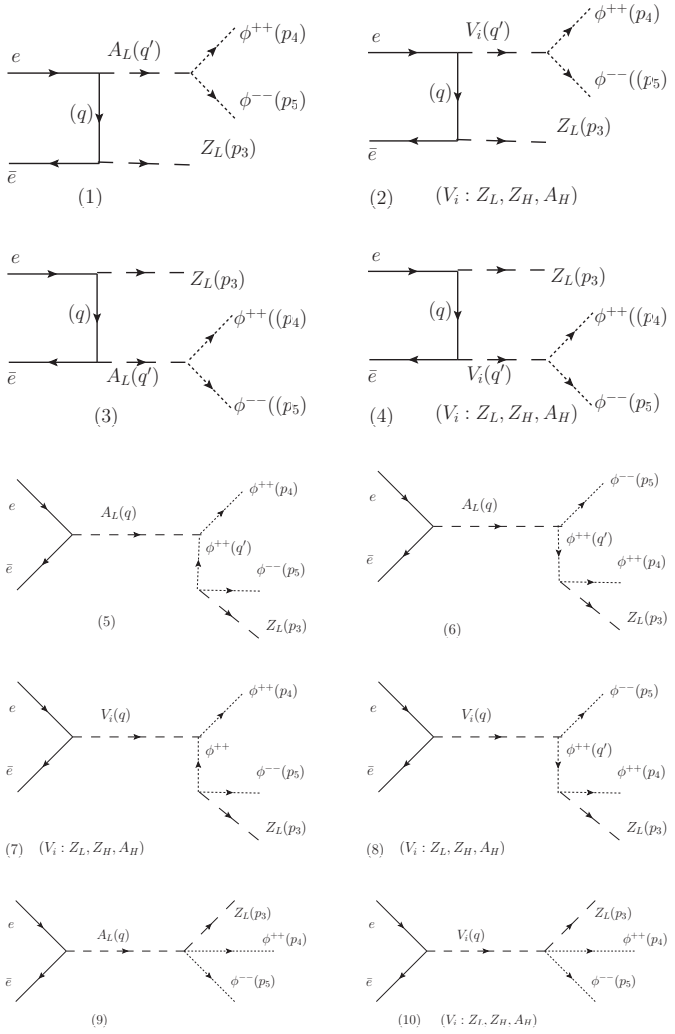

Figure 5.12: Feynman diagrams contributing to $e^+e^- \to Z_L\phi^{++}\phi^{--}$ in littlest Higgs model

In this process the double charged couple is generated by the decay of the neutral scalars at the s channel. The charged vectors W_i do not contribute to this process because our final state does not allow these type couplings. The Feynman diagrams contributing to the process $e^+e^- \rightarrow \phi^{++}\phi^{--}Z_L$ are given in figure 5.12. The amplitudes for the first two diagrams in figure 5.12 are written as:

$$\begin{aligned} M_1 &= \bar{u}[-p_2]i\gamma_\mu(g_{V_1} + g_{A_1}\gamma_5)\epsilon^\mu[p_3]\frac{i\not{q}}{q^2}i\gamma_\nu g_{V_4}u[p_1](i)\frac{g^{\alpha\nu}}{q'^2} \\ &\quad iE_4'^{\phi\phi}(p_4 - p_5)_\alpha, \end{aligned} \tag{5.22}$$

$$\begin{aligned} M_2 &= \sum_{i=1}^{3}\bar{u}[-p_2]i\gamma_\mu(g_{V_1} + g_{A_1}\gamma_5)\epsilon^\mu[p_3]\frac{i\not{q}}{q^2}i\gamma_\nu(g_{V_i} + g_{A_i}\gamma_5)u[p_1] \\ &\quad (i)\frac{g^{\alpha\nu} - \frac{q'^\nu q'^\alpha}{M_i^2}}{q'^2 - M_i^2 + iM_i\Gamma_i}iE_i'^{\phi\phi}(p_4 - p_5)_\alpha, \end{aligned} \tag{5.23}$$

where $q = p_1 - q$ and $q' = p_2 - p_3$, and the vertex factors $E_i'^{\phi\phi}$ are given in table 5.11.

The amplitudes for diagrams 3 and 4 in figure 5.12 are given by:

$$M_3 = \bar{u}[-p_2]i\gamma_\mu(g_{V_4})\frac{ig^{\mu\nu}}{q^2}iE_4'^{\phi\phi}(p_4 - p_5)_\nu\gamma_\alpha(g_{V_1} + g_{A_1}\gamma_5)\epsilon^\alpha[p_3]u[p_1], \tag{5.24}$$

$$\begin{aligned} M_4 &= \sum_{i=1}^{3}\bar{u}[-p_2]i\gamma_\mu(g_{V_i} + g_{A_i}\gamma_5)i\frac{g^{\mu\nu} - \frac{q^\mu q^\nu}{M_i^2}}{q^2 - M_i^2 + iM_i\Gamma_i}iE_i'^{\phi\phi}(p_4 - p_5)_\nu \\ &\quad i\frac{\not{q}}{q^2}i\gamma_\alpha(g_{V_1} + g_{A_1}\gamma_5)\epsilon^\alpha[p_3]u[p_1], \end{aligned} \tag{5.25}$$

where $q = p_1 - p_3$ and $q' = p_2 - q$, and the vertex factors $E_i'^{\phi\phi}$ are given in table 5.11.

The diagrams 5 to 8 in figure 5.12 corresponds to sub processes in which double electric charge is mediated by a double charged scalar, so they will have a double charged scalar propagator. The amplitudes for these diagrams are given by:

$$\begin{aligned} M_5 &= \bar{u}[-p_2]i\gamma_\mu g_{V_4}u[p_1]i\frac{ig^{\mu\nu}}{q^2}iE_4'^{\phi\phi}(p_5 + q')_\nu\frac{i}{q'^2 - M_{\phi^2}} \\ &\quad iE_1'^{\phi\phi}(-q' - p_3)_\sigma\epsilon^\sigma[p_3], \end{aligned} \tag{5.26}$$

$$M_6 = \bar{u}[-p_2]i\gamma_\mu g_{V_4} u[p_1] i\frac{ig^{\mu\nu}}{q^2} iE_4^{\prime\phi\phi}(p_4 - q')_\nu \frac{i}{q'^2 - M_{\phi^2}}$$
$$iE_1^{\prime\phi\phi}(-q' - p_3)_\sigma \epsilon^\sigma[p_3], \tag{5.27}$$

$$M_7 = \sum_{i=1}^{3} \bar{u}[-p_2]i\gamma_\mu(g_{V_i} + g_{A_i}\gamma_5)u[p_1] i\frac{g^{\mu\nu} - \frac{q^\mu q^\nu}{M_i^2}}{q^2 - M_i^2 + iM_i\Gamma_i}$$
$$(iE_i^{\prime\phi\phi})(p_5 + q')_\nu \frac{i}{q'^2 - M_\phi^2}(iE_1^{\prime\phi\phi})(-q' - p_3)_\sigma \epsilon^\sigma[p_3], \tag{5.28}$$

$$M_8 = \sum_{i=1}^{3} \bar{u}[-p_2]i\gamma_\mu(g_{V_i} + g_{A_i}\gamma_5)u[p_1] i\frac{g^{\mu\nu} - \frac{q^\mu q^\nu}{M_i^2}}{q^2 - M_i^2 + iM_i\Gamma_i}$$
$$(iE_i^{\prime\phi\phi})(p_4 - q')_\nu \frac{i}{q'^2 - M_\phi^2}(iE_1^{\prime\phi\phi})(-q' - p_3)_\sigma \epsilon^\sigma[p_3], \tag{5.29}$$

where $q = p_1 + p_2$, $q' = q - p_4$ for diagrams 5 and 7 and $q' = q - p_5$ for diagrams 6 and 8.

The last two diagrams in figure 5.12 correspond to the contributions coming from four point interactions of vectors and double charged scalars. These amplitudes are given by:

$$M_9 = \bar{u}[-p_2]i\gamma_\mu g_{V_4} u[p_1] i\frac{ig^{\mu\nu}}{q^2} iC_{41}^{\prime\phi\phi} g_{\nu\sigma}\epsilon^\sigma[p_3], \tag{5.30}$$

where.

$$M_{10} = \sum_{i=1}^{3} \bar{u}[-p_2]i\gamma_\mu(g_{V_i} + g_{A_i}\gamma_5)u[p_1] i$$
$$\frac{g^{\mu\nu} - \frac{q^\mu q^\nu}{M_i^2}}{q^2 - M_i^2 + iM_i\Gamma_i}(iC_{i1}^{\prime\phi\phi}) g_{\nu\alpha}\epsilon^\alpha[p_3], \tag{5.31}$$

where $q = p_1 + p_2$ and $C_{ij}^{\prime\phi\phi}$ are four point couplings given in table 5.10.

The differential cross sections for the double associated production of double charged scalars associated with Z_L are examined in this section, and their plots with respect to E_Z are given in figure 5.11 for different value of mixing angles at $\sqrt{S} = 3TeV$, for symmetry breaking scale $f = 1TeV$. The total cross section of this production process is plotted in figure 5.13 with

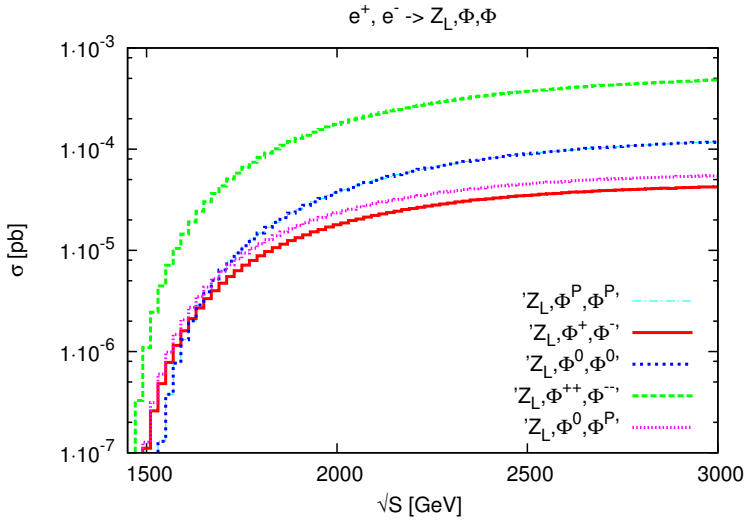

Figure 5.13: Total cross section vs. $\sqrt{S}$ graphs for double associated production of neutral and charged scalars with parameters $f/s/s'$: $1000GeV/0.8/0.6$.

respect to center of mass energy, and the numerical values of total cross sections are given in table 5.12 for parameters of interest. It is seen from figures 5.13 and 5.11 that the process is not sensitive to gauge boson resonances since they are out of the energy reach, due to the heavy mass of scalars presented in table 4.2.

The differential cross section of the production process reaches its maximum value of $10^{-4}\frac{pb}{GeV}$ for model parameters $s/s' = 0.5/0.1$ for $E_Z \sim 100GeV$. For this parameters the total cross section is $8.4 \times 10^{-2} pb$. This will give about 8000 events per year for high luminosities such as $100 fb^{-1}$, and also at least ten events for very low luminosities such as $10 pb^{-1}$. But to get this remarkable number of events(see Fig. 5.14), the total energy of the colliders should be increased to cover $f > 3TeV$ for this production process, since $s/s' = 0.5/0.1$ is out favored by electroweak precision data for $f = 1TeV$.

For the electroweak allowed parameters $s/s' = 0.8/0.6, 0.8/0.7, 0.95/0.6$ for $f = 1TeV$ at $\sqrt{S} = 3TeV$, the differential cross section gets lower values at the order of $10^{-7}\frac{pb}{GeV}$. The resulting cross sections are calculated by integrating over E_Z, and found to be about $4 \sim 8 \times 10^{-4} pb$ (table 5.12) resulting in $40 \sim 80$ events per year for integrated luminosity of

$100 fb^{-1}$. For $\sqrt{S} < 3TeV$, this production channel is not reachable.

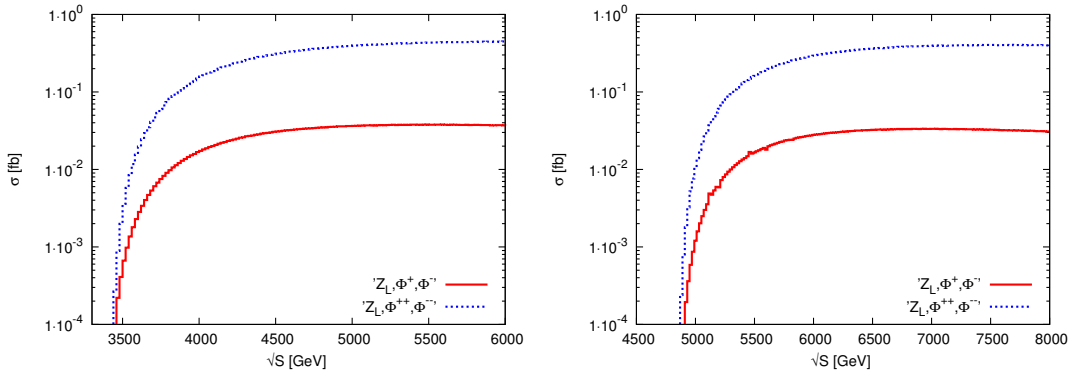

Figure 5.14: Total cross section vs. $\sqrt{S}$ graphs for Z_L associated pair production of charged scalars at (left)$f = 2.5TeV$, and at (right)$f = 3.5TeV$ when parameters s/s' : 0.8/0.7.

This channel is free of SM backgrounds due to lepton number violating decays of doubly charged scalar at the final state. If the lepton mixing term in the Yukawa Lagrangian is considered, the most interesting decay mode of double charged scalar is to leptons, violating lepton number by two. The total number of lepton number violating final states in this channel depends on the branching ratio of the leptonic decays of doubly charged scalar (equation 4.4). The decays into final states from same lepton family is dependant on the Yukawa coupling Y, and to different lepton families to Y'. Since the values of Y' are expected to be small, and Y can get values up to order one, the most promising final state for observing lepton number violation in this process will be $l_i l_i l_j^+ l_j^+$ plus reconstructed Z_L; four leptons violating lepton flavor by four.

For $f = 1TeV$ the leptonic branching ratio of double charged scalars can reach values close to 1 for $Y \to 1$, independent from Y'. If the value of the Yukawa coupling Y is high enough, the number of final state lepton number violating signal can reach 50 events per year, which can be directly detected free from background.

Finally, the behavior of the production processes for higher values of f is also analyzed. The dependence total cross section on $\sqrt{S}$ when $s/s' = 0.8/0.7$ for $f = 2.5TeV, 3.5TeV, 5TeV$ are plotted in figures 5.14(left), 5.14(right) and 5.15(left), respectively. It is seen that the

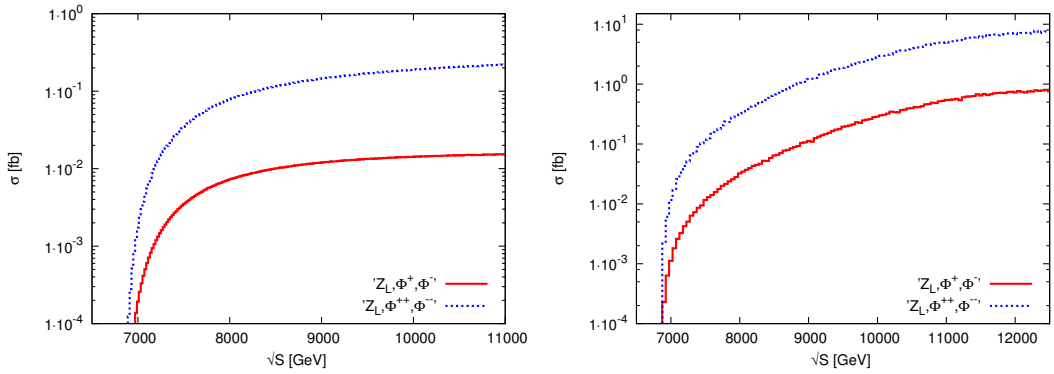

Figure 5.15: Total cross section vs. $\sqrt{S}$ graphs for Z_L associated pair production of charged scalars at $f = 5TeV$ when parameters (left)s/s' : 0.8/0.7 and (right)s/s' : 0.6/0.4.

maximum value of total cross sections, production rates and final lepton flavor violating signals for these f values for both processes remain same, but the required energy is shifted to $\sqrt{S} = 3.8TeV(5.5TeV)\{7.5TeV\}$ for $f = 2.5TeV(3.5TeV)\{5TeV\}$, due to the increase in heavy scalar masses. For $f = 5TeV$, we have also analyzed the case $s/s' = 0.6/0.4$, since the parameters are less constrained. The dependence of total cross sections for associated production of both single and doubly charged pairs are plotted in figure 5.15(right). It is seen that the total cross sections are increased by order one. For the single charged pair, the production cross section is calculated as $0.9fb$ for $\sqrt{S} \gtrsim 10TeV$, resulting in 90 production

Table 5.12: The total cross sections in pb for double production of doubly charged scalars associated with Z_L for $f = 1TeV$ and at $\sqrt{S} = 3TeV$.

s/s'	$\sigma_{Z_L\phi^{++}\phi^{--}}$
0.8/0.6	4.8 10^{-4}
0.8/0.7	4.4 10^{-4}
0.95/0.6	7.8 10^{-4}
0.5/0.1	8.4 10^{-2}

events for luminosities of the order of $100 fb^{-1}$. For the double charged scalar pair, the total cross section is $5 \sim 9 fb$ for $\sqrt{S} \gtrsim 10 TeV$, giving $500 \sim 900$ productions at luminosities $100 fb^{-1}$. In this case the final number of four lepton signals ($l_i l_i l_i^+ l_j^+$) will be around 600 for higher values of Yukawa coupling ($Y \sim 1$). If the values of Yukawa coupling is smaller, in the region $0.1 \leq Y \leq 0.3$, the double charged pair will decay into semi leptonic modes, such as $W_L^+ W_L^+ l_i l_i$, resulting in $200 \sim 400$ signals accessible for luminosities of $100 fb^{-1}$. Finally, if the energy of the colliders can be increased to cover the region $f > 3 TeV$ where the parameters are less constrained, the total number of lepton number violation events per year can reach up to thousands for Y close to one. In this case for even low Y values, the lepton number violations can be observed.

5.3 The Z_L Associated Production of Higgs Boson in the Littlest Higgs Model

In this section the production of SM Higgs boson within Z_L via $e^+e^- \to Z_L H$ and $e^+e^- \to Z_L HH$ processes at high energy electron colliders is discussed in the framework of littlest Higgs model. These production processes are in the reach for both ILC ($\sqrt{S} = 1TeV$) and CLIC ($\sqrt{S} = 3TeV$), since the final state masses are light compared to the new heavy scalars of the littlest Higgs model. Due to the heavy vector propagations in these processes, the productions will be sensitive to the effects of the littlest Higgs model.

5.3.1 $e^+e^- \to Z_L H$

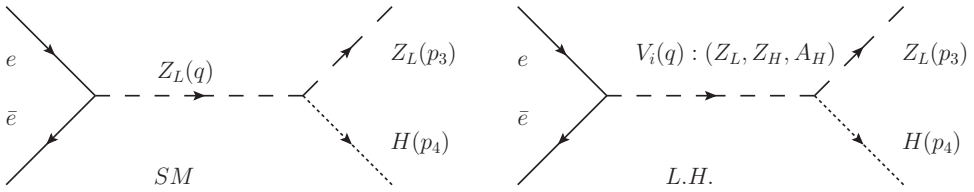

Figure 5.16: Feynman diagram contributing $e^+e^- \to Z_L H$, SM (right) and littlest Higgs model(right).

In standard model the single associated production of Higgs boson associated with Z_L occurs via emitting by a Higgs boson from Z_L in the s channel. The Feynman diagram for this process is given in figure 5.16, and the corresponding amplitude is given by:

$$M = \bar{u}[-p_2] i\gamma_\mu (g_V + g_A\gamma_5) u[p_1](-i) \frac{g^{\mu\nu} - \frac{q^\mu q^\nu}{M_{Z_L}^2}}{q^2 - M_{Z_L}^2 + i\Gamma_{Z_L}} i\frac{gM_{Z_L}}{c_W} g_{\nu\alpha}\epsilon^\alpha[p_3] \ , \tag{5.32}$$

where $g_A = \frac{-g}{2c_W}(-1/2 + s_W^2)$, $g_V = \frac{-g}{4c_W}$ and $q = p_1 + p_2$.

In littlest Higgs model, this process receives contributions from other heavy neutral scalars propagating (fig.5.16 (right)). The amplitude for this process is the sum of the contributions from all sub processes and is given by:

Table 5.13: The Feynman rules for three point $Z_L HH$ and four point $Z_L Z_L HH$ vertices in SM .

λ_{ZZHH}	$\frac{ig^2 g_{\mu\nu}}{2c_W^2}$
λ_{ZHH}	$\frac{ig^2 v g_{\mu\nu}}{2c_W^2}$

$$M = \sum_{i=1}^{3} \bar{u}[-p_2] i\gamma_\mu (g_{V_i} + g_{A_i}\gamma_5) u[p_1](-i) \frac{g^{\mu\nu} - \frac{q^\mu q^\nu}{M_i^2}}{q^2 - M_i^2 + iM_i\Gamma_i} (i) B_{i1}^H g_{\nu\alpha} \epsilon^\alpha[p_3] \ , \tag{5.33}$$

where $q = p_1 + p_2$, and B_{ij}^H are couplings given in table 5.14.

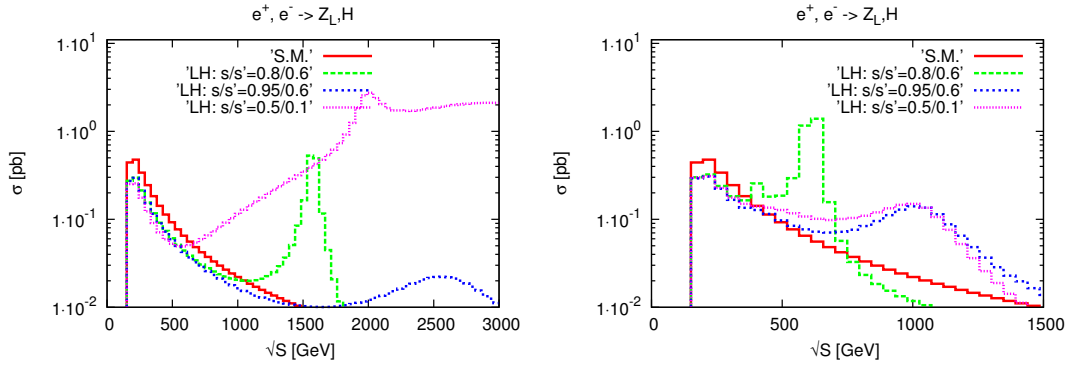

Figure 5.17: For $e^+e^- \to Z_L H$ total cross section(pb) vs. $\sqrt{S}$(GeV) graphs, variations with respect to s/s' for $f = 2460GeV$(left), and for $f = 1000GeV$(right).

For the process $e^+e^- \to Z_L H$ the total cross section in the framework of littlest Higgs model is examined. In SM, the cross section of the process is about $0.48pb$ at $\sqrt{S} = 250GeV$. For the littlest Higgs model total cross section versus energy graphs are presented in figure 5.17, for symmetry breaking scales $f = 1000GeV$ and for $f = 2460GeV$, for electroweak allowed parameter sets of s/s'. For low $\sqrt{S}$ values, total cross section calculated in the littlest Higgs model is slightly below the SM values. But for $\sqrt{S} > 400GeV$ for $f = 1000GeV$, and for

Table 5.14: The three point Feynman rules for HV_iV_j vertices. Their couplings are given in the form $ig_{\mu\nu}B^H_{ij}$ where $g_{\mu\nu}$ carries the Lorentz indices of vectors.

i/j	vertices	$iB^H_{ij}g_{\mu\nu}$
1/1	HZ_LZ_L	$\frac{i}{2}\frac{g^2}{c_w^2}vg_{\mu\nu}\left(1-\frac{v^2}{3f^2}-\frac{1}{2}s_0^2+4\sqrt{2}s_0\frac{v'}{v}\right.$ $\left.-\frac{1}{2}\left((c^2-s^2)^2+5(c'^2-s'^2)^2\right)\frac{v^2}{f^2}\right)$
2/2	HZ_HZ_H	$-\frac{i}{2}g^2vg_{\mu\nu}$
1/2	HZ_LZ_H	$-\frac{i}{2}\frac{g^2}{c_w}\frac{(c^2-s^2)}{2sc}vg_{\mu\nu}$
2/3	HZ_HA_H	$-\frac{i}{4}gg'\frac{(c^2s'^2+s^2c'^2)}{scs'c'}vg_{\mu\nu}$
1/3	HZ_LA_H	$-\frac{i}{2}\frac{gg'}{c_w}\frac{(c'^2-s'^2)}{2s'c'}vg_{\mu\nu}$
3/3	HA_HA_H	$-\frac{i}{2}g'^2vg_{\mu\nu}$

$\sqrt{S} > 1TeV$ for $f = 2460GeV$, the contributions from littlest Higgs gets larger, while the value of the cross section for SM gets very small. This is due to the gauge boson resonances corresponding to the mass of Z_H.

For $f = 2460GeV$, at $s/s' = 0.5/0.1$ highest values of cross sections are achieved for this process at the order of $10pb$, but this set is not allowed by electroweak observable tests. For values $s/s' = 0.8/0.6$, there appears a resonance in the cross section at $\sqrt{S} = 1.5TeV$ corresponding to the Z_H resonance for $M_{Z_H} \simeq 1.6TeV$ given in table 4.2, reaching to a value of $1pb$. For $0.95/0.6$ this resonance occurs at $\sqrt{S} \simeq 2.5TeV$ widely due to larger decay width of heavy Z_H.

For $f = 1TeV$ the peak value of cross section at the order of $1pb$ is reached at $\sqrt{S} = 700GeV$, hitting the heavy Z_H pole for parameters $s/s' = 0.8/0.6$. The resonance for parameters $s/s' = 0.95/0.6$ and $s/s' = 0.5/0.1$ appears at $\sqrt{S} = 1TeV$ at a peak value of $0.5pb$.

It is seen that for this process the total number of production events will reach up to 10^5 events per year at high luminosities such as $100fb^{-1}$. Even at ILC the effects of the littlest Higgs model can be observed for low symmetry breaking scale values.

If the Higgs boson is observed at LHC, this production channel will determine the mass of Z_H by reconstructing the invariant mass of Z_LH pair. If the mass of Z_H is determined at the LHC,

the results obtained from this channel will determine the parameter space of littlest Higgs model.

5.3.2 $e^+e^- \to Z_LHH$

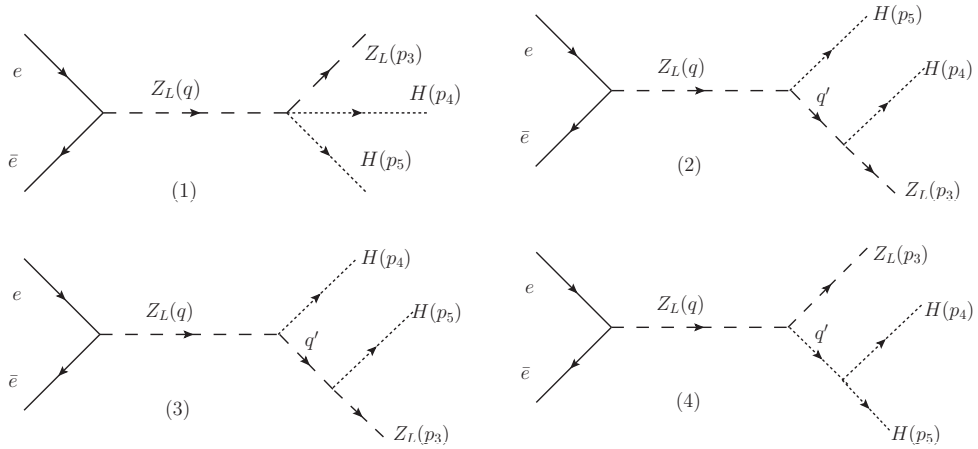

Figure 5.18: Feynman diagrams contributing to $e^+e^- \to Z_LHH$ in SM

In standard model, double production of Higgs boson associated with Z_L has contributions from four point Z_LZ_LHH vertex, from three point Z_LZ_LH vertex and also from three point HHH vertex and the Feynman diagrams contributing to this process are given in figure 5.18. The amplitude corresponding to first diagram in figure 5.18 is given by:

$$M_1 = \bar{u}[-p_2]i\gamma_\mu(g_V + g_A\gamma_5)u[p_1](-i)\frac{g^{\mu\nu} - \frac{q^\mu q^\nu}{M_{Z_L}^2}}{q^2 - M_{Z_L}^2 + i\Gamma_{Z_L}}i\lambda_{ZZHH}g_{\nu\alpha}\epsilon^\alpha[p_3] \ . \tag{5.34}$$

The amplitude corresponding to second and third diagrams in figure 5.18 are given by:

$$M_2 = \bar{u}[-p_2]i\gamma_\mu(g_V + g_A\gamma_5)u[p_1](-i)\frac{g^{\mu\nu} - \frac{q^\mu q^\nu}{M_{Z_L}^2}}{q^2 - M_{Z_L}^2 + i\Gamma_{Z_L}}i\lambda_{ZZH}g_{\nu\alpha}$$
$$(-i)\frac{g^{\alpha\beta} - \frac{q'^\alpha q'^\beta}{M_{Z_L}^2}}{q'^2 - M_{Z_L}^2 + i\Gamma_{Z_L}}i\lambda_{ZZH}g_{\beta\sigma}\epsilon^\sigma[p_3] \ , \tag{5.35}$$

$$M_3 = \bar{u}[-p_2]i\gamma_\mu(g_V + g_A\gamma_5)u[p_1](-i)\frac{g^{\mu\nu} - \frac{q^\mu q^\nu}{M_{Z_L}^2}}{q^2 - M_{Z_L}^2 + i\Gamma_{Z_L}}i\lambda_{ZZH}g_{\nu\alpha}$$
$$(-i)\frac{g^{\alpha\beta} - \frac{q'^\alpha q'^\beta}{M_{Z_L}^2}}{q'^2 - M_{Z_L}^2 + i\Gamma_{Z_L}}i\lambda_{ZZH}g_{\beta\sigma}\epsilon^\sigma[p_3] \ , \tag{5.36}$$

where $q' = q - p_4$ for diagram 3 and $q' = q - p_5$ for diagram 2.

The amplitude corresponding to last diagram in figure 5.18 is given by:

$$M_4 = \bar{u}[p_2]i\gamma_\mu(g_V + g_A\gamma_5)(-i)\frac{g^{\mu\nu} - \frac{q^\mu q^\nu}{M_{Z_L}^2}}{q^2 - M_{Z_L}^2 + i\Gamma_{Z_L}}$$
$$i\lambda_{ZZH}g_{\nu\alpha}(-i)\epsilon^\alpha[p_3]\frac{i}{q'^2 - M_H^2}i\lambda_{HHH} \ , \tag{5.37}$$

where $q' = p_4 + p_5$. For all these four amplitudes $q = p_1 + p_2$ and the SM couplings λ_{ZZH}, λ_{ZZHH} and λ_{HHH} are given in tables 5.13 and 5.16.

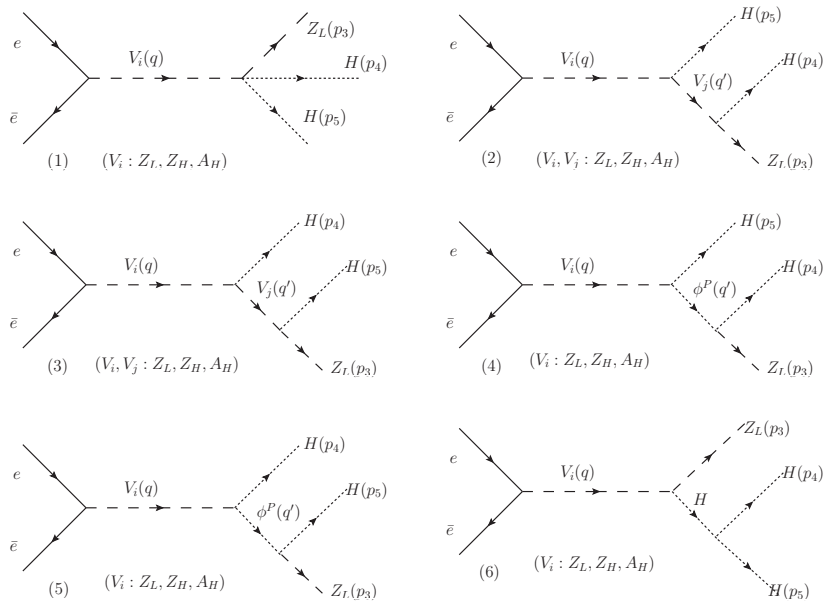

Figure 5.19: Feynman diagrams contributing to $e^+e^- \to Z_L HH$ in littlest Higgs model.

Table 5.15: The four point Feynman rules for HHV_iZ_L vertices. Their couplings are given in the form $iC_ig_{\mu\nu}$.

i	vertices	C_i
1	HHZ_LZ_L	$\frac{i}{2}\frac{g^2}{c_w^2}g_{\mu\nu} + O(v^2/f^2)$
2	HHZ_HZ_L	$-\frac{i}{2}\frac{g^2}{c_w}\frac{(c^2-s^2)}{2sc}g_{\mu\nu}$
3	HHA_HZ_L	$-\frac{i}{2}\frac{gg'}{c_w}\frac{(c'^2-s'^2)}{2s'c'}g_{\mu\nu}$
4	HHA_LZ_L	0

Table 5.16: The three point Feynman rules for HHH vertices for SM (λ_{HHH}) and littlest Higgs model (λ'_{HHH}).

λ_{HHH}	$\frac{-i3M_H^2}{v}$
λ'_{HHH}	$\frac{-i3M_H^2}{v}(1 - \frac{11v^2(4fv'/v^2)}{4f^2(1-(4fv'/v^2)^2)})$

In littlest Higgs model, the double Higgs production associated by a Z_L boson gets contributions from propagation of new neutral vectors besides Z_L and also new pseudo scalar besides H. The Feynman diagrams contributing to this production process are given in figure 5.19. The amplitude corresponding to first diagram in figure 5.19 is due to four point couplings of vectors and Higgs bosons and given by:

$$M_1 = \sum_{i=1}^{3} \bar{u}[-p_2]i\gamma_\mu(g_{V_i} + g_{A_i}\gamma_5)u[p_1](-i)\frac{g^{\mu\nu} - \frac{q^\mu q^\nu}{M_i^2}}{q^2 - M_i^2 + iM_i\Gamma_i}iC_ig^{\nu\alpha}\epsilon^\alpha[p_3], \tag{5.38}$$

where C_i is the vertex factor for Z_LV_iHH given in table 5.15 and $i = 1, 2, 3$.

The amplitudes for the second and third Feynman diagrams in figure 5.19 are given by:

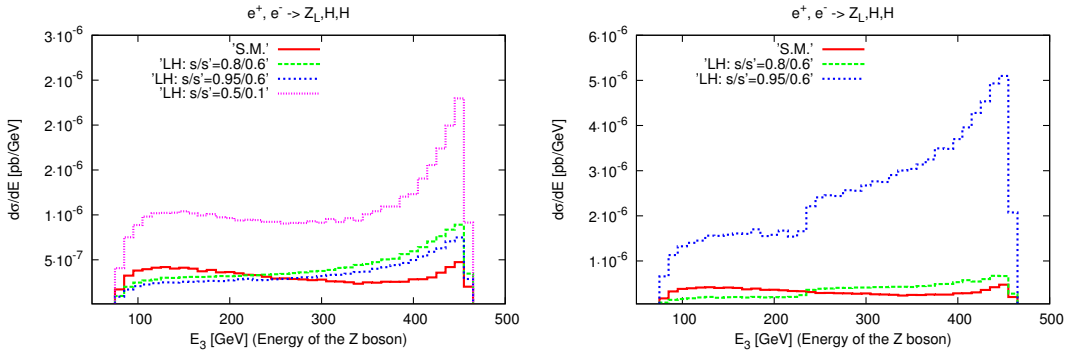

Figure 5.20: For $e^+e^- \to Z_L HH$ differential cross section vs. E_Z graphs, variation with respect to the littlest Higgs model parameters s/s' for $f = 2460GeV$(left) and $f = 1000GeV$(right) at $\sqrt{S} = 1TeV$.

$$M_2 = \sum_{i,j=1,1}^{3,3} \bar{u}[-p_2] i\gamma_\mu (g_{V_i} + g_{A_i}\gamma_5) u[p_1](-i)\frac{g^{\mu\nu} - \frac{q^\mu q^\nu}{M_i^2}}{q^2 - M_i^2 + iM_i\Gamma_i} iB_{ij}^H g^{\nu\alpha}$$
$$(-i)\frac{g^{\beta\alpha} - \frac{q'^\alpha q'^\beta}{M_j^2}}{q'^2 - M_j^2 + iM_j\Gamma_j} iB_{1j}^H g^{\beta\sigma}\epsilon^\sigma[p_3], \tag{5.39}$$

where B_{ij}^H is the vertex factor for V_iV_jH and $q' = q - p_5$. $M_3 = M_2$ with replacing $q' = q - p_4$.

The amplitudes for diagrams 4*and*5 in figure 5.19 are due to contributions from the propagation of pseudo scalar ϕ^P and they are given by:

$$M_4 = \sum_{i=1}^{3} \bar{u}[-p_2] i\gamma_\mu (g_{V_i} + g_{A_i}\gamma_5) u[p_1](-i)\frac{g^{\mu\nu} - \frac{q^\mu q^\nu}{M_i^2}}{q^2 - M_i^2 + iM_i\Gamma_i}$$
$$i(E_{i1}^P P_\nu)\frac{-i}{q'^2 - M_\phi^2}(E_{11}^P P'_\sigma)\epsilon^\sigma[p_3], \tag{5.40}$$

where E_{i1}^P and E_{11}^P are the vertex factors of $V_iH\phi^P$ and $Z_LH\phi^P$ respectively given in table 5.5, and $P_\nu = (p_H - p_{\phi^P})_\nu = (p_5 - q')_\nu$ and $P' = p_4 + q'$. M_5 can be obtained by exchanging p_4 and p_5.

The amplitude for the last diagram in figure 5.19 is given by:

$$M_6 = \sum_{i=1}^{3} \bar{u}[-p_2] i\gamma_\mu (g_{V_i} + g_{A_i}\gamma_5) u[p_1](-i) \frac{g^{\mu\nu} - \frac{q^\mu q^\nu}{M_i^2}}{q^2 - M_i^2 + iM_i\Gamma_i}$$
$$i(B_{i1}^H) g_{\nu\alpha} \epsilon^\alpha[p_3] \frac{-i}{q''^2 - M_H^2} (i\lambda'_{HHH}), \tag{5.41}$$

where B_{i1}^H is the vertex factor for $Z_L H V_i$ and λ'_{HHH} for HHH given in tables 5.14 and5.16.

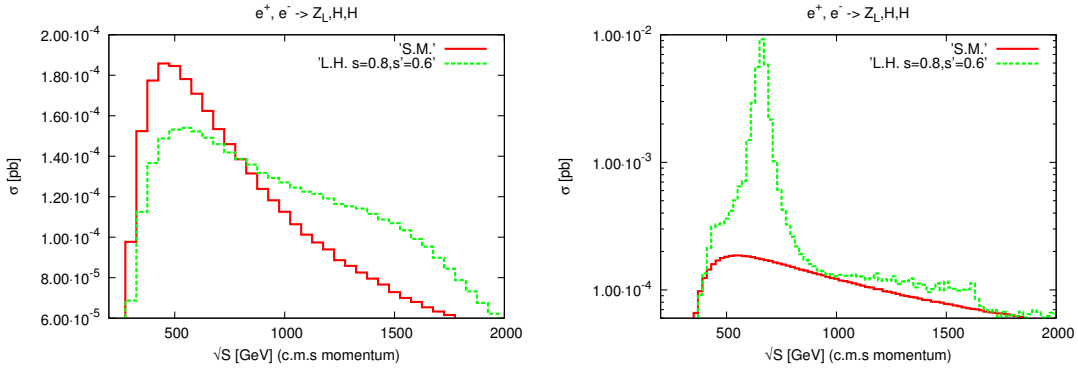

Figure 5.21: Total cross section vs. $\sqrt{S}$ graph for $e^+e^- \to Z_L HH$, for SM and littlest Higgs model for parameters $f/s/s'$: $2460GeV/0.8/0.6$(left), same graph for low f value $f/s/s'$: $1000GeV/0.8/0.6$(right).

For the production of two Higgs boson within Z_L, the differential cross sections of the process, the total cross sections of the process and their dependence on the littlest Higgs model parameters are examined. The differential cross sections are plotted with respect to energy of the Z_L boson for $f = 1TeV$ and $f = 2.46TeV$ at center of mass energy $\sqrt{S} = 1TeV$, and presented in figure 5.20 for SM and also for different values of parameters s/s'. The total cross sections of the process for $f = 1TeV$ and $f = 2.46TeV$ are plotted with the SM total cross sections in figure 5.21.

As in the case of process $e^+e^- \to Z_L H$, the differential cross sections for $f = 2460GeV$ and s/s' being in the range of electroweak observables is slightly smaller in littlest Higgs model than SM values for low energies of Z_L ($E_Z \leq 220GeV$). For higher energies of Z_L the littlest Higgs model contributions dominates the process.

For symmetry breaking scale $f = 2460GeV$, the differential cross section reaches a max-

imum value of order $10^{-6}\frac{pb}{GeV}$ at $E_{Z_L} \simeq 460GeV$ for parameters $s/s' = 0.95/0.6, 0.8/0.6$. For $f = 1TeV$ the differential cross section is maximum within the parameter space allowed by electroweak data, with a peak value of $5 \times 10^{-6}\frac{pb}{GeV}$ for $E_{Z_L} \simeq 460GeV$ for parameters $s/s' = 0.95/0.6$. For mixing angles $s/s' = 0.8/0.6$ the differential cross section is maximum at $E_{Z_L} \simeq 460GeV$ with a value of $10^{-6}\frac{pb}{GeV}$. It is seen from figure 5.20 that this channel is sensitive to littlest Higgs model effects, since the difference in the differential cross section of the SM and the littlest Higgs model is in the range $\pm\%30$ in the parameter space allowed by the electroweak precision data.

The total cross section of the process is calculated by integrating out E_Z for symmetry breaking scales $f = 1TeV$ and $f = 2.46TeV$ at $s/s' = 0.8/0.6$. For $f = 2.46TeV$ the total cross section has a maximum at $\sqrt{S} = 0.5TeV$ with a value of $1.5 \times 10^{-4}pb$ below the SM value of the total cross section which is $1.8 \times 10^{-4}pb$. The littlest Higgs model dominates for $\sqrt{S} > 0.8TeV$ while the value for SM decreases. For $f = 1TeV$ the total cross section for the littlest Higgs model dominates the production process. At $\sqrt{S} \simeq 0.6TeV$, the littlest Higgs model value of cross section gets a resonance from Z_H pole with a value of $10^{-2}pb$ which is two orders higher than the SM value. This will give thousands of events per year observable at ILC and CLIC.

5.4 Production of Higgs Boson Associated with New Neutral Scalars of Littlest Higgs Model

5.4.1 $e^+e^- \to Z_L H\phi^0$

In this section the production of new heavy scalar, ϕ^0, standard model Higgs scalar and Z_L is investigated. The Feynman diagrams contributing to the production of Higgs and heavy scalar associated with Z_L are given in figure 5.22.

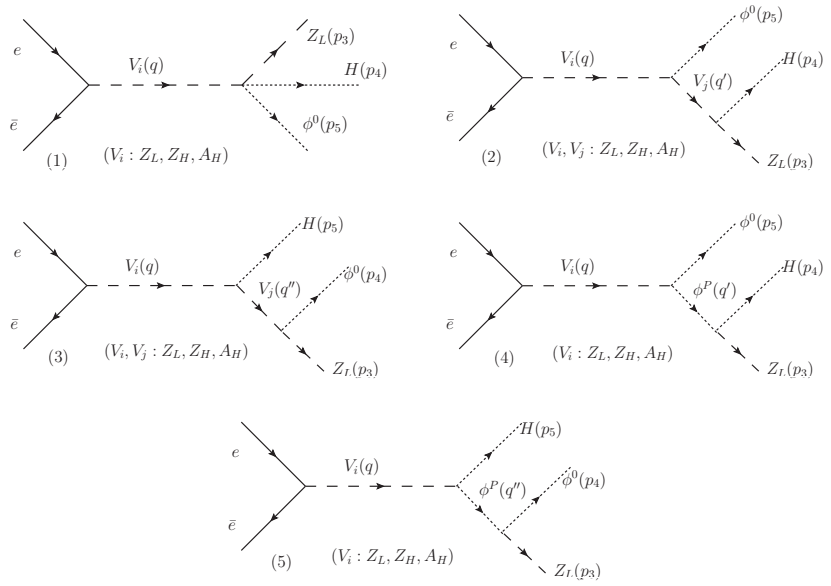

Figure 5.22: Feynman diagrams contributing to $e^+e^- \to Z_L H\phi^0$ in littlest Higgs model.

The amplitude for the first diagram in figure 5.22 is given by:

$$M_1 = \sum_{i=1}^{3} \bar{u}[-p_2] i\gamma_\mu (g_{V_i} + g_{A_i}\gamma_5) u[p_1](-i)\frac{g^{\mu\nu} - \frac{q^\mu q^\nu}{M_i^2}}{q^2 - M_i^2 + iM_i\Gamma_i} iC_{i1}^{H\phi} g^{\nu\alpha}\epsilon^\alpha[p_3], \tag{5.42}$$

where $iC_{i1}^{H\phi} g_{\mu\nu}$ is the vertex factor of $V_i Z_L H\phi^0$ given in table 5.18.

The amplitude for the second diagram in figure 5.22 is given by:

Table 5.17: The total cross sections in pb for production of neutral scalars associated with Higgs boson and Z_L for $f = 1TeV$ and at $\sqrt{S} = 2TeV$.

s/s'	$\sigma_{Z_L H\phi^0}$	$\sigma_{Z_L H\phi^P}$
0.8/0.6	$3.4\ 10^{-3}$	$6.8\ 10^{-7}$
0.95/0.6	$3.0\ 10^{-3}$	$8.9\ 10^{-7}$
0.5/0.1	1.8	$3.5\ 10^{-4}$

$$M_2 = \sum_{i,j=1,1}^{3,3} \bar{u}[-p_2] i\gamma_\mu (g_{V_i} + g_{A_i}\gamma_5) u[p_1](-i) \frac{g^{\mu\nu} - \frac{q^\mu q^\nu}{M_i^2}}{q^2 - M_i^2 + iM_i\Gamma_i}$$
$$i(B_{ij}^{\phi}) g^{\nu\alpha} i \frac{g^{\alpha\beta} - \frac{q'^\alpha q'^\beta}{M_j^2}}{q^2 - M_j^2 + iM_j\Gamma_j} (i(B_{1j}^{H})) g_{\beta\sigma} \epsilon^\sigma[p_3], \tag{5.43}$$

where $iB_{ij}^{\phi} g_{\mu\nu}$ and $iB_{1j}^{H} g_{\mu\nu}$ are the vertex factors of $V_i V_j \phi^0$ and $V_j H Z_L$ respectively given in tables 5.3 and5.14, and $q' = q - p_5$.

The amplitude for the third diagram in figure 5.22 is given by:

$$M_3 = \sum_{i,j=1,1}^{3,3} \bar{u}[-p_2] i\gamma_\mu (g_{V_i} + g_{A_i}\gamma_5) u[p_1](-i) \frac{g^{\mu\nu} - \frac{q^\mu q^\nu}{M_i^2}}{q^2 - M_i^2 + iM_i\Gamma_i}$$
$$i(B_{ij}^{H}) g^{\nu\alpha} i \frac{g^{\alpha\beta} - \frac{q''^\alpha q''^\beta}{M_j^2}}{q^2 - M_j^2 + iM_j\Gamma_j} (i(B_{1j})) g_{\beta\sigma} \epsilon^\sigma[p_3], \tag{5.44}$$

where $iB_{ij}^{H} g_{\mu\nu}$ and $iB_{1j} g_{\mu\nu}$ are the vertex factors of $V_i V_j H$ and $V_j \phi^0 Z_L$ respectively given in tables 5.14 and 5.3, and $q'' = q - p_4$.

The amplitude for diagram 4 in figure 5.22 is given by:

$$M_4 = \sum_{i=1}^{3} \bar{u}[-p_2] i\gamma_\mu (g_{V_i} + g_{A_i}\gamma_5) u[p_1](-i) \frac{g^{\mu\nu} - \frac{q^\mu q^\nu}{M_i^2}}{q^2 - M_i^2 + iM_i\Gamma_i} iE_{i2}^{P}$$
$$P_\nu \frac{-i}{q'^2 - M_\phi^2} iE_{11}^{P} P_\alpha \epsilon^\alpha[p_3], \tag{5.45}$$

where $iE^P_{i2}P_\nu$ and $iE^P_{11}P'_\nu$ are vertex factors of $V_i\phi^P\phi^0$ and $\phi^P HZ_L$ respectively given in table 5.5 and $P = p_5 + q'$.

The amplitude for diagram 5 in figure 5.22 is given by:

$$\begin{aligned} M_5 &= \sum_{i=1}^{3} \bar{u}[-p_2]i\gamma_\mu(g_{V_i} + g_{A_i}\gamma_5)u[p_1](-i)\frac{g^{\mu\nu} - \frac{q^\mu q^\nu}{M_i^2}}{q^2 - M_i^2 + iM_i\Gamma_i} \\ &\quad iE^P_{i1}P_\nu\frac{-i}{q''^2 - M_\phi^2}iE^P_{12}P_\alpha\epsilon^\alpha[p_3], \end{aligned} \tag{5.46}$$

where $iE^P_{i1}P_\nu$ and $iE^P_{12}P'_\alpha$ are vertex factors of $V_i\phi^P H$ and $\phi^P\phi^0 Z_L$ respectively given in table 5.5, and $P' = p_4 + q''$.

Table 5.18: The four point Feynman rules for $H\phi^0V_iV_j$ vertices. Their couplings are given in the form $iC^{H\phi^0}_{ij}g_{\mu\nu}$.

i/j	vertices	$iC^{H\phi^0}_{ij}g_{\mu\nu}$
1/1	$H\phi^0Z_LZ_L$	$\frac{3i}{2}\frac{g^2}{c_w^2}s_0g_{\mu\nu}$
1/2	$H\phi^0Z_HZ_L$	$-\frac{3i}{2}\frac{g^2}{c_w}\frac{(c^2-s^2)}{2sc}s_0g_{\mu\nu}$
1/3	$H\phi^0A_HZ_L$	$-\frac{3i}{2}\frac{gg'}{c_w}\frac{(c'^2-s'^2)}{2s'c'}s_0g_{\mu\nu}$
1/4	$H\phi^0A_LZ_L$	0

For this process the differential cross sections with respect to energy of the Z_L boson for different values of s/s' are plotted in figure 5.23 at $\sqrt{S} = 2TeV$ for symmetry breaking scale $f = 1TeV$ and mass of the Higgs boson is $M_H = 120GeV$. The total cross sections for this process for the parameters of interest are presented in table 5.17. For the parameters $s/s' = 0.5/0.1$ the differential cross section is maximum at the order of $10^{-3}\frac{pb}{GeV}$ for $E_{Z_L} > 200GeV$. The corresponding cross section is found as $1.8pb$.

For the values of mixing parameters $s/s' = 0.8/0.6, 0.8/0.7, 0.95/0.6$, the differential cross section have nearly same behavior for $E_{Z_L} > 180GeV$ with a constant value of $5 \times 10^{-6}\frac{pb}{GeV}$ up to cut off determined by the kinematical constraints. The corresponding total cross section for these parameters sets are at the order of $3 \times 10^{-3}pb$.

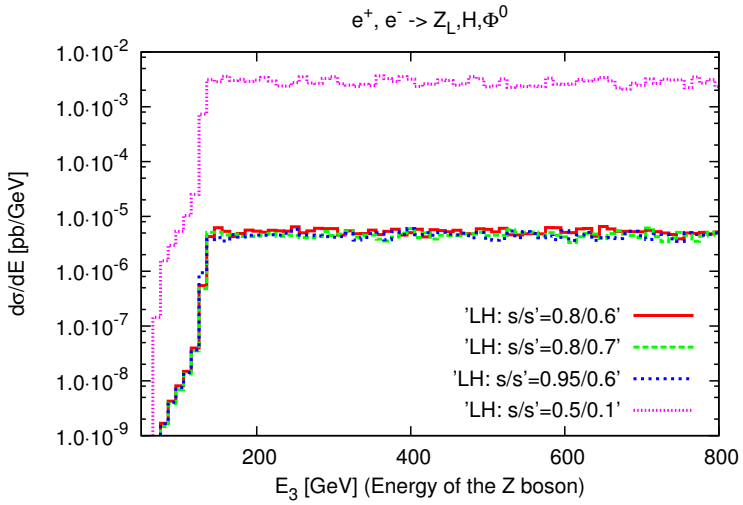

Figure 5.23: Differential cross section vs. E_Z graph for $e^+e^- \rightarrow Z_L\phi^0 H$, variations with respect to s/s' for $f = 1000GeV$ at $\sqrt{S} = 2000GeV$.

These results imply that for electroweak allowed parameters up to hundreds of events can be produced per year at $\sqrt{S} = 2GeV$. For parameters $s/s' = 0.5/0.1$ the number of events will be around 10^5 events per year, but this number can only be reached if the symmetry breaking scale is high enough to cover this parameter set, and the energy of the colliders should be high enough to cover region $f > 3TeV$.

In the final state this channel will provide signals such as Z_LHHH for the dominant decay of neutral scalar to Higgs couple. If the lepton number violating Yukawa coupling is high enough $Y \simeq 1$, the dominant decay of ϕ^0 will be to neutrinos such as; $\nu_i\nu_j + \bar{\nu}_i\bar{\nu}_j$. This will result in a signal of huge missing energy of the order of scalar mass.

5.4.2 $e^+e^- \rightarrow Z_LH\phi^P$

In this section the production of heavy pseudo scalar ϕ^P associated with standard model Higgs boson and heavy vector Z_L is analyzed. The production occurs due to the three point vector Higgs pseudo scalar vertices in the littlest Higgs model. Since the values of these couplings

are quite low, the final production rates are expected to be small.

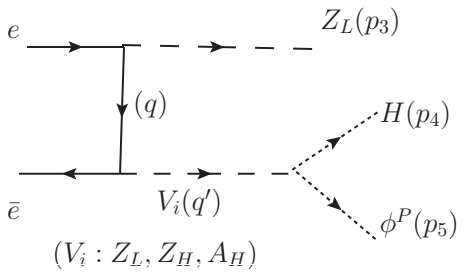

Figure 5.24: Feynman diagrams contributing to $e^+e^- \to Z_L H\phi^P$ in the littlest Higgsmodel.

The Feynman diagram contributing to process $e^+e^- \to Z_L H\phi^P$ is given in figure 5.24 (right), and the corresponding amplitude is given by:

$$\begin{aligned} M &= \sum_{i=1}^{3} \bar{u}[-p_2] i\gamma_\mu (g_{V_1} + g_{A_1}\gamma_5)\epsilon^\mu[p_3] \frac{\not{q}}{q^2} i\gamma_\nu (g_{V_i} + g_{A_i}\gamma_5) u[p_1] \\ &\quad \frac{g^{\nu\alpha} - \frac{q'^\alpha q^\nu}{M_i^2}}{q'^2 - M_i^2 + iM_i\Gamma_i} iE_{i1}^P P_\alpha, \end{aligned} \tag{5.47}$$

where $iE_{i1}^P P_\mu$ is the vertex factor of $V_i H\phi^P$ given in figure 5.5 and $P = q - q'$.

For this production process the differential cross sections are plotted with respect to energy of the Z_L boson and presented in figure 5.25. The values of total cross sections for the parameters of interest for symmetry breaking scale $f = 1TeV$ are given in table 5.17. It is seen that even for $s/s' = 0.5/0.1$, the differential cross section is at the order of $10^{-7}\frac{pb}{GeV}$ corresponding to the cross section of $3.5 \times 10^{-4} pb$. For values of s/s' allowed by electroweak precision data, the total cross section is only at the order of $10^{-7} pb$. This results implies that this production channel is out of reach for near future electron colliders.

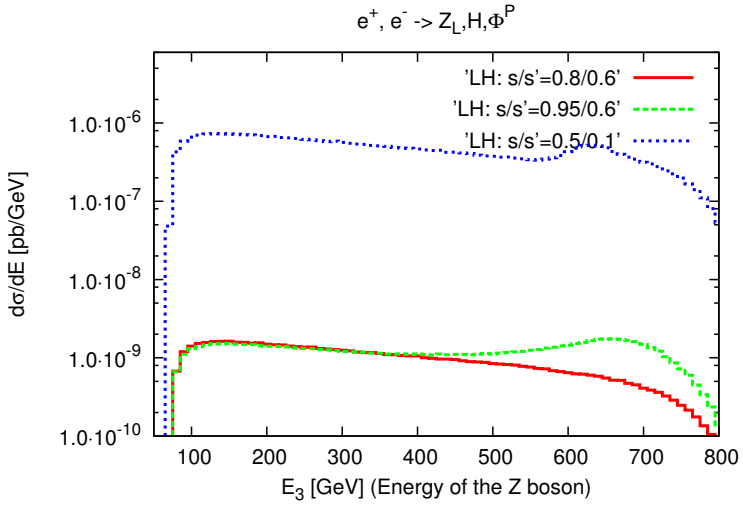

Figure 5.25: Differential cross section vs. E_Z graph for $e^+e^- \rightarrow Z_L H\phi^P$, variations with respect to s/s' for $f = 1000GeV$ at $\sqrt{S} = 2TeV$.

CHAPTER 6

DIRECT PRODUCTION OF SCALARS AT e^+e^- COLLIDERS

In this section, the direct production of scalars without a vector in electron colliders is analyzed. In the littlest Higgs model, the direct productions of all scalars are not allowed at e^+e^- collisions at tree level. The only possible productions are; $H\phi^P$, $\phi^0\phi^P$ and the double productions of charged scalars. These production processes are due to existence of vector scalar vertices.

In the littlest Higgs model the neutral scalar and pseudo scalar ϕ^0 and ϕ^P behaves similar, having same masses, same decay modes and decay widths. One way to distinguish them experimentally is observing ϕ^P with H since H associated production of ϕ^0 is not allowed in the model. The direct production of charged scalars is also important, because they provide direct lepton number and flavor violating signals free from any backgrounds.

6.1 Neutral scalars

6.1.1 $e^+e^- \to H\phi^P$

In the littlest Higgs model the direct production of $\phi^P H$ couple is significant because it will provide signals to distinguish ϕ^P from ϕ^0 . It will be presented here that, for low symmetry breaking scales this channel would be accessible even for ILC. The Feynman diagrams contributing to this process are presented in figure 6.1.

The amplitude corresponding to Feynman diagram in figure 6.1 contributing to Higgs associated ϕ^P production at the s channel is written as:

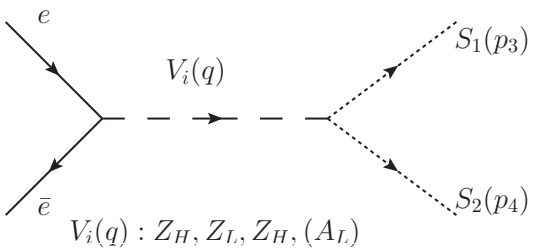

Figure 6.1: Feynman diagrams contributing to $e^+e^- \to S_1S_2$ processes in littlest Higgs model. $S_1 - S_2 : H - \phi^P, \phi^0 - \phi^P, \phi^+ - \phi^-, \phi^{++} - \phi^{--}$ and A_L contributes to charged productions only.

$$M = \sum_{i=1}^{3} \bar{u}[-p_2] i\gamma_\mu (g_{V_i} + g_{A_i}\gamma_5) u[p_1] \; i\frac{g^{\mu\alpha} - \frac{q^\alpha q^\mu}{M_i^2}}{q^2 - M_i^2 + iM_i\Gamma_i} iE_{i1}^P P_\alpha, \tag{6.1}$$

where $iE_{i1}^P P_\mu$ is the vertex factor of $V_i H \phi^P$ given in figure 5.5 and $P = p_3 - p_4$.

For this process, total cross section versus energy graphs are presented in 6.2 for $f = 1TeV$. Production process is significant even for low energies such as $\sqrt{S} = 0.9 \sim 1TeV$ accessible for ILC. For parameters $s/s' = 0.8/0.6$, the cross section receives a maximum value of $10^{-4} pb$ resulting in 10 events per year. For parameters $s/s' = 0.8/0.7$ the cross section exhibits a peak due to heavy vector resonances at a value of $8 \times 10^{-4} pb$ at $\sqrt{S} = 1.1TeV$. This will result hundred of events produced per year accessible for both ILC and CLIC.

At the final state, the pseudo scalar will decay into neutrinos giving a high missing energy accompanying the Higgs boson.

6.1.2 $e^+e^- \to \phi^0\phi^P$

In the littlest Higgs model the scalar ϕ^0 and the pseudo scalar ϕ^P are degenerate in mass, and their properties are similar. They can also be produced via $e^+e^- \to \phi^0\phi^P$ process in electron colliders. The Feynman diagrams contributing to this process are given in figure 6.1.

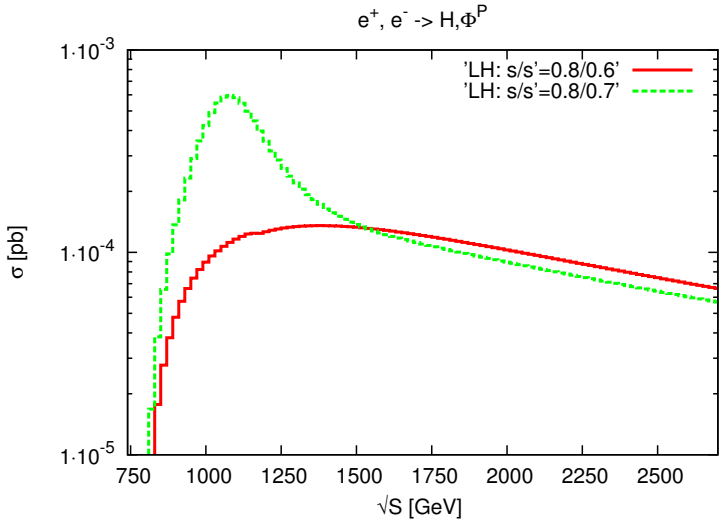

Figure 6.2: Total cross section vs. $\sqrt{S}$ graphs for $e^+e^- \to H\phi^P$, for parameters $f = 1000GeV$ and s/s'.

The amplitude corresponding to Feynman diagram in figure 6.1 contributing to $\phi^0\phi^P$ production is written by:

$$M = \sum_{i=1}^{3} \bar{u}[-p_2]i\gamma_\mu(g_{V_i} + g_{A_i}\gamma_5)u[p_1] \frac{g^{\mu\alpha} - \frac{q^\alpha q^\mu}{M_i^2}}{q^2 - M_i^2 + iM_i\Gamma_i} iE_i' P_\alpha, \tag{6.2}$$

where $iE_i'P_\mu$ is the vertex factor of $V_i\phi^0\phi^P$, $P = p_3 - p_4$, and $E_i' = E_{i2}^P$ are given in table 5.5.

The total cross section versus energy graphs for this production channel are presented in figure 6.3. For $f = 1TeV$ and mixing angles $s/s' = 0.8/0.6, 0.95/0.6$, the total cross section of the process reaches up to $10^{-2}pb$ implying that there will be $100 \sim 1000$ production events per year for luminosities $100fb^{-1}$ at electron colliders at energies $\sqrt{S} > 1.5TeV$.

The lepton violating decay modes of pseudo scalar and scalar are the same as they decay into neutrinos violating lepton number. But these violations cannot be observed at high energy colliders, since the only signature they can leave is the missing energy.

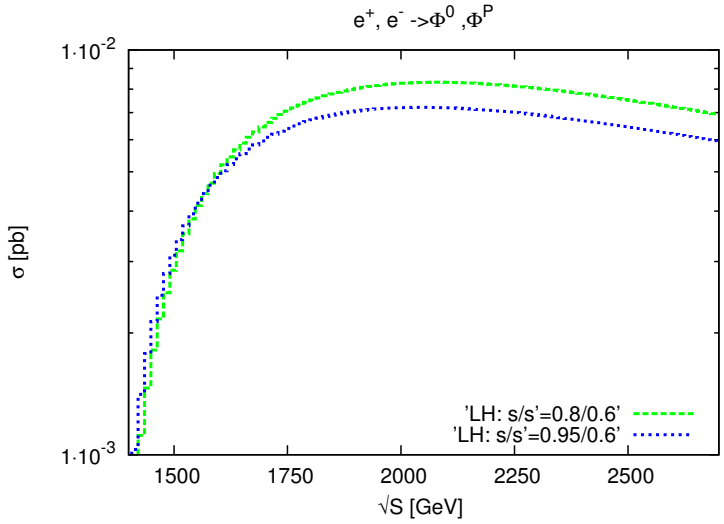

Figure 6.3: Total cross section vs. $\sqrt{S}$ graphs for $e^+e^- \to \phi^0\phi^P$, for parameters $f = 1000GeV$ and s/s'.

If the lepton number violation is not considered, or Yukawa coupling Y is not sufficient to produce violation signals, ϕ^0 dominantly decays into HH pair and ϕ^P to ZH pair. However the final state $ZHHH$ is dominated by a high background from standard model, and even if the Higgs is discovered and can be reconstructed, the final state analysis will be challenging.

6.2 Charged scalars

6.2.1 $e^+e^- \to \phi^+\phi^-$

In the littlest Higgs model neutral gauge bosons, including photon, have three point interaction vertices with charged scalars, enabling the production of charged scalars via $e^+e^- \to \phi^+\phi^-$ process at electron colliders. These process is strongly dependent on the littlest Higgs model parameter set $f/s/s'$ due to the vector single charged scalar couplings given in table 5.7.

The Feynman diagrams for s channel double production of single charged scalars are presented in figure 6.1. The amplitudes corresponding to these Feynman diagrams are written

as:

$$M_1 = \bar{u}[-p_2]i\gamma_\mu g_{V_4} u[p_1](i)\frac{g^{\alpha\mu}}{q^2} iE_4^{\phi\phi}(p_3 - p_4)_\alpha, \tag{6.3}$$

$$M_2 = \sum_{i=1}^{3} \bar{u}[-p_2]i\gamma_\mu(g_{V_i} + g_{A_i}\gamma_5)u[p_1] (i)\frac{g^{\alpha\mu} - \frac{q^\mu q^\alpha}{M_i^2}}{q^2 - M_i^2 + iM_i\Gamma_i} iE_i^{\phi\phi}(p_3 - p_4)_\alpha, \tag{6.4}$$

where $q = p_1 + p_2$ and coefficients $E_i^{\phi\phi}$ are given in table 5.7 and M_1 for the photon propagating diagram.

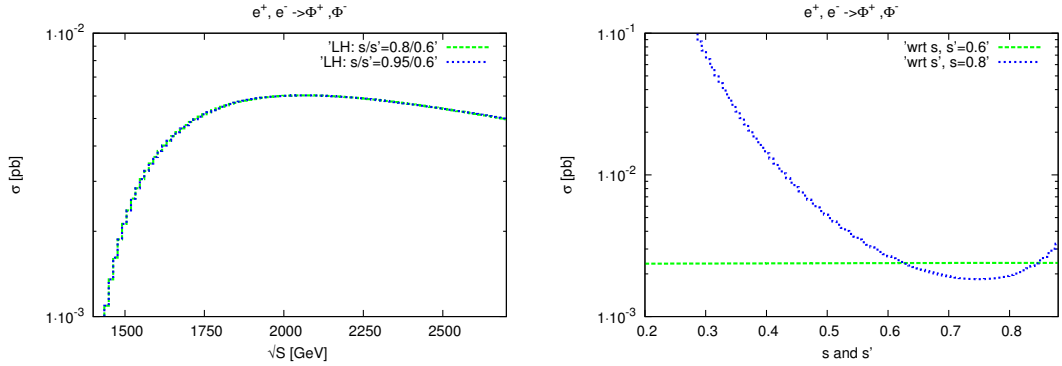

Figure 6.4: Total cross section vs. $\sqrt{S}$ graphs for $e^+e^- \to \phi^+\phi^-$, for parameters $f = 1000GeV$ and s/s'(left), and cross section vs. $s(s')$ graphs (right).

For this process the calculated cross sections are plotted in figure 6.4 with respect to center of mass energy. The dependence of total cross section on model parameters s/s' at $f = 1TeV$ are also presented in figure 6.4(right). It is seen that the change in the total cross section with respect to s is significant. On the other hand, the total cross section is strongly dependent on s', increasing up to order to two orders f magnitude at $f = 1TeV$.

Within the range of electroweak precision data, the direct production cross section gets a value of $8 \times 10^{-3} pb$ for $s/s' = 0.8/0.6, 0.95/0.6$ and $f = 1TeV$ for energies $\sqrt{S} > 1.5TeV$. This will give up to 800 productions per year for luminosities of $100 fb^{-1}$. For higher values of symmetry breaking scale parameter ($f > 1TeV$), the production process is not accessible for ILC and CLIC because of the kinematical constraints of high scalar mass.

At the final state, the lepton flavor violating signals of this channel will be $l_i^- \nu_i l_j^+ \bar{\nu}_j$, two leptons of same or different families plus missing energy of the neutrinos. If the leptons are from same generation such as $e^+e^-, \mu^-\mu^+$, the final state is not observed as a lepton number violating signal, even if it occurs by violating lepton number. The promising final state signatures are two leptons of different families plus missing energy, such as; $e^-\mu^+, \mu^-e^+$. The branching ratio of such signals are calculated as $\frac{2}{3} BR[Y]^2$, which is strongly dependent on Yukawa coupling Y. For high values of $Y \to 1$, this can give events up to a hundred lepton number violating final signatures.

If the lepton number violation is not considered, or the value of Y is close to zero, the charged couple of scalars will decay into SM vectors $W_L^\pm Z_L$ dominantly, giving a signal of $W_L^+ Z_L W_L^- Z_L$. At the final state the charged scalars can be reconstructed from $W_L^\pm Z_L$ invariant mass distributions.

6.2.2 $e^+e^- \to \phi^{++}\phi^{--}$

In the littlest Higgs model, as a consequence of new scalar triplet, there exist double charged scalars with interesting features. The existence of vector double charged scalar vertices in the model enables the charged scalars produced via $e^+e^- \to \phi^{++}\phi^{--}$ process in electron colliders.

The Feynman diagrams for s channel double production of double charged scalars are presented in figure 6.1. The amplitudes corresponding to these Feynman diagrams are written as:

$$\begin{aligned} M_1 &= \bar{u}[-p_2] i\gamma_\mu g_{V_4} u[p_1](i)\frac{g^{\alpha\mu}}{q^2} \\ &\quad iE_4'^{\phi\phi}(p_3 - p_4)_\alpha, \end{aligned} \tag{6.5}$$

$$M_2 = \sum_{i=1}^{3} \bar{u}[-p_2] i\gamma_\mu (g_{V_i} + g_{A_i}\gamma_5) u[p_1]$$
$$(i)\frac{g^{\alpha\mu} - \frac{q^\mu q^\alpha}{M_i^2}}{q^2 - M_i^2 + iM_i\Gamma_i} iE_i'^{\phi\phi}(p_3 - p_4)_\alpha, \quad (6.6)$$

where $q = p_1 + p_2$, and the vertex factors $E_i'^{\phi\phi}$ are given in table 5.11.

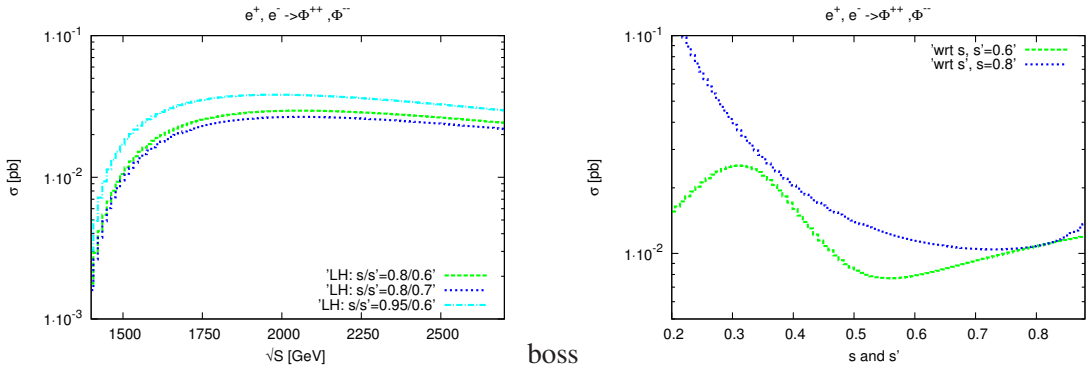

boss

Figure 6.5: Total cross section vs. $\sqrt{S}$ graphs for $e^+e^- \to \phi^{++}\phi^{--}$, for parameters $f = 1000GeV$ and s/s'(left), and cross section vs. $s(s')$ graphs (right).

For this process the total cross section of the production event at $f = 1TeV$ are analyzed. The dependence of the total cross section on the model parameters s/s' at $\sqrt{S} = 3TeV$ are presented in figure 6.5 (right). It is seen that the cross section is less sensitive to changes in s, but for changes in s' the total cross section increases rapidly with low values of s' by two orders of magnitude. The cross section versus total center of mass energy graphs are presented in figure 6.5(left) for parameters allowed by electroweak precision observables. The cross section of the production process gets remarkable values of the same order for parameters $s/s' = 0.8/0.6, 0.8/0.7, 0.95/0.6$ for energies $\sqrt{S} > 1.5TeV$ accessible in CLIC. The maximum value of cross section reaches to $3 \times 10^{-2} pb$ for the considered parameter sets resulting up to 3000 events produced per year for integrated luminosities of $100 fb^{-1}$.

If the lepton number violating final states are considered, for large values of Yukawa coupling $Y \simeq 1$, $\phi^{++}\phi^{--}$ couple will decay into $l_i l_i l_j^+ l_j^+$; four leptons violating lepton number by four,

and into $l_i l_i l_i^+ l_j^+$ and $l_i l_j l_j^+ l_j^+$ four leptons violating lepton number by two. The branching ratio of the final states violating lepton number by four such as $e^- e^- \mu^+ \mu^+$ is calculated as $BR^{l_i l_i l_j^+ l_j^+}(i \neq j) = \frac{2}{3} BR[Y]^2 \simeq 04$. This will result in 120 events per year for a luminosity of $100 fb^{-1}$ violating lepton number by four free from any backgrounds directly accessible for $\sqrt{S} > 1.5 TeV$. The final states such as $e^- e^+ e^- e^+$ also happens by violating lepton number by two at each scalar vertex, but can not be lepton number violation signals. Their branching ratio is calculated as $BR^{l_i l_i l_i^+ l_i^+} = \frac{1}{3} BR[Y]^2$.

For the final states violating lepton number by two such as $e^- e^+ e^- \mu^+$, the branching ratios are dependent on the flavor mixing Yukawa coupling Y', and calculated as $BR^{l_i l_i l_i^+ l_j^+} = BR[Y] \times BR[Y']$. For $Y' \geq 0.01$ the branching ratios will reach up to 2% resulting tens of accessible events per year.

The final states $l_i l_j l_i^+ l_j^+$ occur by violating lepton number by two at each scalar decay, but can not be observed as violation signals. Also these kind of events are not accessible due to the strong dependence on Y'.

This channel will also provide lepton number violation by two for even low values of Yukawa coupling Y, such as $Y \simeq 0.1$. For these values the charged scalars decay into $W_L^\pm W_L^\pm$ dominantly with a branching ratio of 0.9 and to leptons with a branching ratio of 0.1. At the final state tens of signals such as $W_L^+ W_L^+ e^- e^-$ can be achieved per year for $Y \simeq 0.1$ and 50 signals per year for $Y \simeq 0.4$ accessible at energies $\sqrt{S} > 1.5 TeV$.

If the lepton number violation is not considered, or the Yukawa coupling Y is not sufficient to produce violation ($Y < 0.1$), the double charged scalar will decay in to $W_L^+ W_L^+ W_L^- W_L^-$. The scalars in this case can be reconstructed from invariant mass of same sign W_L bosons.

Finally, this direct production process is in the reach for observing double charged scalars. And for $0.1 \leq Y \leq 1$ lepton number violations by number four and two are accessible for energies $\sqrt{S} > 1.5 TeV$ accessible at CLIC.

CHAPTER 7

CONCLUSION

In this thesis, the scalar phenomenology of the littlest Higgs model at e^+e^- colliders is studied. The dependance of cross sections and number of production events on model parameters s, s' and f are analyzed. Also possible lepton flavor violating signals are examined.

For the processes that exist at the SM, such as $e^+e^- \rightarrow Z_L H(H)$, it is found that the effects of the model, so called the resonances of the new heavy gauge bosons can be seen in decays into SM Higgs boson. The littlest Higgs model can be well understood if these effects can be observed at future colliders.

For the associated production of new heavy scalars with SM Higgs bosons, with or without SM vector boson Z_L, it is shown that the cross sections and the event rates are not remarkable.

For the production of neutral heavy scalars associated with Z_L, the production rates are dependant on the mass of the scalar and so on the symmetry breaking scale f, and the mixing angles s, s'. The production of ϕ^0 via $e^+e^- \rightarrow Z_L\phi^0$ shows a vector resonance at $\sqrt{S} \simeq 1TeV$ for $f = 1TeV$ and $s/s' = 0.95/0.6$ corresponding to heavy gauge boson Z_H. In this channel, the production is achieved for $\sqrt{S} > 0.75TeV$ for $f = 1TeV$ with a cross section of order $10^{-3}pb$, and for $\sqrt{S} > 1.8TeV$ for $f = 2.64TeV$ with a cross section of order $10^{-4}pb$. For the production of scalar and pseudo scalar pairs, the processes can happen at energies $\sqrt{S} > 2TeV$ for low symmetry breaking scale values, $f = 1TeV$, and reach production cross sections up to the order of $10^{-4}pb$ for electroweak allowed values of mixing angles. The value of the rates for the production of $\phi^0\phi^P$ associated with Z_L are reduced by one order. The expected number of production events is about $10 \sim 100$ for single ϕ^0, and pairs of $\phi^0\phi^0$ and $\phi^P\phi^P$ at luminosities $100fb^{-1}$, and at the order of one for $\phi^0\phi^P$ couple. At the final state, the scalar

and the pseudo scalar decays in to neutrino couples violating lepton flavor, if the value of the Yukawa coupling Y is close to one, else to SM Higgs and Z_L pairs.

The most interesting results are found in the charged sector. For the production of charged couple associated with Z_L, it is found that at an e^+e^- collider of $\sqrt{S} \geq 2TeV$ with a luminosity of $100fb^{-1}$, the Z_L associated production of charged scalars will be in the reach, being the single charged pair is quite challenging due to low production rates, and the production of doubly charged scalar pair is more promising for the electroweak allowed parameters at $f = 1TeV$. The final states will contain lepton flavor violating signals if the value of Yukawa coupling Y is close to unity. For larger values of f the mixing angles s/s' are less constrained, e.g. for $f = 5TeV$ and $s/s' = 0.6/0.4$, the production rates increases allowing remarkable final lepton number violating events for $0.1 \leq Y \leq 1$, but for these set of parameters the center of mass energy of the colliders should be increased.

For the direct production of charged scalars, the cross sections for pair production of charged and doubly charged Higgs bosons exhibits strong dependence on the value of s', and for $s' \leq 0.5$ the cross section increases up to order two when values of s' is decreasing. For the process $e^+e^- \rightarrow \phi^+\phi^-$, the cross section reaches a value of $8 \times 10^{-3} pb$, and therefore around 800 per year are expected at a luminosity of $100fb^{-1}$. Depending on the values of Y and Y', the final states can be leptonic such as $l_i\nu_i\bar{l}_i\bar{\nu}_i$ and $l_i\nu_i\bar{l}_j\bar{\nu}_j$. For $Y \simeq 1$ the branching ratio to leptonic modes is as high as 0.6 giving hundreds of final leptonic signals for $\sqrt{S} \geq 1.7TeV$. The pair production of doubly charged scalars via $e^+e^- \rightarrow \phi^{++}\phi^{--}$, the maximum of the cross section is $3 \times 10^{-2} pb$ for $s/s' : 0.95/0.6$, and results in 3000 events are expected for per year at luminosities of $100fb^{-1}$ for $\sqrt{S} \geq 1.7TeV$. The final state decay modes of the doubly charged pair is leptonic, semi leptonic or bosonic, depending on Y and Y'. For $Y \simeq 1$ final signal will be four leptons; two leptons and two anti leptons dominantly. It is found that the most interesting modes are the semi leptonic signals; $l_il_iW_L^+Z_L(W_L^+H)$, produced when $Y \simeq 0.2$ violating the lepton number by two giving 600 events per year. Finally, the pair production of charged scalars can occur in future e^+e^- colliders at $\sqrt{S} \geq 1.7TeV$. At the final state final lepton flavor and number violating modes are reachable if the Yukawa coupling $Y > 0.1$.

In conclusion, the littlest Higgs model, can be detected at e^+e^- colliders. The neutral heavy scalars will be produced but the final states will be challenging to analyze, since they do not carry charge. For charged scalars, the productions will be achieved, and they will provide

unique collider signals.

The results of this thesis are either published or to be published as following articles:

1. A. Çağıl and M. T. Zeyrek, *"Z_L associated pair production of charged Higgs bosons in the littlest Higgs model at e^+e^- colliders"*, Phys.Rev.**D80**(2009)055021, `arXiv/hep-ph:0908.3581`.

2. A. Çağıl and M. T. Zeyrek, *"Analyzing the neutral scalar productions associated with Z_L in the littlest Higgs model at ILC and CLIC"*, to be submitted.

3. A. Çağıl, *"Pair production of charged scalars in the littlest Higgs model at e^+e^- colliders"*, to be submitted.

REFERENCES

[1] N. Arkani-Hamed, A.G. Cohen, E. Katz, and A.E. Nelson, JHEP**0207**(2002)034, arXiv:hep-ph/0206021.

[2] N. Arkani-Hamed *et al.*, JHEP**0208**(2002)021, arXiv:hep-ph/0206020.

[3] M. Schmaltz, Nucl.Phys.Proc.Suppl.**117**(2003),arXiv:hep-ph/0210415.

[4] D.E.Kaplan and M. Schmaltz, JHEP**0310**(2003)039, arXiv:hep-ph/0302049.

[5] M. Perelstein, Prog.Part.Nucl.Phys.**58**(2007)247-291, arXiv:hep-ph/0512128.

[6] T. Han, H. E. Logan, B. McElrath and L-T. Wang, Phys.Rev. **D67**(2003)095004, arXiv:hep-ph/0301040.

[7] M. Schmaltz and D. Tucker-Smith, Ann.Rev.Nucl.Part.Sci.**55**(2005)229-270, arXiv:hep-ph/0502182.

[8] H. Georgi, *Weak Interactions And Modern Particle Theory*, Menlo Park: Benjamin/Cummings, 1984.

[9] J. Hubisz, P. Maeda, A. Noble and M. Perelstein, JHEP**01**(2006)135.

[10] J. L. Hewett, F. J. Petriello and T. G. Rizzo, JHEP **0310** (2003) 062 , arXiv:hep-ph/0211218.

[11] T. Aaltonen, *et al*, CDF Collaboration, Phys.Rev.Lett.99:171802,2007.

[12] M-C. Chen and S. Dawson, Phys.Rev.**D70**(2004)015003, arXiv:hep-ph/0311032.

[13] W. Killian and J. Reuter, Phys.Rev. **D70** (2004) 015004, arXiv:hep-ph/0311095.

[14] A.G. Dias, C.A. de S. Pires P.S. Rodrigues da Silva, Phys.Rev.**D77**(2008)055001, arXiv:hep-ph/0711.1154.

[15] C. Csaki, J. Hubisz, G. D. Kribs, P. Maede and J. Terning, Phys.Rev. **D68** (2003) 035009 , arXiv:hep-ph/0303236.

[16] G. Azuelos *et al.*, Eur. Phys. J. C. **3952** (2005) 13.

[17] F. Ledroit, AIPConf.Proc.**903**(2007)245-248, arXiv:hep-ex/0610005.

[18] W. Kilian, D. Rainwater and J. Reuter, Phys. Rev. D **74**, 095003 (2006), arXiv:hep-ph/0609119.

[19] C-X. Yue, W. Yang and F. Zhang, Nucl.Phys. **B716** (2005) 199-214, arXiv:hep-ph/0409066.

[20] O. C. W. Kong, Phys.Rev.**D70**(2004)075021, arXiv:hep-ph/0409238, O. C. W. Kong,"*Talk given at 12th International Conference on Supersymmetry and Unification of Fundamental Interactions (SUSY 04), Tsukuba, Japan, June 2004*", arXiv:hep-ph/0409211.

[21] G.A. Gonzales-Sprinberg, R. Martinez and J-A. Rodriguez, Phys.Rev. **D71** (2005) 035003, arXiv:hep-ph/0406178.

[22] C-X. Yue, W. Yang and F. Zhang,Nucl.Phys. **B716** (2005) 199-214, arXiv:hep-ph/0409066.

[23] G-C. Cho and A. Omote, Talk given at the *International Conference on Linear Colliders*, LCWS04, 19-23 April 2004, Paris, France, arXiv:hep-ph/0408270.

[24] C-X. Yue, S. Zhao and W. Ma, Nucl.Phys.**B784**(2007)36-48, arXiv:hep-ph/0706.0232.

[25] C-X. Yue, S. Yang and L-H. Wang, Europhys.Lett.76(2006)381-387, arXiv:hep-ph/0609107.

[26] C-X. Yue, S. Wang and D. Yu, Phys.Rev. **D68** (2003) 115004, arXiv:hep-ph/0309113.

[27] C-X. Yue, L-L Due and X-L. Wang, J.Phys.**G33**(2007)577-586, arXiv:hep-ph/0609208.

[28] C-X. Yue, W. Wang, Z-J. Zong and F. Zhang, Eur.Phys.J.**C42**(2005)331-339, arXiv:hep-ph/0504253.

[29] X. Wang, Q. Zeng, Z. Jin and S. Liu, arXiv:hep-ph/0702064.

[30] F. M. L. de Almeida Jr., Y. A. Coutinho, J. A. Martins Simoes, A.J. Ramalho, S. Wulck and M. A. B. do Vale, arXiv:hep-ph/0702137.

[31] X. Wang, J. Chen, Y. Liu and H. Yang, Phys.Rev.**D74**(2006)015006, arXiv:hep-ph/0606093.

[32] C-X. Yue, W. Wang and F. Zhang, Nucl.Phys. **B716** (2005) 199-214 , arXiv:hep-ph/0409066.

[33] T. M. Aliev, O. Cakir, Eur.Phys.J.C54:149-158(2008), arXiv:hep-ph/0707.3096.

[34] A. J. Buras, A. Poschenrieder and S. Uhlig, Nucl. Phys. B **716**, 173 (2005) [arXiv:hep-ph/0410309].

[35] A. J. Buras, A. Poschenrieder and S. Uhlig, TUM-HEP-573-05, Jan 2005, arXiv:hep-ph/0501230.

[36] S. R. Choudhury, N. Gaur, A. Goyal and N. Mahajan, Phys. Lett. B **601**, 164 (2004) [arXiv:hep-ph/0407050].

[37] S. R. Choudhury, N. Gaur, G. C. Joshi and B. H. J. McKellar, arXiv:hep-ph/0408125.

[38] W. j. Huo and S. h. Zhu, Phys. Rev. D **68**, 097301 (2003) [arXiv:hep-ph/0306029].

[39] J. Y. Lee, JHEP **0412**, 065 (2004) [arXiv:hep-ph/0408362].

[40] T. Han, H.E. Logan, B. Mukhopadhyaya and R. Srikanth, Phys.Rev. **D72** (2005) 053007 , arXiv:hep-ph/0505260.

[41] S.R. Choudhury, N. Gaur and A. Goyal, Phys.Rev. **D72** (2005) 097702 , arXiv:hep-ph/0508146.

[42] C-X. Yue and S. Zhao, Eur.Phys.J.**C50**(2007)897-903, arXiv:hep-ph/0701017.

[43] S.R. Choudhury *et al.*, Phys.Rev.**D75**(2007)055011, arXiv:hep-ph/0612327.

[44] G.L. Fogli *et al*, Phys. Rev. D**70**, 113003(2004); M. Tegmark *et al*, SDSS Collabration, Phys. Rev. D**69**, 103501(2004).

[45] J. Brau (Ed.) *et al*, By ILC Collaboration, *LC Reference Design Report: ILC Global Design Effort and World Wide Study.*, FERMILAB-APC, Aug 2007, arXiv:acc-ph/0712.1950.

[46] R.W. Assmann *et al.*, The CLIC Study Team, *A 3 TeV e^+e^- linear collider based on CLIC technology*, CERN 2000-008, Geneva, 2000; E. Accomando *et al.*, By CLIC Physics Working Group, *Physics at the CLIC multi-TeV linear collider.*, CERN-2004-005, arXiv:hep-ph/0412251; H. Braun *et al.*, By CLIC Study Team, *CLIC 2008 parameters*, CERN-OPEN-2008-021, CLIC-NOTE-764.

[47] T.N.P.H. working group, for CDF and DØ collabrations, arXiv:hep-ex/0903.4001

[48] J. Ellis, lectures given in *"SUSPE65, Scottish Universities Summer School in Physics"*, August 2009, St. Andrews, Scotland.

[49] S. R. Coleman and E. Weinberg, Phys. Rev. D **7**, 1888 (1973).

[50] H. C. Cheng and I. Low, JHEP **0309**, 051 (2003) [arXiv:hep-ph/0308199].

[51] H. C. Cheng and I. Low, JHEP **0408**, 061 (2004) [arXiv:hep-ph/0405243].

[52] I. Low, JHEP **0410**, 067 (2004) [arXiv:hep-ph/0409025].

[53] J. Hubisz and P. Meade, Phys. Rev. D **71**, 035016 (2005) [arXiv:hep-ph/0411264].

[54] H. C. Cheng, I. Low and L. T. Wang, arXiv:hep-ph/0510225.

[55] C. Amsler et al. (Particle Data Group), Phys. Lett. B**667**(2008)1.

[56] A. Pukhov *et al.*, CalcHEP/CompHEP Collab., hep-ph/9908288 ; hep-ph/0412191.

[57] A. Çağıl and M. T. Zeyrek, Phys.Rev.**D80**(2009)055021, arXiv/hep-ph:0908.3581.

APPENDIX A

FEYNMAN RULES FOR THE LITTLEST HIGGS MODEL

The Feynman rules are taken from reference [6]. In these Feynman rules, all particles are the mass eigenstates, and are assumed to be outgoing.

The three point interaction vertices are given in tables A.1 and A.2. The four point interaction vertices are given in tables A.3 and A.4. The scalar-fermion couplings are listed in Table A.8.

The gauge boson self-couplings are given as follows, with all momenta out-going. The three-point couplings take the form:

$$V_1^\mu(k_1)V_2^\nu(k_2)V_3^\rho(k_3): \quad -ig_{V_1V_2V_3}\left[g^{\mu\nu}(k_1-k_2)^\rho + g^{\nu\rho}(k_2-k_3)^\mu + g^{\rho\mu}(k_3-k_1)^\nu\right]. \tag{A.1}$$

The four-point couplings take the form:

$$\begin{aligned} W_1^{+\mu}W_2^{+\nu}W_3^{-\rho}W_4^{-\sigma}: &\qquad -ig_{W_1^+W_2^+W_3^-W_4^-}(2g^{\mu\nu}g^{\rho\sigma} - g^{\mu\rho}g^{\nu\sigma} - g^{\nu\rho}g^{\mu\sigma}) \\ V_1^\mu V_2^\nu W_1^{+\rho}W_2^{-\sigma}: &\qquad ig_{V_1V_2W_1^+W_2^-}(2g^{\mu\nu}g^{\rho\sigma} - g^{\mu\rho}g^{\nu\sigma} - g^{\nu\rho}g^{\mu\sigma}). \end{aligned} \tag{A.2}$$

The coefficients $g_{V_1V_2V_3}$, $g_{V_1V_2W_1^+W_2^-}$ and $g_{W_1^+W_2^+W_3^-W_4^-}$ are given in Table A.5.

The couplings between gauge bosons and fermions are given in Tables A.6 and A.7. The charged gauge boson couplings to fermions in Table A.6 are all left-handed. It is defined as; $x_L \equiv \lambda_1^2/(\lambda_1^2+\lambda_2^2)$ to shorten the notation.

For the neutral gauge bosons in Table A.7, we write the couplings to fermions in the form $i\gamma^\mu(g_V + g_A\gamma^5)$. The fermions are charged under the two $U(1)$ groups . The additional requirement that the two $U(1)$ groups be anomaly-free fixes $y_u = -2/5$ and $y_e = 3/5$.

Table A.1: Three-point couplings of two gauge bosons to one scalar. All particles are the mass eigenstates.

particles	vertices	particles	vertices
$W^+_{L\mu}W^-_{L\nu}H$	$\frac{i}{2}g^2 v g_{\mu\nu}\left(1-\frac{v^2}{3f^2}+\right.$ $\left.\frac{1}{2}(c^2-s^2)^2\frac{v^2}{f^2}-\frac{1}{2}s_0^2-2\sqrt{2}s_0\frac{v'}{v}\right)$	$W^+_{H\mu}W^-_{H\nu}H$	$-\frac{i}{2}g^2 v g_{\mu\nu}$
$Z_{L\mu}Z_{L\nu}H$	$\frac{i}{2}\frac{g^2}{c_w^2}v g_{\mu\nu}\left(1-\frac{v^2}{3f^2}-\frac{1}{2}s_0^2+4\sqrt{2}s_0\frac{v'}{v}\right.$ $\left.-\frac{1}{2}\left((c^2-s^2)^2+5(c'^2-s'^2)^2\right)\frac{v^2}{f^2}\right)$	$Z_{H\mu}Z_{H\nu}H$ $A_{H\mu}A_{H\nu}H$	$-\frac{i}{2}g^2 v g_{\mu\nu}$ $-\frac{i}{2}g'^2 v g_{\mu\nu}$
$W^+_{L\mu}W^-_{H\nu}H$	$-\frac{i}{2}g^2\frac{(c^2-s^2)}{2sc}v g_{\mu\nu}$	$Z_{L\mu}Z_{H\nu}H$	$-\frac{i}{2}\frac{g^2}{c_w}\frac{(c^2-s^2)}{2sc}v g_{\mu\nu}$
$Z_{L\mu}A_{H\nu}H$	$-\frac{i}{2}\frac{gg'}{c_w}\frac{(c'^2-s'^2)}{2s'c'}v g_{\mu\nu}$	$Z_{H\mu}A_{H\nu}H$	$-\frac{i}{4}gg'\frac{(c^2s'^2+s^2c'^2)}{scs'c'}v g_{\mu\nu}$
$W^+_{L\mu}W^-_{L\nu}\Phi^0$	$-\frac{i}{2}g^2(s_0 v-2\sqrt{2}v')g_{\mu\nu}$	$W^+_{H\mu}W^-_{H\nu}\Phi^0$	$\frac{i}{2}g^2(s_0 v-2\sqrt{2}v')g_{\mu\nu}$
$W^+_{L\mu}W^-_{H\nu}\Phi^0$	$\frac{i}{2}g^2\frac{(c^2-s^2)}{2sc}(s_0 v-2\sqrt{2}v')g_{\mu\nu}$		
$Z_{L\mu}Z_{L\nu}\Phi^0$	$-\frac{i}{2}\frac{g^2}{c_w^2}(v s_0-4\sqrt{2}v')g_{\mu\nu}$	$Z_{H\mu}Z_{H\nu}\Phi^0$	$\frac{i}{2}g^2\left(v s_0+\frac{(c^2-s^2)^2}{s^2c^2}\sqrt{2}v'\right)g_{\mu\nu}$
$Z_{L\mu}Z_{H\nu}\Phi^0$	$\frac{i}{2}\frac{g^2}{c_w}\frac{(c^2-s^2)}{2sc}(v s_0-4\sqrt{2}v')g_{\mu\nu}$	$Z_{L\mu}A_{H\nu}\Phi^0$	$\frac{i}{2}\frac{gg'}{c_w}\frac{(c'^2-s'^2)}{2s'c'}(v s_0-4\sqrt{2}v')g_{\mu\nu}$
$A_{H\mu}Z_{H\nu}\Phi^0$	$\frac{i}{4}gg'\frac{1}{scs'c'}\left((c^2s'^2+s^2c'^2)v s_0\right.$ $\left.+2\sqrt{2}(c^2-s^2)(c'^2-s'^2)v'\right)g_{\mu\nu}$	$A_{H\mu}A_{H\nu}\Phi^0$	$\frac{i}{2}g'^2\left(v s_0+\frac{(c'^2-s'^2)^2}{s'^2c'^2}\sqrt{2}v'\right)g_{\mu\nu}$
$W^+_{L\mu}A_{L\nu}\Phi^-$	0	$W^+_{H\mu}A_{L\nu}\Phi^-$	0
$W^+_{L\mu}Z_{L\nu}\Phi^-$	$-i\frac{g^2}{c_w}v' g_{\mu\nu}$	$W^+_{H\mu}Z_{L\nu}\Phi^-$	$i\frac{g^2}{c_w}\frac{(c^2-s^2)}{2sc}v' g_{\mu\nu}$
$W^+_{L\mu}A_{H\nu}\Phi^-$	$-\frac{i}{2}gg'\frac{(c'^2-s'^2)}{2s'c'}(v s_+-4v')g_{\mu\nu}$	$W^+_{H\mu}A_{H\nu}\Phi^-$	$-\frac{i}{2}gg'\frac{(c^2c'^2+s^2s'^2)}{scs'c'}v' g_{\mu\nu}$
$W^+_{L\mu}Z_{H\nu}\Phi^-$	$ig^2\frac{(c^2-s^2)}{2sc}v' g_{\mu\nu}$	$W^+_{H\mu}Z_{H\nu}\Phi^-$	$-ig^2\frac{(c^4+s^4)}{2s^2c^2}v' g_{\mu\nu}$
$W^+_{L\mu}W^+_{L\nu}\Phi^{--}$	$2ig^2 v' g_{\mu\nu}$	$W^+_{H\mu}W^+_{H\nu}\Phi^{--}$	$2ig^2\frac{(c^4+s^4)}{2s^2c^2}v' g_{\mu\nu}$
$W^+_{L\mu}W^+_{H\nu}\Phi^{--}$	$-2ig^2\frac{(c^2-s^2)}{2sc}v' g_{\mu\nu}$		

Table A.2: Three-point couplings of one gauge boson to two scalars. The momenta are assigned according to $V_\mu S_1(p_1)S_2(p_2)$. All particles are the mass eigenstates and all momenta are out-going.

particles	vertices	particles	vertices
$W^+_{L\mu}H\Phi^-$	$-\frac{ig}{2}\left(\sqrt{2}s_0 - s_+\right)(p_1-p_2)_\mu$	$W^+_{H\mu}H\Phi^-$	$\frac{ig}{2}\frac{(c^2-s^2)}{2sc}\left(\sqrt{2}s_0 - s_+\right)(p_1-p_2)_\mu$
$W^+_{L\mu}\Phi^0\Phi^-$	$-\frac{ig}{\sqrt{2}}(p_1-p_2)_\mu$	$W^+_{H\mu}\Phi^0\Phi^-$	$\frac{ig}{\sqrt{2}}\frac{(c^2-s^2)}{2sc}(p_1-p_2)_\mu$
$W^+_{L\mu}\Phi^P\Phi^-$	$\frac{g}{\sqrt{2}}(p_1-p_2)_\mu$	$W^+_{H\mu}\Phi^P\Phi^-$	$-\frac{g}{\sqrt{2}}\frac{(c^2-s^2)}{2sc}(p_1-p_2)_\mu$
$W^+_{L\mu}\Phi^+\Phi^{--}$	$-ig(p_1-p_2)_\mu$	$W^+_{H\mu}\Phi^+\Phi^{--}$	$ig\frac{(c^2-s^2)}{2sc}(p_1-p_2)_\mu$
$A_{L\mu}H\Phi^P$	0	$A_{H\mu}H\Phi^P$	$-\frac{1}{2}g'\frac{(c'^2-s'^2)}{2s'c'}(s_P-2s_0)(p_1-p_2)_\mu$
$A_{L\mu}\Phi^0\Phi^P$	0	$A_{H\mu}\Phi^0\Phi^P$	$g'\frac{(c'^2-s'^2)}{2s'c'}(p_1-p_2)_\mu$
$A_{L\mu}\Phi^+\Phi^-$	$-ie(p_1-p_2)_\mu$	$A_{H\mu}\Phi^+\Phi^-$	$ig'\frac{(c'^2-s'^2)}{2s'c'}(p_1-p_2)_\mu$
$A_{L\mu}\Phi^{++}\Phi^{--}$	$-2ie(p_1-p_2)_\mu$	$A_{H\mu}\Phi^{++}\Phi^{--}$	$ig'\frac{(c'^2-s'^2)}{2s'c'}(p_1-p_2)_\mu$
$Z_{L\mu}H\Phi^P$	$\frac{1}{2}\frac{g}{c_w}(s_P-2s_0)(p_1-p_2)_\mu$	$Z_{H\mu}H\Phi^P$	$-\frac{1}{2}g\frac{(c^2-s^2)}{2sc}(s_P-2s_0)(p_1-p_2)_\mu$
$Z_{L\mu}\Phi^0\Phi^P$	$-\frac{g}{c_w}(p_1-p_2)_\mu$	$Z_{H\mu}\Phi^0\Phi^P$	$g\frac{(c^2-s^2)}{2sc}(p_1-p_2)_\mu$
$Z_{L\mu}\Phi^+\Phi^-$	$i\frac{g}{c_w}s_w^2(p_1-p_2)_\mu$	$Z_{H\mu}\Phi^+\Phi^-$	$O(v^2/f^2)$
$Z_{L\mu}\Phi^{++}\Phi^{--}$	$-i\frac{g}{c_w}\left(1-2s_w^2\right)(p_1-p_2)_\mu$	$Z_{H\mu}\Phi^{++}\Phi^{--}$	$ig\frac{(c^2-s^2)}{2sc}(p_1-p_2)_\mu$

Table A.3: Four-point gauge boson-scalar couplings.

particles	vertices	particles	vertices
$W^+_{L\mu}W^-_{L\nu}HH$	$\frac{i}{2}g^2 g_{\mu\nu} + O(v^2/f^2)$	$W^+_{H\mu}W^-_{H\nu}HH$	$-\frac{i}{2}g^2 g_{\mu\nu}$
$Z_{L\mu}Z_{L\nu}HH$	$\frac{i}{2}\frac{g^2}{c_w^2} g_{\mu\nu} + O(v^2/f^2)$	$Z_{H\mu}Z_{H\nu}HH$	$-\frac{i}{2}g^2 g_{\mu\nu}$
		$A_{H\mu}A_{H\nu}HH$	$-\frac{i}{2}g'^2 g_{\mu\nu}$
$W^+_{L\mu}W^-_{H\nu}HH$	$-\frac{i}{2}g^2\frac{(c^2-s^2)}{2sc} g_{\mu\nu}$	$Z_{L\mu}Z_{H\nu}HH$	$-\frac{i}{2}\frac{g^2}{c_w}\frac{(c^2-s^2)}{2sc} g_{\mu\nu}$
$Z_{L\mu}A_{H\nu}HH$	$-\frac{i}{2}\frac{gg'}{c_w}\frac{(c'^2-s'^2)}{2s'c'} g_{\mu\nu}$	$Z_{H\mu}A_{H\nu}HH$	$-\frac{i}{4}gg'\frac{(c^2s'^2+s^2c'^2)}{scs'c'} g_{\mu\nu}$
$W^+_{L\mu}W^-_{L\nu}H\Phi^0$	$\frac{i}{2}g^2 s_0 g_{\mu\nu}$	$W^+_{H\mu}W^-_{H\nu}H\Phi^0$	$-\frac{i}{2}g^2 s_0 g_{\mu\nu}$
$Z_{L\mu}Z_{L\nu}H\Phi^0$	$\frac{3i}{2}\frac{g^2}{c_w^2} s_0 g_{\mu\nu}$	$Z_{H\mu}Z_{H\nu}H\Phi^0$	$\frac{i}{2}g^2\left[1+\frac{(c^2-s^2)^2}{s^2c^2}\right] s_0 g_{\mu\nu}$
		$A_{H\mu}A_{H\nu}H\Phi^0$	$\frac{i}{2}g'^2\left[1+\frac{(c'^2-s'^2)^2}{s'^2c'^2}\right] s_0 g_{\mu\nu}$
$W^+_{L\mu}W^-_{H\nu}H\Phi^0$	$-\frac{i}{2}g^2\frac{(c^2-s^2)}{2sc} s_0 g_{\mu\nu}$	$Z_{L\mu}Z_{H\nu}H\Phi^0$	$-\frac{3i}{2}\frac{g^2}{c_w}\frac{(c^2-s^2)}{2sc} s_0 g_{\mu\nu}$
$Z_{L\mu}A_{H\nu}H\Phi^0$	$-\frac{3i}{2}\frac{gg'}{c_w}\frac{(c'^2-s'^2)}{2s'c'} s_0 g_{\mu\nu}$	$Z_{H\mu}A_{H\nu}H\Phi^0$	$\frac{i}{4}gg'\frac{1}{scs'c'}\Big[(c^2s'^2+s^2c'^2)$ $+2(c^2-s^2)(c'^2-s'^2)\Big] s_0 g_{\mu\nu}$
$W^+_{L\mu}A_{L\nu}H\Phi^-$	$-\frac{i}{2}eg(s_+ - \sqrt{2}s_0) g_{\mu\nu}$	$W^+_{H\mu}A_{L\nu}H\Phi^-$	$\frac{i}{2}eg\frac{(c^2-s^2)}{2sc}(s_+ - \sqrt{2}s_0) g_{\mu\nu}$
$W^+_{L\mu}Z_{L\nu}H\Phi^-$	$\frac{i}{2}\frac{g^2}{c_w}\Big[s_+ s_w^2$ $-\sqrt{2}s_0(1+s_w^2)\Big] g_{\mu\nu}$	$W^+_{H\mu}Z_{L\nu}H\Phi^-$	$-\frac{i}{2}\frac{g^2}{c_w}\frac{(c^2-s^2)}{2sc}\Big[s_+ s_w^2$ $-\sqrt{2}s_0(1+s_w^2)\Big] g_{\mu\nu}$
$W^+_{L\mu}A_{H\nu}H\Phi^-$	$-\frac{i}{2}gg'\frac{(c'^2-s'^2)}{2s'c'}(s_+ - 2\sqrt{2}s_0) g_{\mu\nu}$	$W^+_{H\mu}A_{H\nu}H\Phi^-$	$-\frac{i}{4}gg'\frac{1}{scs'c'}\Big[(c^2s'^2+s^2c'^2)s_+$ $+\sqrt{2}(c^2-s^2)(c'^2-s'^2)s_0\Big] g_{\mu\nu}$
$W^+_{L\mu}Z_{H\nu}H\Phi^-$	$\frac{i}{2}g^2\frac{(c^2-s^2)}{2sc} s_0 g_{\mu\nu}$	$W^+_{H\mu}Z_{H\nu}H\Phi^-$	$-\frac{i}{2}g^2\frac{(c^4+s^4)}{2s^2c^2} s_0 g_{\mu\nu}$
$W^+_{L\mu}W^+_{L\nu}H\Phi^{--}$	$\sqrt{2}ig^2 s_0 g_{\mu\nu}$	$W^+_{H\mu}W^+_{H\nu}H\Phi^{--}$	$\sqrt{2}ig^2\frac{(c^4+s^4)}{2s^2c^2} s_0 g_{\mu\nu}$
$W^+_{L\mu}W^+_{H\nu}H\Phi^{--}$	$-\sqrt{2}ig^2\frac{(c^2-s^2)}{2sc} s_0 g_{\mu\nu}$		
$W^+_{L\mu}W^-_{L\nu}\Phi^0\Phi^0$	$ig^2 g_{\mu\nu}$	$W^+_{H\mu}W^-_{H\nu}\Phi^0\Phi^0$	$-ig^2 g_{\mu\nu}$
$Z_{L\mu}Z_{L\nu}\Phi^0\Phi^0$	$2i\frac{g^2}{c_w^2} g_{\mu\nu}$	$Z_{H\mu}Z_{H\nu}\Phi^0\Phi^0$	$2ig^2\frac{(c^2-s^2)^2}{4s^2c^2} g_{\mu\nu}$
		$A_{H\mu}A_{H\nu}\Phi^0\Phi^0$	$2ig'^2\frac{(c'^2-s'^2)^2}{4s'^2c'^2} g_{\mu\nu}$
$W^+_{L\mu}W^-_{H\nu}\Phi^0\Phi^0$	$-ig^2\frac{(c^2-s^2)}{2sc} g_{\mu\nu}$	$Z_{L\mu}Z_{H\nu}\Phi^0\Phi^0$	$-2i\frac{g^2}{c_w}\frac{(c^2-s^2)}{2sc} g_{\mu\nu}$
$Z_{L\mu}A_{H\nu}\Phi^0\Phi^0$	$-2i\frac{gg'}{c_w}\frac{(c'^2-s'^2)}{2s'c'} g_{\mu\nu}$	$Z_{H\mu}A_{H\nu}\Phi^0\Phi^0$	$2igg'\frac{(c^2-s^2)(c'^2-s'^2)}{4scs'c'} g_{\mu\nu}$
$W^+_{L\mu}A_{L\nu}\Phi^0\Phi^-$	$-\frac{i}{\sqrt{2}}egg_{\mu\nu}$	$W^+_{H\mu}A_{L\nu}\Phi^0\Phi^-$	$\frac{i}{\sqrt{2}}eg\frac{(c^2-s^2)}{2sc} g_{\mu\nu}$
$W^+_{L\mu}Z_{L\nu}\Phi^0\Phi^-$	$-\frac{i}{\sqrt{2}}\frac{g^2}{c_w}(1+s_w^2) g_{\mu\nu}$	$W^+_{H\mu}Z_{L\nu}\Phi^0\Phi^-$	$\frac{i}{\sqrt{2}}\frac{g^2}{c_w}\frac{(c^2-s^2)}{2sc}(1+s_w^2) g_{\mu\nu}$
$W^+_{L\mu}A_{H\nu}\Phi^0\Phi^-$	$\sqrt{2}igg'\frac{(c'^2-s'^2)}{2s'c'} g_{\mu\nu}$	$W^+_{H\mu}A_{H\nu}\Phi^0\Phi^-$	$-\frac{i}{2\sqrt{2}}gg'\frac{(c^2-s^2)(c'^2-s'^2)}{scs'c'} g_{\mu\nu}$
$W^+_{L\mu}Z_{H\nu}\Phi^0\Phi^-$	$\frac{i}{\sqrt{2}}g^2\frac{(c^2-s^2)}{2sc} g_{\mu\nu}$	$W^+_{H\mu}Z_{H\nu}\Phi^0\Phi^-$	$-\frac{i}{\sqrt{2}}g^2\frac{(c^4+s^4)}{2s^2c^2} g_{\mu\nu}$
$W^+_{L\mu}W^+_{L\nu}\Phi^0\Phi^{--}$	$\sqrt{2}ig^2 g_{\mu\nu}$	$W^+_{H\mu}W^+_{H\nu}\Phi^0\Phi^{--}$	$\sqrt{2}ig^2\frac{(c^4+s^4)}{2s^2c^2} g_{\mu\nu}$
$W^+_{L\mu}W^+_{H\nu}\Phi^0\Phi^{--}$	$-\sqrt{2}ig^2\frac{(c^2-s^2)}{2sc} g_{\mu\nu}$		

Table A.4: Four-point gauge boson-scalar couplings, continued.

particles	vertices	particles	vertices
$W^+_{L\mu}W^-_{L\nu}\Phi^P\Phi^P$	$ig^2 g_{\mu\nu}$	$W^+_{H\mu}W^-_{H\nu}\Phi^P\Phi^P$	$-ig^2 g_{\mu\nu}$
$Z_{L\mu}Z_{L\nu}\Phi^P\Phi^P$	$2i\frac{g^2}{c_w^2} g_{\mu\nu}$	$Z_{H\mu}Z_{H\nu}\Phi^P\Phi^P$	$2ig^2\frac{(c^2-s^2)^2}{4s^2c^2} g_{\mu\nu}$
		$A_{H\mu}A_{H\nu}\Phi^P\Phi^P$	$2ig'^2\frac{(c'^2-s'^2)^2}{4s'^2c'^2} g_{\mu\nu}$
$W^+_{L\mu}W^-_{H\nu}\Phi^P\Phi^P$	$-ig^2\frac{(c^2-s^2)}{2sc} g_{\mu\nu}$	$Z_{L\mu}Z_{H\nu}\Phi^P\Phi^P$	$-2i\frac{g^2}{c_w}\frac{(c^2-s^2)}{2sc} g_{\mu\nu}$
$Z_{L\mu}A_{H\nu}\Phi^P\Phi^P$	$-2i\frac{gg'}{c_w}\frac{(c'^2-s'^2)}{2s'c'} g_{\mu\nu}$	$Z_{H\mu}A_{H\nu}\Phi^P\Phi^P$	$2igg'\frac{(c^2-s^2)(c'^2-s'^2)}{4scs'c'} g_{\mu\nu}$
$W^+_{L\mu}A_{L\nu}\Phi^P\Phi^-$	$\frac{1}{\sqrt{2}}egg_{\mu\nu}$	$W^+_{H\mu}A_{L\nu}\Phi^P\Phi^-$	$\frac{1}{\sqrt{2}}eg\frac{(c^2-s^2)}{2sc} g_{\mu\nu}$
$W^+_{L\mu}Z_{L\nu}\Phi^P\Phi^-$	$\frac{1}{\sqrt{2}}\frac{g^2}{c_w}(1+s_w^2) g_{\mu\nu}$	$W^+_{H\mu}Z_{L\nu}\Phi^P\Phi^-$	$-\frac{1}{\sqrt{2}}\frac{g^2}{c_w}\frac{(c^2-s^2)}{2sc}(1+s_w^2) g_{\mu\nu}$
$W^+_{L\mu}A_{H\nu}\Phi^P\Phi^-$	$-\sqrt{2}gg'\frac{(c'^2-s'^2)}{2s'c'} g_{\mu\nu}$	$W^+_{H\mu}A_{H\nu}\Phi^P\Phi^-$	$\frac{1}{2\sqrt{2}}gg'\frac{(c^2-s^2)(c'^2-s'^2)}{scs'c'} g_{\mu\nu}$
$W^+_{L\mu}Z_{H\nu}\Phi^P\Phi^-$	$-\frac{1}{\sqrt{2}}g^2\frac{(c^2-s^2)}{2sc} g_{\mu\nu}$	$W^+_{H\mu}Z_{H\nu}\Phi^P\Phi^-$	$\frac{1}{\sqrt{2}}g^2\frac{(c^4+s^4)}{2s^2c^2} g_{\mu\nu}$
$W^+_{L\mu}W^+_{L\nu}\Phi^P\Phi^{--}$	$-\sqrt{2}g^2 g_{\mu\nu}$	$W^+_{H\mu}W^+_{H\nu}\Phi^P\Phi^{--}$	$-\sqrt{2}g^2\frac{(c^4+s^4)}{2s^2c^2} g_{\mu\nu}$
$W^+_{L\mu}W^+_{H\nu}\Phi^P\Phi^{--}$	$\sqrt{2}g^2\frac{(c^2-s^2)}{2sc} g_{\mu\nu}$		
$W^+_{L\mu}W^-_{L\nu}\Phi^+\Phi^-$	$2ig^2 g_{\mu\nu}$	$W^+_{H\mu}W^-_{H\nu}\Phi^+\Phi^-$	$2ig^2\frac{(c^2-s^2)^2}{4s^2c^2} g_{\mu\nu}$
$Z_{L\mu}Z_{L\nu}\Phi^+\Phi^-$	$2i\frac{g^2}{c_w^2}s_w^4 g_{\mu\nu}$	$Z_{H\mu}Z_{H\nu}\Phi^+\Phi^-$	$-2ig^2\frac{1}{4s^2c^2} g_{\mu\nu}$
$A_{L\mu}A_{L\nu}\Phi^+\Phi^-$	$2ie^2 g_{\mu\nu}$	$A_{H\mu}A_{H\nu}\Phi^+\Phi^-$	$2ig'^2\frac{(c'^2-s'^2)^2}{4s'^2c'^2} g_{\mu\nu}$
$A_{L\mu}Z_{L\nu}\Phi^+\Phi^-$	$-2ie\frac{g}{c_w}s_w^2 g_{\mu\nu}$	$A_{H\mu}Z_{H\nu}\Phi^+\Phi^-$	$O(v^2/f^2)$
$W^+_{L\mu}W^-_{H\nu}\Phi^+\Phi^-$	$-2ig^2\frac{(c^2-s^2)}{2sc} g_{\mu\nu}$	$A_{L\mu}A_{H\nu}\Phi^+\Phi^-$	$-2ieg'\frac{(c'^2-s'^2)}{2s'c'} g_{\mu\nu}$
		$Z_{L\mu}Z_{H\nu}\Phi^+\Phi^-$	$O(v^2/f^2)$
$A_{L\mu}Z_{H\nu}\Phi^+\Phi^-$	$O(v^2/f^2)$	$Z_{L\mu}A_{H\nu}\Phi^+\Phi^-$	$2i\frac{gg'}{c_w}\frac{(c'^2-s'^2)}{2s'c'}s_w^2 g_{\mu\nu}$
$W^+_{L\mu}A_{L\nu}\Phi^+\Phi^{--}$	$3ieg g_{\mu\nu}$	$W^+_{H\mu}A_{L\nu}\Phi^+\Phi^{--}$	$-3ieg\frac{(c^2-s^2)}{2sc} g_{\mu\nu}$
$W^+_{L\mu}Z_{L\nu}\Phi^+\Phi^{--}$	$i\frac{g^2}{c_w}(1-3s_w^2) g_{\mu\nu}$	$W^+_{H\mu}Z_{L\nu}\Phi^+\Phi^{--}$	$-i\frac{g^2}{c_w}\frac{(c^2-s^2)}{2sc}(1-3s_w^2) g_{\mu\nu}$
$W^+_{L\mu}A_{H\nu}\Phi^+\Phi^{--}$	$2igg'\frac{(c'^2-s'^2)}{2s'c'} g_{\mu\nu}$	$W^+_{H\mu}A_{H\nu}\Phi^+\Phi^{--}$	$-\frac{i}{2}gg'\frac{(c^2-s^2)(c'^2-s'^2)}{scs'c'} g_{\mu\nu}$
$W^+_{L\mu}Z_{H\nu}\Phi^+\Phi^{--}$	$-\frac{1}{\sqrt{2}}g^2\frac{(c^2-s^2)}{2sc} g_{\mu\nu}$	$W^+_{H\mu}Z_{H\nu}\Phi^+\Phi^{--}$	$\frac{1}{\sqrt{2}}g^2\frac{(c^4+s^4)}{2s^2c^2} g_{\mu\nu}$
$W^+_{L\mu}W^-_{L\nu}\Phi^{++}\Phi^{--}$	$ig^2 g_{\mu\nu}$	$W^+_{H\mu}W^-_{H\nu}\Phi^{++}\Phi^{--}$	$-ig^2 g_{\mu\nu}$
$Z_{L\mu}Z_{L\nu}\Phi^{++}\Phi^{--}$	$2i\frac{g^2}{c_w^2}(1-2s_w^2)^2 g_{\mu\nu}$	$Z_{H\mu}Z_{H\nu}\Phi^{++}\Phi^{--}$	$2ig^2\frac{(c^2-s^2)^2}{4s^2c^2} g_{\mu\nu}$
$A_{L\mu}A_{L\nu}\Phi^{++}\Phi^{--}$	$8ie^2 g_{\mu\nu}$	$A_{H\mu}A_{H\nu}\Phi^{++}\Phi^{--}$	$2ig'^2\frac{(c'^2-s'^2)^2}{4s'^2c'^2} g_{\mu\nu}$
$A_{L\mu}Z_{L\nu}\Phi^{++}\Phi^{--}$	$4ie\frac{g}{c_w}(1-2s_w^2) g_{\mu\nu}$	$A_{H\mu}Z_{H\nu}\Phi^{++}\Phi^{--}$	$-2igg'\frac{(c^2-s^2)(c'^2-s'^2)}{4scs'c'} g_{\mu\nu}$
$W^+_{L\mu}W^-_{H\nu}\Phi^{++}\Phi^{--}$	$-ig^2\frac{(c^2-s^2)}{2sc} g_{\mu\nu}$	$A_{L\mu}A_{H\nu}\Phi^{++}\Phi^{--}$	$-4ieg'\frac{(c'^2-s'^2)}{2s'c'} g_{\mu\nu}$
		$Z_{L\mu}Z_{H\nu}\Phi^{++}\Phi^{--}$	$2i\frac{g^2}{c_w}\frac{(c^2-s^2)}{2sc}(1-2s_w^2) g_{\mu\nu}$
$A_{L\mu}Z_{H\nu}\Phi^{++}\Phi^{--}$	$4ieg\frac{(c^2-s^2)}{2sc} g_{\mu\nu}$	$Z_{L\mu}A_{H\nu}\Phi^{++}\Phi^{--}$	$-2i\frac{gg'}{c_w}\frac{(c'^2-s'^2)}{2s'c'}(1-2s_w^2) g_{\mu\nu}$

Table A.5: Gauge boson self-couplings.

particles	g_{WWV}	particles	g_{WWV}
$W_L^+W_L^-A_L$	$-e$	$W_L^+W_L^-Z_L$	$-ec_\mathrm{w}/s_\mathrm{w}$
$W_L^+W_L^-A_H$	$\frac{e}{s_\mathrm{w}}\frac{v^2}{f^2}c_\mathrm{w}x_Z^{B'}$	$W_L^+W_L^-Z_H$	$\frac{e}{s_\mathrm{w}}\frac{v^2}{f^2}\left(c_\mathrm{w}x_Z^{W'}+sc(c^2-s^2)\right)$
$W_L^+W_H^-A_L$	0	$W_L^+W_H^-Z_L$	$-\frac{e}{s_\mathrm{w}}\frac{v^2}{f^2}x_Z^{W'}$
$W_L^+W_H^-A_H$	$-\frac{e}{s_\mathrm{w}}\frac{v^2}{f^2}x_H$	$W_L^+W_H^-Z_H$	$-e/s_\mathrm{w}$
$W_H^+W_H^-A_L$	$-e$	$W_H^+W_H^-Z_L$	$-ec_\mathrm{w}/s_\mathrm{w}$
$W_H^+W_H^-A_H$	$\frac{e}{s_\mathrm{w}}\frac{v^2}{f^2}\left(x_H\frac{(c^2-s^2)}{sc}+c_\mathrm{w}x_Z^{B'}\right)$	$W_H^+W_H^-Z_H$	$\frac{e}{s_\mathrm{w}}\frac{(c^2-s^2)}{sc}$

particles	$g_{W_1^+W_2^+W_3^-W_4^-}$	particles	$g_{W_1^+W_2^+W_3^-W_4^-}$
$W_L^+W_L^+W_L^-W_L^-$	$-g^2$	$W_L^+W_L^+W_L^-W_H^-$	$-g^2sc(c^2-s^2)v^2/4f^2$
$W_L^+W_L^+W_H^-W_H^-$	$-g^2$	$W_L^+W_H^+W_L^-W_H^-$	$-g^2/4$
$W_H^+W_H^+W_L^-W_H^-$	$g^2(c^2-s^2)/2sc$	$W_H^+W_H^+W_H^-W_H^-$	$-g^2(c^6+s^6)/s^2c^2$

particles	$g_{V_1V_2W_1^+W_2^-}$	particles	$g_{V_1V_2W_1^+W_2^-}$
$A_LA_LW_L^+W_L^-$	$-g^2s_\mathrm{w}^2$	$A_LA_LW_H^+W_H^-$	$-g^2s_\mathrm{w}^2$
$Z_LZ_LW_L^+W_L^-$	$-g^2c_\mathrm{w}^2$	$Z_LZ_LW_H^+W_H^-$	$-g^2c_\mathrm{w}^2$
$A_LZ_LW_L^+W_L^-$	$-g^2s_\mathrm{w}c_\mathrm{w}$	$A_LZ_LW_H^+W_H^-$	$-g^2s_\mathrm{w}c_\mathrm{w}$
$A_LA_HW_L^+W_L^-$	$g^2s_\mathrm{w}c_\mathrm{w}x_Z^{B'}v^2/f^2$	$A_LA_HW_H^+W_H^-$	$g^2s_\mathrm{w}c_\mathrm{w}x_Z^{B'}v^2/f^2$ $+g^2s_\mathrm{w}x_H\frac{v^2}{f^2}(c^2-s^2)/sc$
$A_LZ_HW_L^+W_L^-$	$g^2s_\mathrm{w}c_\mathrm{w}x_Z^{W'}v^2/f^2$ $-g^2s_\mathrm{w}sc(c^2-s^2)v^2/2f^2$	$A_LZ_HW_H^+W_H^-$	$g^2s_\mathrm{w}(c^2-s^2)/sc$
$Z_LZ_HW_L^+W_L^-$	$g^2(c_\mathrm{w}^2-s_\mathrm{w}^2)x_Z^{W'}v^2/f^2$	$Z_LZ_HW_H^+W_H^-$	$g^2c_\mathrm{w}(c^2-s^2)/sc$
$Z_LA_HW_L^+W_L^-$	$g^2c_\mathrm{w}^2x_Z^{B'}v^2/f^2$	$Z_LA_HW_H^+W_H^-$	$g^2c_\mathrm{w}^2x_Z^{B'}v^2/f^2$ $+g^2c_\mathrm{w}x_H\frac{v^2}{f^2}(c^2-s^2)/sc$
$A_HA_HW_L^+W_L^-$	$O(v^4/f^4)$	$A_HA_HW_H^+W_H^-$	$O(v^4/f^4)$
$Z_HZ_HW_L^+W_L^-$	$-g^2$	$Z_HZ_HW_H^+W_H^-$	$-g^2(c^6+s^6)/s^2c^2$
$Z_HA_HW_L^+W_L^-$	$-g^2x_Hv^2/f^2$	$Z_HA_HW_H^+W_H^-$	$-g^2x_H\frac{v^2}{f^2}(c^6+s^6)/s^2c^2$ $-g^2c_\mathrm{w}x_Z^{B'}\frac{v^2}{f^2}(c^2-s^2)/sc$
$A_LA_LW_L^+W_H^-$	0	$A_HA_HW_L^+W_H^-$	$O(v^4/f^4)$
$Z_LZ_LW_L^+W_H^-$	$-2g^2c_\mathrm{w}x_Z^{W'}v^2/f^2$	$Z_HZ_HW_L^+W_H^-$	$g^2(c^2-s^2)/sc$
$Z_LA_LW_L^+W_H^-$	$-g^2s_\mathrm{w}x_Z^{W'}v^2/2f^2$	$Z_HA_HW_L^+W_H^-$	$g^2x_H\frac{v^2}{f^2}(c^2-s^2)/sc$ $+g^2c_\mathrm{w}x_Z^{B'}v^2/f^2$
$A_LA_HW_L^+W_H^-$	$-g^2s_\mathrm{w}x_Hv^2/f^2$	$A_LZ_HW_L^+W_H^-$	$-g^2s_\mathrm{w}$
$Z_LA_HW_L^+W_H^-$	$-g^2c_\mathrm{w}x_Hv^2/f^2$	$Z_LZ_HW_L^+W_H^-$	$-g^2c_\mathrm{w}$

Table A.6: Charged gauge boson-fermion couplings. They are purely left-handed, and the projection operator $P_L = (1 - \gamma^5)/2$ is implied.

particles	vertices	particles	vertices
$W_L^{+\mu}\bar{u}_L d_L$	$\frac{ig}{\sqrt{2}}\left[1 - \frac{v^2}{2f^2}c^2(c^2 - s^2)\right]\gamma^\mu V_{ud}^{\rm SM}$	$W_H^{+\mu}\bar{u}_L d_L$	$-\frac{ig}{\sqrt{2}}\frac{c}{s}\gamma^\mu V_{ud}^{\rm SM}$
$W_L^{+\mu}\bar{t}_L b_L$	$\frac{ig}{\sqrt{2}}\left[1 - \frac{v^2}{f^2}\left(\frac{1}{2}x_L^2 + \frac{1}{2}c^2(c^2 - s^2)\right)\right]\gamma^\mu V_{tb}^{\rm SM}$	$W_H^{+\mu}\bar{t}_L b_L$	$-\frac{ig}{\sqrt{2}}\frac{c}{s}\gamma^\mu V_{tb}^{\rm SM}$
$W_L^{+\mu}\bar{T}_L b_L$	$\frac{g}{\sqrt{2}}\frac{v}{f}x_L\gamma^\mu V_{tb}^{\rm SM}$	$W_H^{+\mu}\bar{T}_L b_L$	$-\frac{g}{\sqrt{2}}\frac{v}{f}x_L\frac{c}{s}\gamma^\mu V_{tb}^{\rm SM}$

Table A.7: Neutral gauge boson-fermion couplings. Anomaly cancelation requires $y_u = -2/5$ and $y_e = 3/5$.

particles	g_V	g_A
$A_L\bar{f}f$	$-eQ_f$	0
$Z_L\bar{u}u$	$-\frac{g}{2c_\mathrm{w}}\left\{(\frac{1}{2}-\frac{4}{3}s_\mathrm{w}^2)-\frac{v^2}{f^2}\left[c_\mathrm{w}x_Z^{W'}c/2s+\frac{s_\mathrm{w}x_Z^{B'}}{s'c'}\left(2y_u+\frac{7}{15}-\frac{1}{6}c'^2\right)\right]\right\}$	$-\frac{g}{2c_\mathrm{w}}\left\{-\frac{1}{2}-\frac{v^2}{f^2}\left[-c_\mathrm{w}x_Z^{W'}c/2s+\frac{s_\mathrm{w}x_Z^{B'}}{s'c'}\left(\frac{1}{5}-\frac{1}{2}c'^2\right)\right]\right\}$
$Z_L\bar{d}d$	$-\frac{g}{2c_\mathrm{w}}\left\{(-\frac{1}{2}+\frac{2}{3}s_\mathrm{w}^2)-\frac{v^2}{f^2}\left[-c_\mathrm{w}x_Z^{W'}c/2s+\frac{s_\mathrm{w}x_Z^{B'}}{s'c'}\left(2y_u+\frac{11}{15}+\frac{1}{6}c'^2\right)\right]\right\}$	$-\frac{g}{2c_\mathrm{w}}\left\{\frac{1}{2}-\frac{v^2}{f^2}\left[c_\mathrm{w}x_Z^{W'}c/2s+\frac{s_\mathrm{w}x_Z^{B'}}{s'c'}\left(-\frac{1}{5}+\frac{1}{2}c'^2\right)\right]\right\}$
$Z_L\bar{e}e$	$-\frac{g}{2c_\mathrm{w}}\left\{(-\frac{1}{2}+2s_\mathrm{w}^2)-\frac{v^2}{f^2}\left[-c_\mathrm{w}x_Z^{W'}c/2s+\frac{s_\mathrm{w}x_Z^{B'}}{s'c'}\left(2y_e-\frac{9}{5}+\frac{3}{2}c'^2\right)\right]\right\}$	$-\frac{g}{2c_\mathrm{w}}\left\{\frac{1}{2}-\frac{v^2}{f^2}\left[c_\mathrm{w}x_Z^{W'}c/2s+\frac{s_\mathrm{w}x_Z^{B'}}{s'c'}\left(-\frac{1}{5}+\frac{1}{2}c'^2\right)\right]\right\}$
$Z_L\bar{\nu}\nu$	$-\frac{g}{2c_\mathrm{w}}\left\{\frac{1}{2}-\frac{v^2}{f^2}\left[c_\mathrm{w}x_Z^{W'}c/2s+\frac{s_\mathrm{w}x_Z^{B'}}{s'c'}\left(y_e-\frac{4}{5}+\frac{1}{2}c'^2\right)\right]\right\}$	$-\frac{g}{2c_\mathrm{w}}\left\{-\frac{1}{2}-\frac{v^2}{f^2}\left[-c_\mathrm{w}x_Z^{W'}c/2s+\frac{s_\mathrm{w}x_Z^{B'}}{s'c'}\left(-y_e+\frac{4}{5}-\frac{1}{2}c'^2\right)\right]\right\}$
$Z_L\bar{t}t$	$-\frac{g}{2c_\mathrm{w}}\left\{(\frac{1}{2}-\frac{4}{3}s_\mathrm{w}^2)-\frac{v^2}{f^2}\left[-x_L^2/2+c_\mathrm{w}x_Z^{W'}c/2s+\frac{s_\mathrm{w}x_Z^{B'}}{s'c'}\left(2y_u+\frac{9}{5}-\frac{3}{2}c'^2+\left(\frac{7}{15}-\frac{2}{3}c'^2\right)\frac{\lambda_1^2}{\lambda_1^2+\lambda_2^2}\right)\right]\right\}$	$-\frac{g}{2c_\mathrm{w}}\left\{-\frac{1}{2}-\frac{v^2}{f^2}\left[x_L^2/2-c_\mathrm{w}x_Z^{W'}c/2s+\frac{s_\mathrm{w}x_Z^{B'}}{s'c'}\left(\frac{1}{5}-\frac{1}{2}c'^2-\frac{1}{5}\frac{\lambda_1^2}{\lambda_1^2+\lambda_2^2}\right)\right]\right\}$
$Z_L\bar{T}T$	$2gs_\mathrm{w}^2/3c_\mathrm{w}$	$O(v^2/f^2)$
$Z_L\bar{T}t$	$igx_Lv/4fc_\mathrm{w}$	$-igx_Lv/4fc_\mathrm{w}$
$A_H\bar{u}u$	$\frac{g'}{2s'c'}\left(2y_u+\frac{17}{15}-\frac{5}{6}c'^2\right)$	$\frac{g'}{2s'c'}\left(\frac{1}{5}-\frac{1}{2}c'^2\right)$
$A_H\bar{d}d$	$\frac{g'}{2s'c'}\left(2y_u+\frac{11}{15}+\frac{1}{6}c'^2\right)$	$\frac{g'}{2s'c'}\left(-\frac{1}{5}+\frac{1}{2}c'^2\right)$
$A_H\bar{e}e$	$\frac{g'}{2s'c'}\left(2y_e-\frac{9}{5}+\frac{3}{2}c'^2\right)$	$\frac{g'}{2s'c'}\left(-\frac{1}{5}+\frac{1}{2}c'^2\right)$
$A_H\bar{\nu}\nu$	$\frac{g'}{2s'c'}\left(y_e-\frac{4}{5}+\frac{1}{2}c'^2\right)$	$\frac{g'}{2s'c'}\left(-y_e+\frac{4}{5}-\frac{1}{2}c'^2\right)$
$A_H\bar{t}t$	$\frac{g'}{2s'c'}\left(2y_u+\frac{17}{15}-\frac{5}{6}c'^2-\frac{1}{5}\frac{\lambda_1^2}{\lambda_1^2+\lambda_2^2}\right)$	$\frac{g'}{2s'c'}\left(\frac{1}{5}-\frac{1}{2}c'^2-\frac{1}{5}\frac{\lambda_1^2}{\lambda_1^2+\lambda_2^2}\right)$
$A_H\bar{T}T$	$\frac{g'}{2s'c'}\left(2y_u+\frac{14}{15}-\frac{4}{3}c'^2+\frac{1}{5}\frac{\lambda_1^2}{\lambda_1^2+\lambda_2^2}\right)$	$\frac{g'}{2s'c'}\frac{1}{5}\frac{\lambda_1^2}{\lambda_1^2+\lambda_2^2}$
$A_H\bar{T}t$	$\frac{g'}{2s'c'}\frac{1}{5}\frac{\lambda_1\lambda_2}{\lambda_1^2+\lambda_2^2}$	$\frac{g'}{2s'c'}\frac{1}{5}\frac{\lambda_1\lambda_2}{\lambda_1^2+\lambda_2^2}$
$Z_H\bar{u}u$	$gc/4s$	$-gc/4s$
$Z_H\bar{d}d$	$-gc/4s$	$gc/4s$
$Z_H\bar{e}e$	$-gc/4s$	$gc/4s$
$Z_H\bar{\nu}\nu$	$gc/4s$	$-gc/4s$
$Z_H\bar{t}t$	$gc/4s$	$-gc/4s$
$Z_H\bar{T}T$	$O(v^2/f^2)$	$O(v^2/f^2)$
$Z_H\bar{T}t$	$-igx_Lvc/4fs$	$igx_Lvc/4fs$

Table A.8: Scalar-fermion couplings.

particles	vertices	particles	vertices
$H\bar{u}u$	$-i\frac{m_u}{v}\left(1-\frac{1}{2}s_0^2+\frac{v}{f}\frac{s_0}{\sqrt{2}}-\frac{2v^2}{3f^2}\right)$	$H\bar{d}d$	$-i\frac{m_d}{v}\left(1-\frac{1}{2}s_0^2+\frac{v}{f}\frac{s_0}{\sqrt{2}}-\frac{2v^2}{3f^2}\right)$
$H\bar{t}t$	$-i\frac{m_t}{v}\left[1-\frac{1}{2}s_0^2+\frac{v}{f}\frac{s_0}{\sqrt{2}}-\frac{2v^2}{3f^2}+\frac{v^2}{f^2}\frac{\lambda_1^2}{\lambda_1^2+\lambda_2^2}\left(1+\frac{\lambda_1^2}{\lambda_1^2+\lambda_2^2}\right)\right]$	$H\bar{T}T$	$-i\frac{\lambda_1^2}{\sqrt{\lambda_1^2+\lambda_2^2}}\left(1+\frac{\lambda_1^2}{\lambda_1^2+\lambda_2^2}\right)\frac{v}{f}$
$H\bar{T}t$	$\frac{m_t}{v}\frac{v}{f}\left(1+\frac{\lambda_1^2}{\lambda_1^2+\lambda_2^2}\right)P_R+\frac{\lambda_1^2}{\sqrt{\lambda_1^2+\lambda_2^2}}P_L$	$H\bar{t}T$	$-\frac{m_t}{v}\frac{v}{f}\left(1+\frac{\lambda_1^2}{\lambda_1^2+\lambda_2^2}\right)P_L-\frac{\lambda_1^2}{\sqrt{\lambda_1^2+\lambda_2^2}}P_R$
$HH\bar{t}t$	$i\frac{2m_t}{f^2}\left[1-\frac{2fv'}{v^2}-\frac{1}{2}\frac{\lambda_1^2}{\lambda_1^2+\lambda_2^2}\right]$	$HH\bar{T}T$	$-\frac{i}{f}\frac{\lambda_1^2}{\sqrt{\lambda_1^2+\lambda_2^2}}$
$HH\bar{T}t$	$-\frac{2v}{f^2}\frac{\lambda_1^2}{\sqrt{\lambda_1^2+\lambda_2^2}}\left[1-\frac{2fv'}{v^2}-\frac{1}{2}\frac{\lambda_1^2}{\lambda_1^2+\lambda_2^2}\right]P_L+\frac{m_t}{vf}P_R$	$HH\bar{t}T$	$\frac{2v}{f^2}\frac{\lambda_1^2}{\sqrt{\lambda_1^2+\lambda_2^2}}\left[1-\frac{2fv'}{v^2}-\frac{1}{2}\frac{\lambda_1^2}{\lambda_1^2+\lambda_2^2}\right]P_R-\frac{m_t}{vf}P_L$
$\Phi^0\bar{u}u$	$-\frac{im_u}{\sqrt{2}v}\left(\frac{v}{f}-\sqrt{2}s_0\right)$	$\Phi^0\bar{d}d$	$-\frac{im_d}{\sqrt{2}v}\left(\frac{v}{f}-\sqrt{2}s_0\right)$
$\Phi^P\bar{u}u$	$-\frac{m_u}{\sqrt{2}v}\left(\frac{v}{f}-\sqrt{2}s_P\right)\gamma^5$	$\Phi^P\bar{d}d$	$\frac{m_d}{\sqrt{2}v}\left(\frac{v}{f}-\sqrt{2}s_P\right)\gamma^5$
$\Phi^+\bar{u}d$	$-\frac{i}{\sqrt{2}v}\left(m_uP_L+m_dP_R\right)\left(\frac{v}{f}-2s_+\right)$	$\Phi^-\bar{d}u$	$-\frac{i}{\sqrt{2}v}\left(m_uP_R+m_dP_L\right)\left(\frac{v}{f}-2s_+\right)$
$\Phi^0\bar{T}t$	$-\frac{im_t}{\sqrt{2}v}\left(\frac{v}{f}-\sqrt{2}s_0\right)\frac{\lambda_1}{\lambda_2}P_L$	$\Phi^0\bar{t}T$	$-\frac{im_t}{\sqrt{2}v}\left(\frac{v}{f}-\sqrt{2}s_0\right)\frac{\lambda_1}{\lambda_2}P_R$
$\Phi^P\bar{T}t$	$\frac{m_t}{\sqrt{2}v}\left(\frac{v}{f}-\sqrt{2}s_0\right)\frac{\lambda_1}{\lambda_2}P_L$	$\Phi^P\bar{t}T$	$\frac{m_t}{\sqrt{2}v}\left(\frac{v}{f}-\sqrt{2}s_0\right)\frac{\lambda_1}{\lambda_2}P_R$
$\Phi^+\bar{T}b$	$-\frac{im_t}{\sqrt{2}v}\left(\frac{v}{f}-2s_+\right)\frac{\lambda_1}{\lambda_2}P_L$	$\Phi^-\bar{b}T$	$-\frac{im_t}{\sqrt{2}v}\left(\frac{v}{f}-2s_+\right)\frac{\lambda_1}{\lambda_2}P_R$

VITA

Ayşe Çağıl was born in İstanbul, Turkey, in 1979. She received her BS degree in physics at Midle East Echnical University(METU) in Ankara, Turkey, in 2001. Having completed the BS program, she started MS studies at physics department of METU, Ankara, Turkey and received her MS degree in 2003. She started her Ph.D. studies in high energy physics at METU, in 2003.